

Division of Surgical Research

Annual Report 2011

Department of Surgery
University Hospital Zurich
Switzerland



Division of Surgical Research
Department of Surgery
University Hospital
Rämistrasse 100
CH - 8091 Zurich

Content

Preface	5
1. Organisation	6
2. Research and Development	8
Cardiovascular Surgery	8
Cardiovascular Regenerative Medicine	8
Hybrid and Minimally Invasive Technologies	16
Mechanical Circulatory Support	20
Visceral & Transplant Surgery	22
Hepatobiliary & Transplantation Surgery	22
Machine liver perfusion	27
Liver Embolization	29
Pancreatitis Research Laboratory	31
Bariatric Surgery	33
Trauma Surgery	34
Pathophysiology	34
Osteology	37
Translational Research	42
Cooperation Trauma Surgery and Plastic, Hand & Reconstructive Surgery	45
Plastic, Hand & Reconstructive Surgery	50
Motion analysis Laboratory	50
Connective tissue healing	52
Microcirculation	54
Protein profiling	60
Thoracic Surgery	62
Transplantation Immunology	62
Oncology	70
Urology	81
Oncology	81
Tissue Engineering for Urologic Tissues	84
Cranio-Maxillofacial Surgery	100
Oral Biotechnology and Bioengineering	100
Oral Oncology	103
Orofacial Deformities	104
Computer-assisted surgery and imaging	104
Surgical Intensive Care Units	106
New and improved anaesthesia methods	114
3. Services	117
Surgical Skill Laboratories	117
Microsurgical Laboratory	117
Histology	117
Photo and Graphic Services	118
Administration	119
Teaching Coordination	119
4. Events and Workshops	120
5. Publications	122
6. Grants	128
7. Awards	133



Preface

Dear Colleagues



Prof. Dr.
Gregor Zünd, MD
Head Division of
Surgical Research

It is my privilege to present the Annual Report 2011 of the Division of Surgical Research at the Department of Surgery, University Hospital Zurich.

The major investments of laboratory equipment made in the past year include the purchase of four CO₂ incubators. In order to comply with the new animal protection regulations, we also had to replace the old animal cabinet by a microbiological airflow safety cabinet for the housing of laboratory rodents.

For teaching activities, several wet lab events for surgeons and microsurgery classes for surgical residents were offered. The weekly lectures held by the Division of Surgical Research at the University Hospital Zurich were regularly attended by the members of our Division and other scientists representing an integrative part of the academic curriculum within the University, University Hospital and the Swiss Federal Institute of Technology.

It is my great pleasure to thank all members within our Division as well as our research partners of the University, University Hospital and the Swiss Federal Institute of Technology for last year's excellent contributions and fruitful collaborations.

Yours sincerely

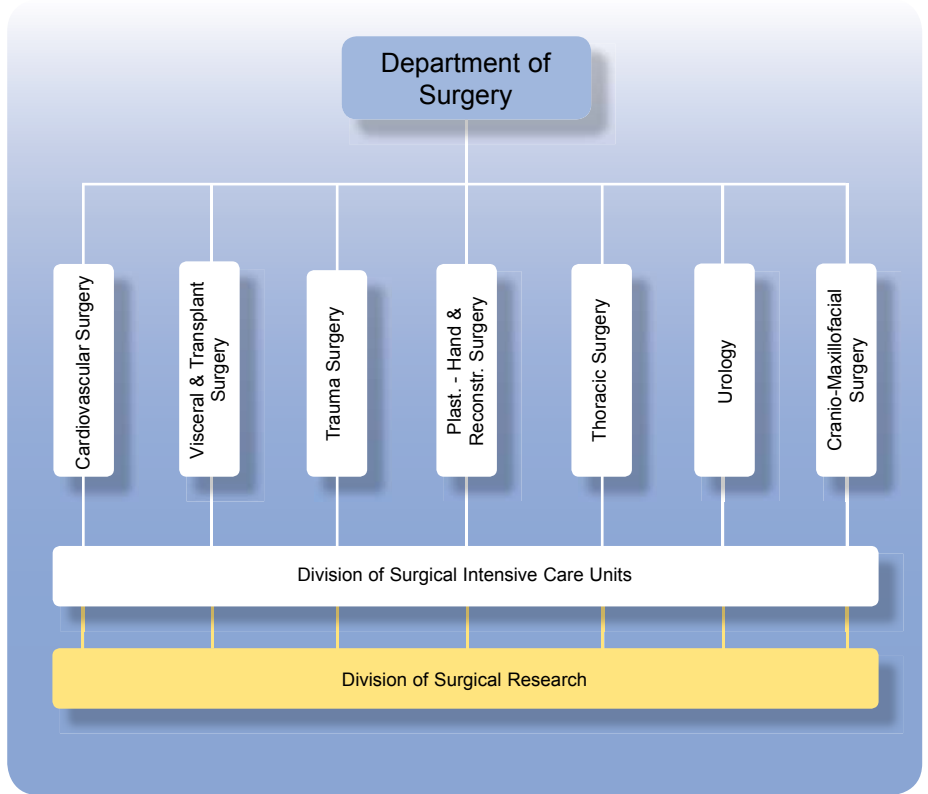
A handwritten signature in black ink, appearing to read 'G. Zünd', written in a cursive style.

Prof. Dr. Gregor Zünd, MD
Head Division of Surgical Research

1. Organisation

1.1 Position of the Division of Surgical Research within the Department of Surgery

 <p>Prof. Dr. Pierre-Alain Clavien, MD, PhD Director Clinic of Visceral & Transpl. Surgery</p>	 <p>Prof. Dr. Hans-Peter Simmen, MD Director Clinic of Trauma Surgery</p>	 <p>Prof. Dr. Walter Weder, MD Director Clinic of Thoracic Surgery</p>
 <p>Prof. Dr. Volkmar Falk, MD Director Clinic of Cardiovascular Surgery</p>	 <p>Prof. Dr. Pietro Giovanoli, MD Director Clinic of Plastic - Hand & Reconstr. Surgery</p>	 <p>Prof. Dr. Tullio Sulser, MD Director Clinic of Urology</p>
 <p>Prof. Dr. Klaus W. Grätz, MD Director Clinic of Cranio-Maxillofacial Surgery</p>	 <p>Prof. Dr. John Stover, MD Head of Intensive Care Unit</p>	
 <p>Prof. Dr. Gregor Zünd, MD Head Division of Surgical Research</p>		



1.2 Structural Organisation of the Division of Surgical Research



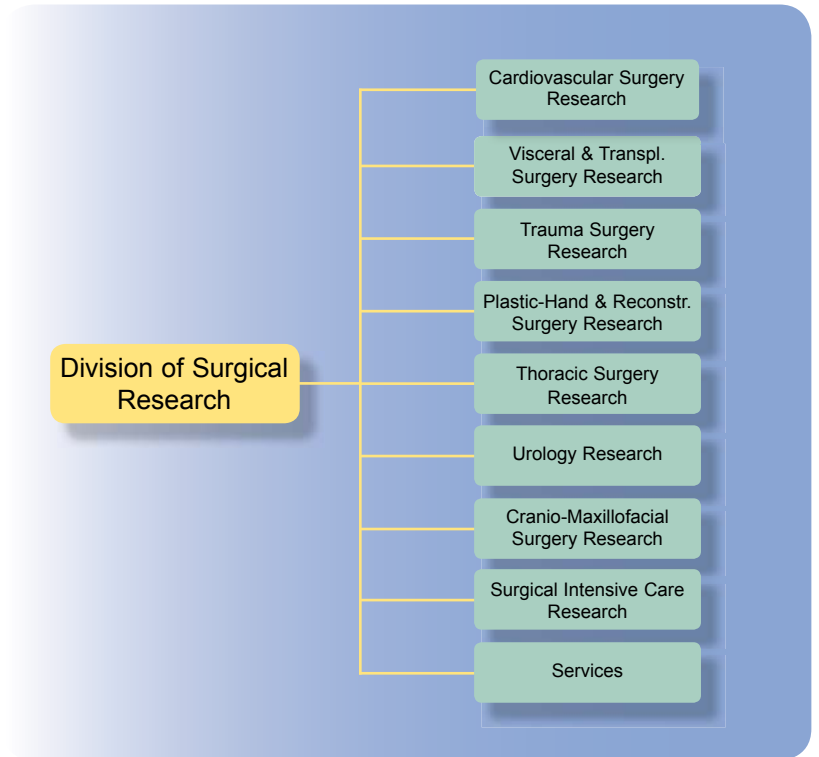
Prof. Dr.
Gregor Zünd, MD
Head Division of
Surgical Research



Prof. Dr.
Rolf Graf, PhD
Co-Head Division of
Surgical Research



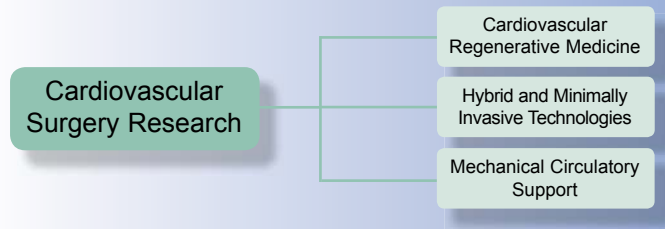
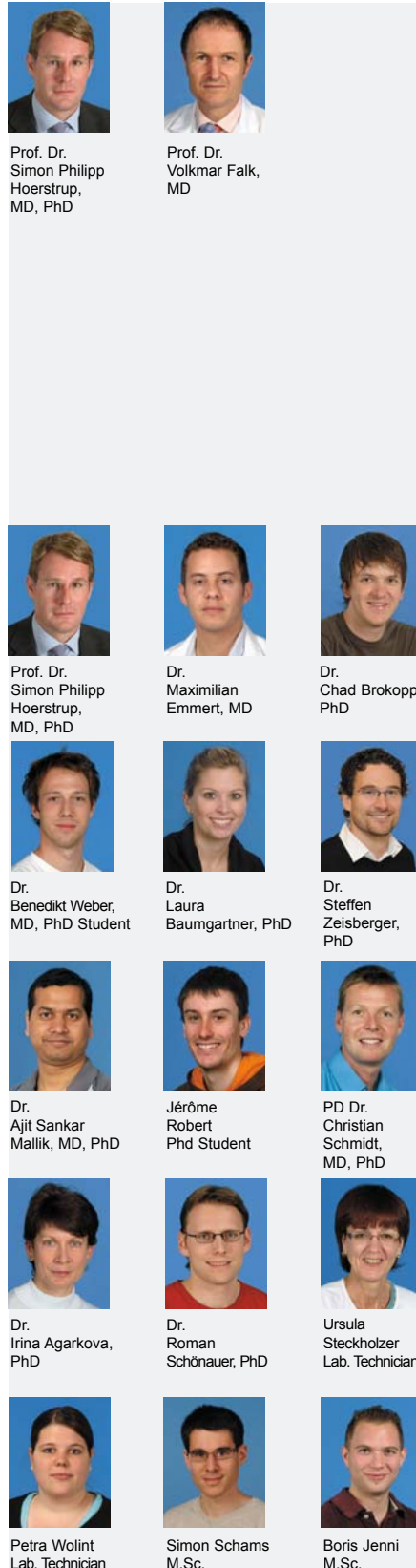
Susanne Frehner
Administration
Division of Surgical
Research



2. Research and Development

8

2.1 Cardiovascular Surgery Research



2.1.1 Cardiovascular Regenerative Medicine

2.1.1.1 Stem Cells

M. Emmert, S.P. Hoerstrup

Cardiac Diseases and Limitations of Conventional Therapies

Ischemic heart disease is the primary cause of death throughout the western society and has tremendous socio-economic impact. Obstruction of the coronary arteries leads to myocardial infarction (heart attack) followed by death of the heart cells. The adult heart cannot regenerate after ischemic injury as cardiomyocytes do not possess an ability to divide and the heart lacks sufficient reserve of precursor or stem cells. The loss of myocytes leads to progressive dilation of the myocardial wall and eventually to cardiac failure. So far, conventional medication or heart transplantation is the only option for patients with cardiac failure. However, conventional medication can treat only the symptoms and the disproportion between the number of donor organs and the number of potential transplantation candidates limits transplantation to a minority of patients. About 20% of patients die during waiting time. Therefore, unmet therapeutic demand requires novel therapy options to be developed.

Stem Cell based cardiac therapy – a future strategy?

As a next generation therapeutic approach, stem cells have shown significant promise in regenerative medicine in particular with regard to the treatment of the failing heart e.g. due to myocardial infarction or other cardiomyopathies. On the basis of encouraging preclinical studies, there are growing numbers of early phase patient trials that aim to demonstrate the feasibility and potential efficacy of cell-based therapies in the clinical setting.

Stem Cell types

Several categories of stem cells are being examined for their ability to promote cardiac repair: crude bone marrow-derived/circulating progenitor cells (BMPCs) and their subpopulations, such as marrow stromal derived stem



Tom Sasse
M.Sc.



Francesca
Papadopulos,
M.Sc.



Yves Wyss
cand. med.



Pascal Heye
M.Sc.



Thomas
Baumgartner
Study Coordination
and Administration

cells (MSCs) and endothelial progenitor cells (EPCs); skeletal myoblasts (SM), umbilical cord derived stem cells (UPCs), embryonic stem cells (ESCs), induced pluripotent cells (iPS) and resident cardiac stem (or cardiomyocyte progenitor) cells (CSCs). While ESCs and iPS displaying the highest plasticity are still in preclinical evaluation due to ethical and safety issues, the other aforementioned adult stem cells have advanced to clinical applications. Marrow stromal derived stem cells (MSCs) are considered as a clinical benchmark cell for cardiac repair and have been repeatedly investigated in animal as well as human trials as they are considered safe and easily available in clinically relevant numbers. Importantly, recent reports indicate that MSCs can be programmed into a cardiac committed stage (cardiopoietic MSC) when applying a specific cardiopoietic conditioning.

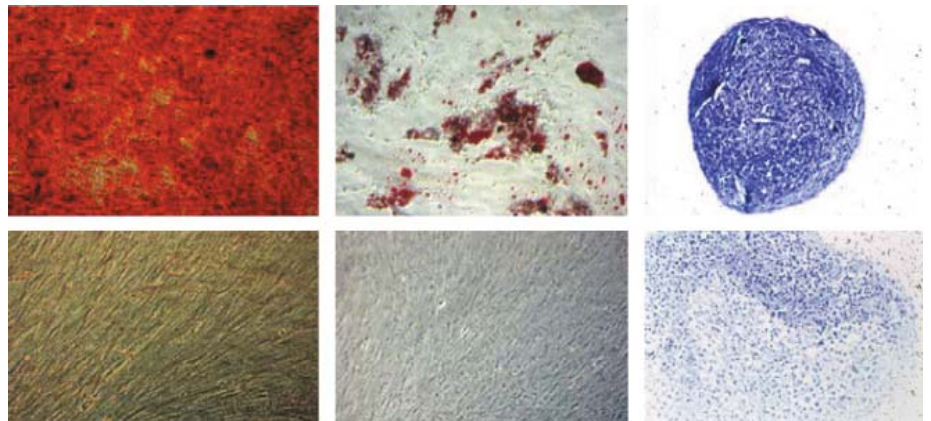


Figure 1: Differentiation assays of MSC into adipogenic, chondrogenic and osteogenic lineage

Cell retention and Integration

The possible causes for the limited effects of stem cell in curing heart failure are the low retention and poor integration of the injected cells. Single cell injections display a high cellular wash out and low survival rate. It was shown, that after single cell injections the MSC migrated to the myocardium and dispersed from the infarcted heart to other organs via the vascular system. The amount of stem cells settled in the myocardium decreased drastically to only ~1.49%. Within another study of five million implanted cardiomyocytes, only 1000 viable cardiomyocytes could be detected after 4 months, representing an integration rate of 0.2%. In responses to these problems, we have to develop new strategies. Recently there has been a series of publications on aggregation of MSC to increase their therapeutic potential. These 3D aggregates, also called microtissues, are produced using gravity-enforced self-assembly of mono-dispersed primary cells and are aimed at improving cellular retention and integration by providing cellular aggregates in a more organized functional state already in-vitro. Applying this technology in previous studies has enabled in-vitro generation of artificial myocardium from neonatal and adult cardiomyocytes, which produce pro-angiogenic factors such as VEGF.

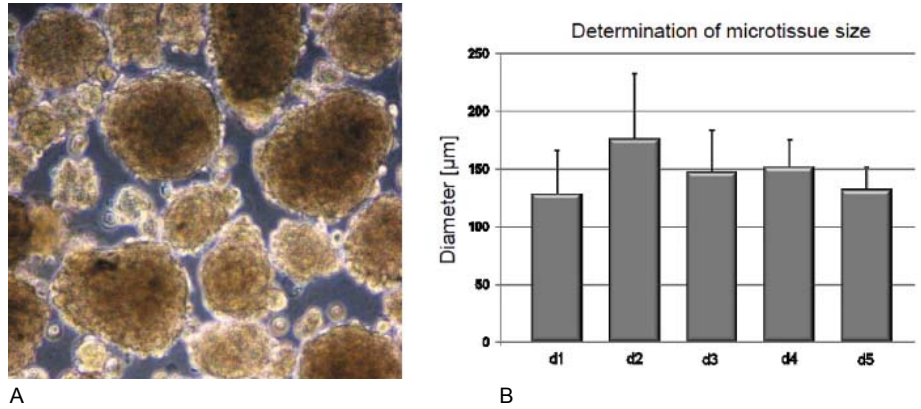


Figure 2: (A) Formation of microtissues (MT) after 4 days and (B) determination of MT-size

Assessment in a large animal model

To assess the effect of MT application *in vivo*, a model of myocardial infarction in pig has been established. We used a navigation system that takes advantage of electrical mapping to detect the border zone of the infarct (NOGA, Cordis Webster). Furthermore, the system is coupled to an injection device to deliver cells at the appropriate location in the infarcted heart.

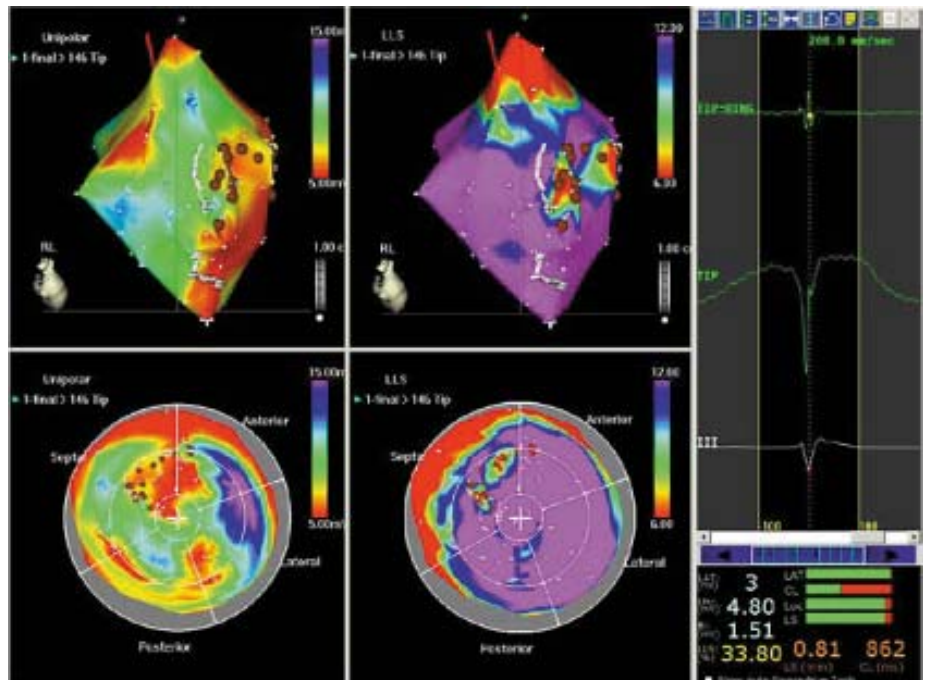


Figure 3: Assessment and definition of injection zone (infarction border zone) of an infarcted pig heart using the NOGA system.

2.1.1.2 Cardiovascular Tissue Engineering

B. Weber, S.P. Hoerstrup

The strategy of cardiovascular tissue engineering

The main focus of cardiovascular tissue engineering is the development and *in vitro* generation of living tissues for cardiovascular surgery including tissue engineered blood vessels, heart valves as well as patches. Currently utilized heart valve and blood vessel prostheses carry disadvantages for the patients mainly because non-living, artificial devices are inserted into the human organism. Tissue engineering enables the *in vitro* production of autologous, living and functional replacements with the capacity of regeneration and growth the latter being of particular importance for pediatric application as an alternative to state of the art artificial replacements.

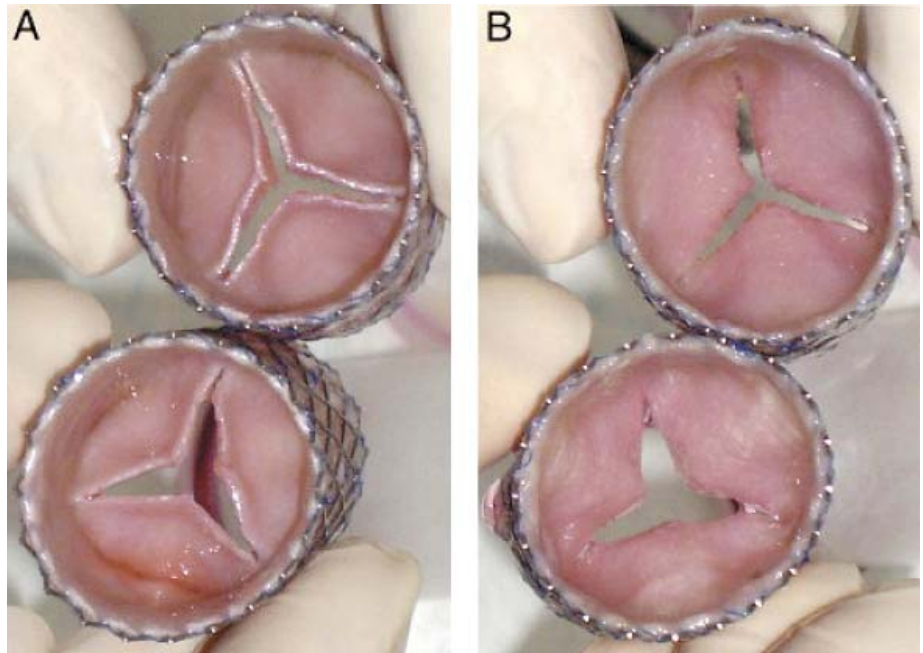
Tissue engineering of cardiovascular structures

To address the substantial limitations of state of the art artificial heart valve and vascular prostheses, the ultimate goal of tissue engineering is to construct living tissues, which combine most of the characteristics of the native original. The success of tissue engineered heart valves is dependent on three main issues: (1) the proliferation and differentiation potential of the cell source from which a living neo-tissue is grown; (2) the scaffold matrix, which determines the three-dimensional shape and serves as an initial guiding structure for cell attachment and tissue development; and (3) the *in vitro* culture conditions of the living construct before implantation. This *in vitro* "conditioning" can be influenced by the culture media and mechanical stimulation such as pulsatile flow by using bioreactors.

Pre-clinical trials in sheep

In recent years, research has demonstrated the principle feasibility of the autologous tissue engineering concept for cardiovascular applications in heart valves and blood vessels. Tissue-engineered large diameter vascular grafts have been successfully used in low and systemic pressure applications in sheep, and technology transfer to human cells and has been shown.

In a large animal study, Hoerstrup et al. (Circulation 2006) investigated the function and growth in tissue-engineered living main pulmonary arteries over a period of 100 weeks in a lamb model, covering the full growth of this animal model. Their investigation provides first evidence of functional growth in living pulmonary arteries engineered from vascular cells in a full growth animal model. These findings support the potential of the tissue-engineering concept for congenital applications and may provide a further experimental basis to justify the large-scale clinical implementation in the near future.



Tissue engineered heart valve prior to *in vivo* implantation (Schmidt et al., JACC 2011).

First-in-man clinical pilot trial

Based on the above described tissue engineering technologies developed in the cardiac surgery research laboratories, living tissue engineered blood vessels were demonstrated to be functional in preclinical large animal trials up to 4 years (*Circulation* 2006). Important observations were (A) the *in vivo* remodeling of the tissue engineered arteries into the typical three-layered architecture observed in their native counterparts, and (B) the ability of the tissue engineered arteries to follow the normal anatomical growth of the animal and their remodeling to a stable, mature tissue composition. Based on these results, a first-in-man clinical pilot trial for patients with congenital heart malformations (single ventricle pathology) using tissue engineered vascular grafts has been initiated by the University of Zurich.

2.1.1.3 Disease Modeling

C. Brokopp, J. Robert, S.P. Hoerstrup

Atherosclerosis builds up inflamed fatty plaques in the arterial wall. Over several decades, unstable atherosclerotic plaques may form in high-risk patients. These life-threatening unstable plaques have a so-called necrotic core that is separated from the blood by a layer of connective tissue called the fibrous cap. Degradation of the fibrous cap causes unstable plaque to rupture open. Plaque rupture brings the blood in contact with the plaque's necrotic core, which triggers occlusive thrombus formation. If these events occur in a major artery, a life-threatening infarction (heart attack or stroke) may be triggered.

Tissue Engineered Atherosclerosis Modeling

To date, atherosclerosis mechanistic studies have been limited either to simple two dimensional in-vitro cell culture systems or animal models. Findings derived from such experimental settings suffer from large deviations from the human context. As a next generation approach, we employ a hybrid strategy to combine traditional cell culture assays with tissue engineered vascular systems. By investigating atherogenesis in biomimetic human-based tissue engineered vessels complete with haemodynamics and three-dimensional vascular histology, we observe unique bio-phenomena more congruent with human atherogenesis than conventional modeling.

HDL transport in tissue engineered vessels

We now demonstrated the possibility to engineer functional artery equivalents as a model to study lipid transport under pathophysiological conditions, with a key advantages of superior bio-mimetic conditions (i.e. flow and 3D histology) compared to current best-in-class vascular cell culture models (**Figure 1A**). High density lipoproteins (HDL) are hypothesized to exert atheroprotective functions including: reduced oxidative damage, inhibition of inflammation, and reverse cholesterol transport away from the vessel wall. While it is known that anti-atherogenic functions of HDL are exerted within the arterial wall, the mechanisms by which HDL is transported through the vascular endothelium into the vascular wall are not known. A better understanding of these mechanisms are anticipated to identify promising drug targets in the context of infarction prevention medications. To this end, proof-of-concept experiments have demonstrated an uptake of HDL in the 3D tissue engineered model (**Figure 1B**), and have set the stage for future lipid transport studies using this model, with the aim of identifying next-generation therapeutic targets.

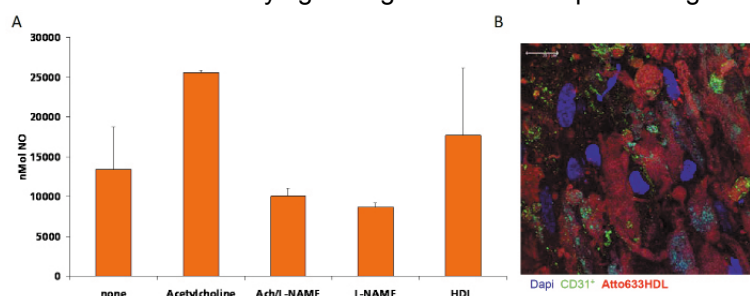


Figure 1. A. Functionality of the endothelium of the engineered vessel. Nitric oxide (NO) production is measured using Electron spin resonance. Acetylcholine, an eNOS agonist induced the production of NO by the artery whereas the eNOS inhibitor L-NAME abolished the increase of NO due to acetylcholine. HDL also induced the production of NO by the endothelial cells of the artery. **B. Localisation of HDL in the engineered artery.** Confocal image of the localisation of HDL (red) in the engineered artery. HDL demonstrated a vesicular localization in the periphery of the nuclei (blue) of the endothelial cells (green).

2.1.1.4. Novel Targets for Infarction Prevention Strategies

C. Brokopp, S.P. Hoerstrup

Unmet clinical needs in myocardial infarction prevention

There is currently important need to identify patients at risk of infarction. Specifically, current clinical blood tests only identify myocardial infarctions after necrosis has already occurred, but cannot predict myocardial infarctions before a coronary event. Moreover, current best-in-class medications for infarction prevention are inadequate. For example, statins prevent life-threatening events in an average of 1 out of 167 patients with elevated CRP after 1.9 years of use, whereas Plavix® is often given after an infarction for re-infarction prevention, to justify the drug's potential side effect risks. Therefore, a significant unmet clinical need remains for diagnostics that identify who to treat and therapeutics to reduce these patients' risk of infarction.

Targeting FAP for myocardial infarction prevention?

Results our research shows that serine protease Fibroblast Activation Protein (FAP) contributes to infarction by: 1. cleaving the structural support (Type I collagen) of the unstable atherosclerotic plaques, thereby making them prone to rupture, and 2. by accelerating the formation of occluding thrombi by activating a key inhibitor of plasmin ($\alpha 2$ antiplasmin). Furthermore, soluble FAP in blood plasma is increased in patients with ACS compared to healthy probands suggesting its potential as a diagnostic biomarker in the context of ACS. However, the causal role of FAP in atherothrombosis and human infarction remains to be determined.

FAP associates with life-threatening coronary plaque rupture

Previous studies from our research show that FAP is expressed as a trans-membrane protein in endothelial and smooth muscle cells of life-threatening unstable atherosclerotic plaques in coronary arteries (**Figure 2A**; *Brokopp et al EHJ, 2011*). Moreover, we have found that FAP is also increased in neutrophils of human coronary thrombi involved in a STEMI heart attack, and is elevated as a soluble biomarker in ACS patients (**Figure 2B**). Furthermore, FAP was found to contribute to arterial occlusion in a murine carotid artery injury model, suggesting a contribution to obstructive thrombosis (**Figure 2C**).

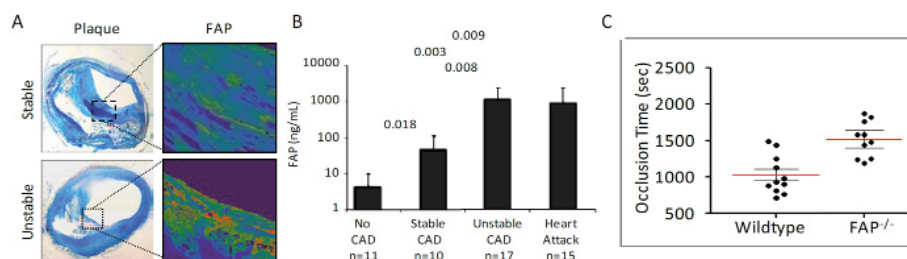
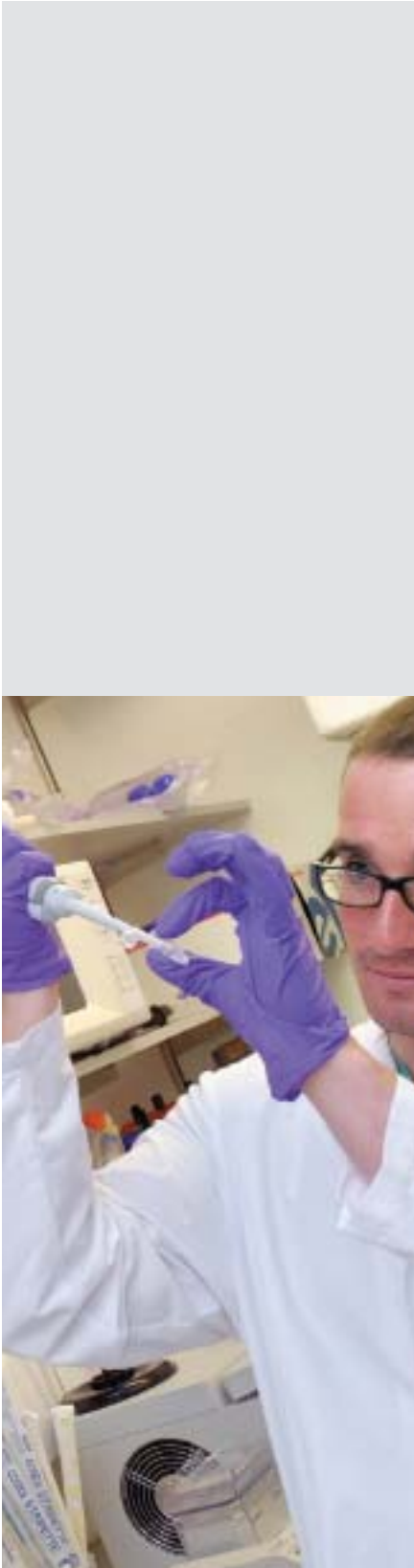


Figure 2: The contribution of FAP to infarction. **A.** FAP (in red) is increased in fibrous cap of unstable vs. stable coronary plaques in autopsy specimens from patients who have suffered a myocardial infarction. **B.** FAP blood plasma levels associate with the degree of acute coronary syndrome (Two-Way ANOVA). **C.** Carotid arteries of FAP^{-/-} mice occlude significantly slower than carotid arteries of wildtype mice when injured with a laser, suggesting that FAP contributes to thrombosis in-vivo ($p < 0.05$, Student's T-Test).



Future Directions

The knowledge and technologies resulting from this project are designed to contribute to:

1. a blood test with potential to identify patients at risk of a myocardial infarction, and
2. validation of FAP as an auspicious drug target for infarction prevention strategies.

Collaborations

- Department of Neurosurgery, UniversityHospital Zurich, Switzerland
- Department of Biomedical Engineering, Technical University Eindhoven, The Netherlands
- Center for Integrative Human Physiology, University of Zurich, Switzerland
- Department of Materials, Federal Institute of Technology, Zurich, Switzerland
- Department of Biochemistry, University of Zurich, Switzerland
- Department of Mathematics, Federal Institute of Technology, Zurich, Switzerland
- Department of Computational Science, Federal Institute of Technology, Zurich, Switzerland
- Department of Veterinary Surgery, MSRU Vetclinics, University of Zurich, Switzerland
- Department of Cardiology, UniversityHospital Zurich, Switzerland
- Department of Cardiac Surgery, Children's Hospital, Harvard Medical School, Boston, MA, USA
- Department of Pathology, Brigham and Women's Hospital, Harvard Medical School, Boston, MA, USA
- Massachusetts Institute of Technology (MIT), Cambridge, MA, USA
- Laboratory for Tissue Engineering, German Heart Centre, Berlin, Germany
- Department of Cardiology, Medical University of Vienna, Austria
- Institute of Nuclear Medicine, University of Debrecen, Hungary
- Laboratory for Transplantation Immunology, UniversityHospital Zurich, Switzerland
- Institute of Chemistry and Applied Biosciences, Federal Institute of Technology Zurich, Switzerland
- Institute of Anatomy, University of Bern, Switzerland
- Human Genetics Laboratory, Genetica AG, Zurich, Switzerland
- Department of Pathology, UniversityHospital Zurich, Switzerland
- Randall Division of Cell and Molecular Biophysics, King's College London, UK
- Fraunhofer Institute for Biomedical Engineering IBMT, St. Ingbert, Germany
- Embryonic Stem Cell Laboratory
- Department of Pathology and Immunology, Geneva University, Switzerland
- Experimental Cardiology Unit, Department of Medicine, University of Lausanne Medical School, Switzerland



Prof. Dr.
Volkmar Falk,
MD



Prof. Dr.
Jürg Grünenfelder,
MD



PD Dr.
Stefan Jacobs,
MD



Dr.
André Plass,
MD



Dr.
Michael Gessat,
Dipl. Ing.



Dr.
Simon Sündermann,
MD



Christoph Russ,
Dipl. Ing.



Raoul Hopf,
Dipl. Ing.



Thomas
Baumgartner
Study Coordination
and Administration

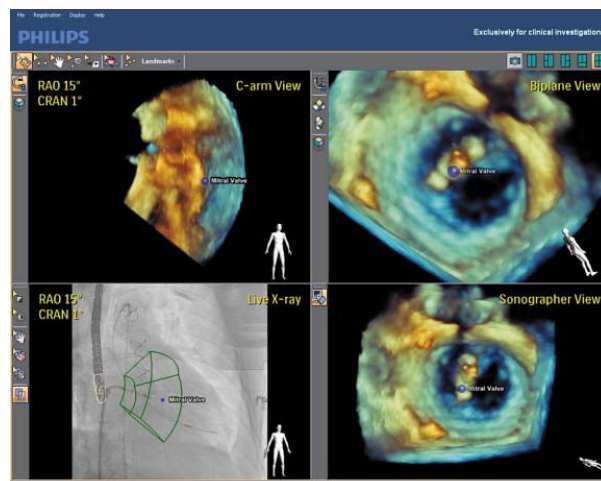
2.1.2. Hybrid and Minimally Invasive Technologies

2.1.2.1. The Advanced Role of Imaging in Transcatheter Cardiac Valve Treatment

M. Gessat, J. Grünenfelder

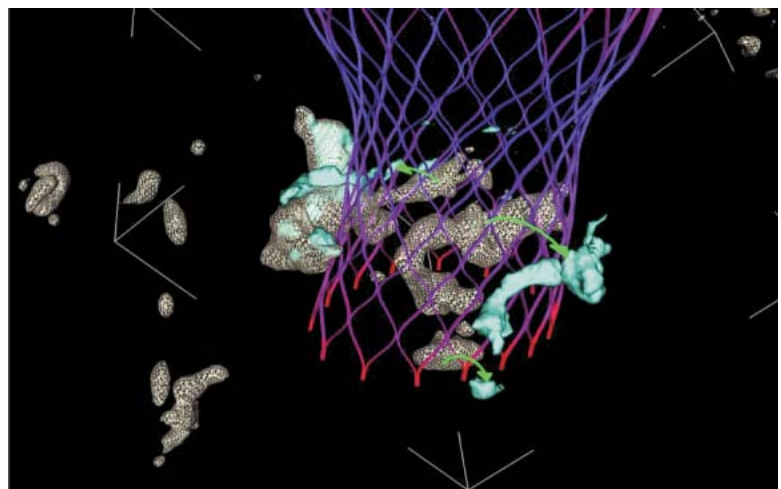
Transcatheter treatment of heart valve disease has been established as an important treatment option for both mitral and aortic valve dysfunction. In 2011, about 20% of the valve treatments at USZ were performed interventionally. Pre-, intra-, and postoperative imaging of the heart and the vascular pathway used for catheterization is of paramount importance in such treatments, since -unlike to open surgery- no direct visual assessment of the pathology or the treatment result is possible. Preoperatively, computer-tomography (CT), magnet resonance imaging (MRI) and transthoracic as well as transesophageal echocardiography are routinely used to assess cardiac function and valvular pathologies. Accurate treatment planning requires various quantitative analyses to be performed on these images which help to decide which surgical or interventional treatment option offers the optimal trade-off between outcome quality and perioperative risk. Our interdisciplinary team of cardiac surgeons, cardiologists, radiologists, and engineers is constantly developing and assessing new image analysis methods and tools to increase the reliability of clinical decisions.

High-quality intraoperative images and an optimal representation of the image content are key ingredients to a successful intraoperative catheter guidance. The hybrid operating room (Hybrid OR) opened in 2011 at USZ contains state-of-the-art imaging equipment and was designed to allow for an optimal integration of the different imaging modalities in order to help surgeons and interventionists in creating a virtual image of the beating heart, the catheters, and the devices at the tip of the catheters. Together with engineers at the ETH Zürich and Philips Healthcare in Best (Netherlands) we are exploring the capabilities offered by the new infrastructure and software available in this facility with respect to optimizing the way, transcatheter valve treatment is supported by intraoperative imaging and the combination of intraoperative images with preoperatively generated models.



Registration of angiography and TEE images to facilitate MitraClip placement in the Hybrid OR

Finally, imaging plays an important role in postoperative assessment of treatment outcome in clinical practice as well as in understanding the principles behind the onset of certain complications frequently seen after transcatheter valve treatment. In TAVI, for instance, we developed a method to measure the displacement and the loss of calcifications at the aortic root by comparing pre- and postoperative images. Released calcium clusters yield a high risk for embolic complications.



Calcium shift analysis after TAVI

2.1.2.2. Computational Models in Cardiac Surgery

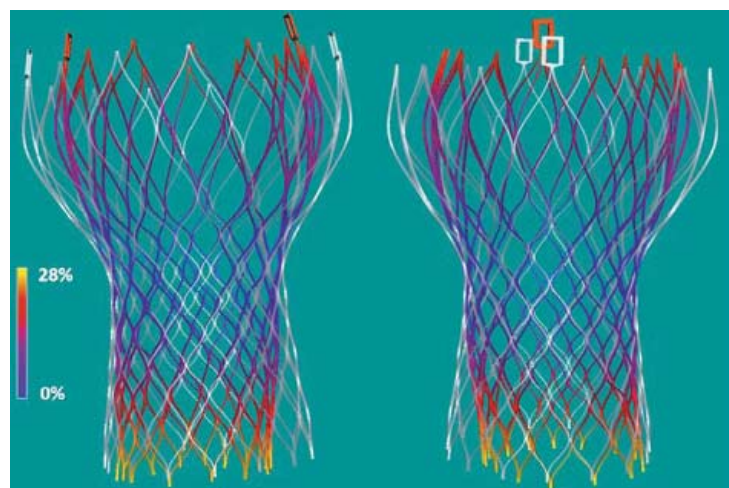
M. Gessat, S. Sündermann, St. Jacobs

Computational models play an increasingly important role in our attempts to understand the heart, to diagnose heart disease, and to plan and deliver treatment to the heart. Computational models are in-silico representations of our general understanding of the physics and biology behind heart function in a way which allow for analysis of physiology and pathology or for prediction of treatment outcomes. The Hybrid Laboratory for Cardiovascular Technologies, which was founded by the Division for Cardiovascular Surgery and the Department of Surgical Research in 2011, is determined to promote the clinical application of model-based techniques in the field of cardiovascular surgery. The laboratory works closely together with partner laboratories from technical disciplines at ETH Zürich and other institutions where research in biophysical modelling and simulation is pursued from a technical perspective. Our laboratory focusses on translating their results to clinical application by providing the infrastructure for pre-clinical in-vitro and in-vivo testing and clinical evaluation, but also by offering clinical input to help steering developments into a direction where they may solve real clinical problems.

On particularly important application of computational models in cardiac surgery is the determination of patient-specifically optimal treatment plans. The (structural as well as functional) complexity of the heart makes the estimation of treatment effects and side-effects a challenging task for a surgeon. In open heart surgery, where optimal access to all structures is possible, this challenge can often be mastered in situ by the operating surgeon. Minimally invasive surgery and catheter-based interventions limit the possibilities of the surgeon to directly assess the effects and side-effects of his actions in situ. Computational models generated from pre-operative medical images and other data sources are applied in treatment planning to create a-priory estimations of the effects a certain treatment has on the treated structure (e.g. a dysfunctional heart valve) and the surrounding structures (e.g. the remaining three heart valves or the coronary system).

Biomechanics of Transcatheter Aortic Valve Implantation

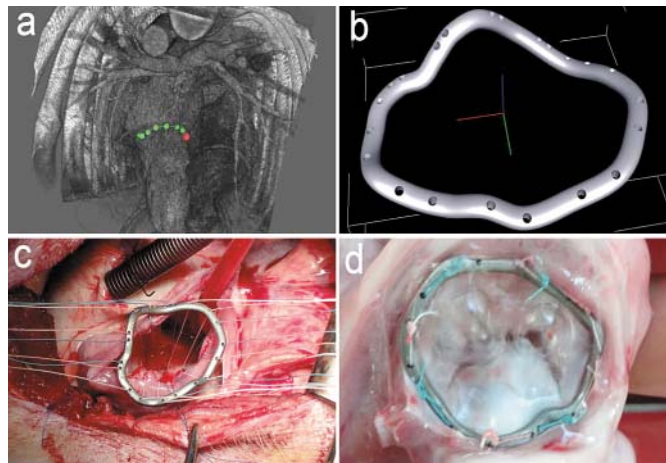
In transcatheter aortic valve implantation (TAVI), the mechanical strains induced by the stent onto the tissues in the aortic root and left ventricular outflow tract (LVOT), are important factors to the effectiveness of the treatment as well as to the onset of complications such as left ventricular arrhythmia. On the one hand, these strains keep the implant in place and provide the sealing between the implant's cuff and the native valve, preventing paravalvular leakage. On the other hand, exceeding mechanical stress on the tissue can lead to impairment of the conductive system or even to annular or LVOT ruptures. In 2011, we established the SNF project "Biomechanical Simulation of Transcatheter Aortic Valve Implantation" which is an interdisciplinary attempt between the USZ and two laboratories of the ETH Zürich. The aim of this project is to establish modelling techniques for predicting the outcome of TAVI. Since the project started in August 2011, we have established an automatic method for analysing the radial strain on a TAVI stent after implantation from follow-up CT images. This analysis allows us to study the postoperative scenario of real-life cases and correlating stent deformation with patient specific outcomes.



Radial strain on CoreValve stent after implantation

Patient-Specific Annuloplasty Rings

Mitral valve annuloplasty is a central component of most techniques in reconstructive mitral valve surgery. Thereby, a ring is implanted onto the mitral annulus with the aim to optimize leaflet co-aptation by modulating the shape and reducing the cross sectional area of the valves circumference. There is a number of off-the-shelf rings available provided for different underlying pathologies. Those rings partly respect the three dimensional shape of the mitral valve annulus, but do not account for the inter-individual variability. A number of studies has shown for different ring designs which were introduced between the 1970's and today, that, depending of the specific anatomy and pathology, the impact on valve competence and the onset of complications such as suture ruptures varies strongly with the ring shape. In 2011 we have successfully proven the concept of an approach to individually manufacture annuloplasty rings tailored to the specific anatomy of a subject as obtained from CT images. A computer program was developed for this purpose which computes a 3D model of an annuloplasty ring optimally fitting the mitral annulus. Based on this mode, a custom-made Titanium ring is created in a rapid manufacturing process called Selective Laser Melting. The processed Titanium alloy (Ti6Al4V) is biocompatible. In order to support ring alignment and suturing, predefined suturing holes are present on the rings. The proof of concept was performed in an animal trial, where rings were produced and successfully implanted in four porcine models.



a) Segmentation of the mitral annulus in CTA. b) 3D computer model of the specimen-specific mitral annuloplasty ring. c) Implantation of patient-specific mitral annuloplasty ring. Suturing holes are used to ensure alignment of annulus and ring. d) Explanted mitral valve complex after annuloplasty.

Collaborations:

- Philips Healthcare (Best, Netherlands)
- Swiss Federal Institute of Technology (ETH) Zurich, Computer Vision Laboratory (Zurich, Switzerland)
- Swiss Federal Institute of Technology (ETH) Zurich, Center for Mechanics (Zurich, Switzerland)
- University of Stanford, Living Matter Lab (Stanford, USA)
- University of Pavia, Structural Mechanics Department (Pavia, Italy)
- Hochschule Karlsruhe, Fakultät für Informatik (Karlsruhe, Germany)

2.1.3. Mechanical Circulatory Support



Dr.
Christoph Starck,
MD



Prof. Dr.
Volkmar Falk,
MD

Development of a new assist device concept

Ch. Starck

Assist devices play an important role in the treatment of heart failure. There are numerous different products on the market. All available devices have two major disadvantages: the need for anticoagulation and at least one connection from inside the body to the outside (power line, cannulas, etc.). Anticoagulation puts the patient at risk for bleeding or thromboembolic complications. The intra- to extracorporeal connection plays an important role for infectious complications.

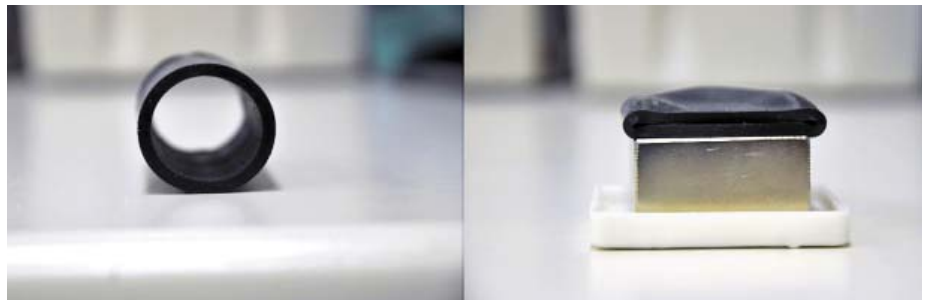
An ideal assist device would avoid the mentioned complications. The goal of this research project which is performed in collaboration with the Functional Materials Laboratory at ETH Zurich is to develop a new assist device concept based on a ferromagnetic polymer. By crosslinking metal nanoparticles into the polymer backbone of hydrogels (*Fuhrer et. al. Small 2009*) or silicones a magnetic field responsive polymer can be formed.

Combining the advantages of this material with the principle of extra-aortic counter pulsation led to the development of a ferromagnetic extra-aortic cuff. The driving force for its assist function will be generated by an external magnetic field which leads to contraction of the magnetic cuff on ECG triggered activation.

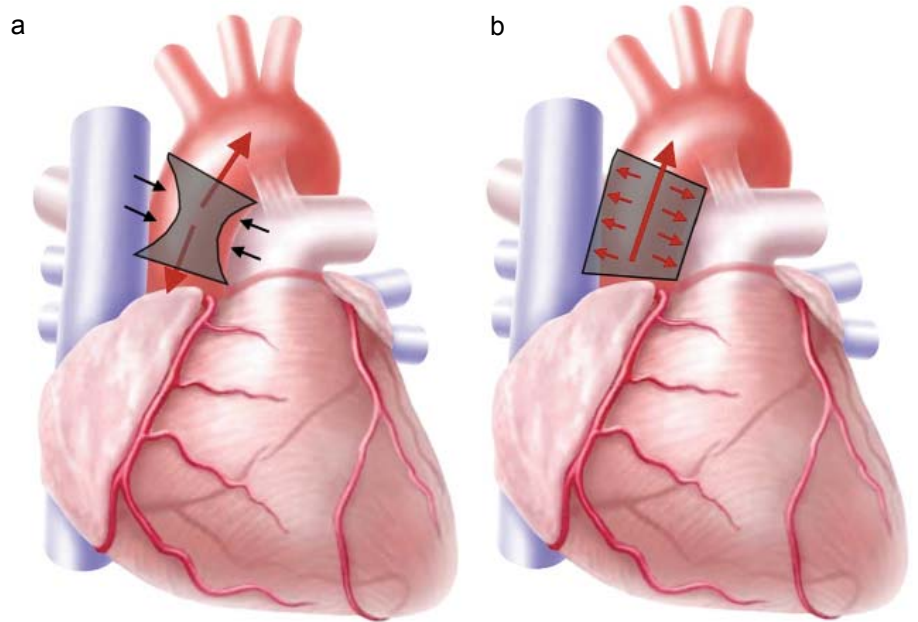
Potential advantages of this assist device concept are:

- Due to the missing contact of the device to the bloodstream anticoagulation is not needed.
- With regard to the magnetic principle of action there exists no intra- to extracorporeal connection.

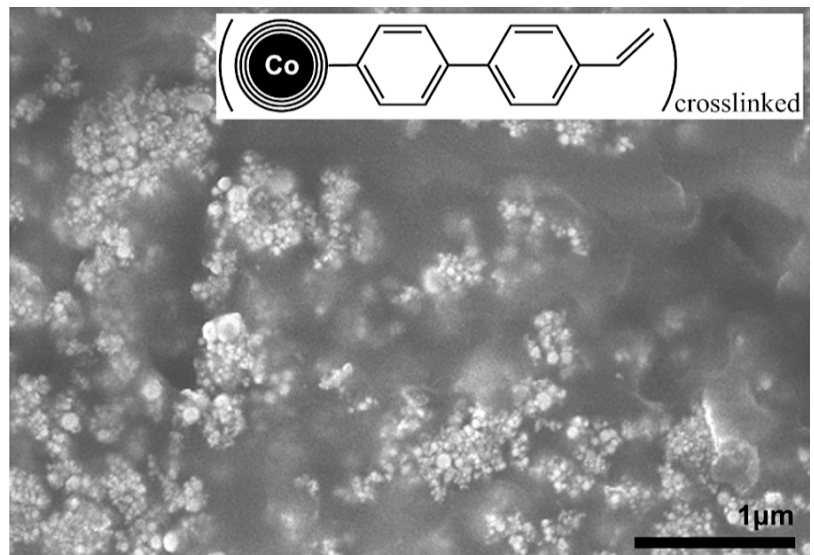
Furthermore this device can be applied in a patient-tailored manner because of the properties of the material which allows individual adaptation of the material to the anatomic conditions of the patient.



a. Ferromagnetic extraaortic silicone cuff in relaxed position. b. Cuff in contracted position in a magnetic field (1.2 T).



Schematic illustration of the principle of extra-aortic counterpulsation.
 a. During contraction in diastole coronary blood flow is increased.
 b. Due to relaxation at the beginning of systole cardiac afterload is decreased.

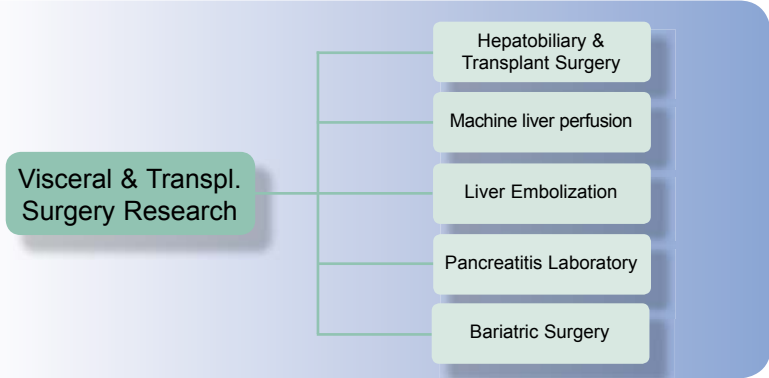
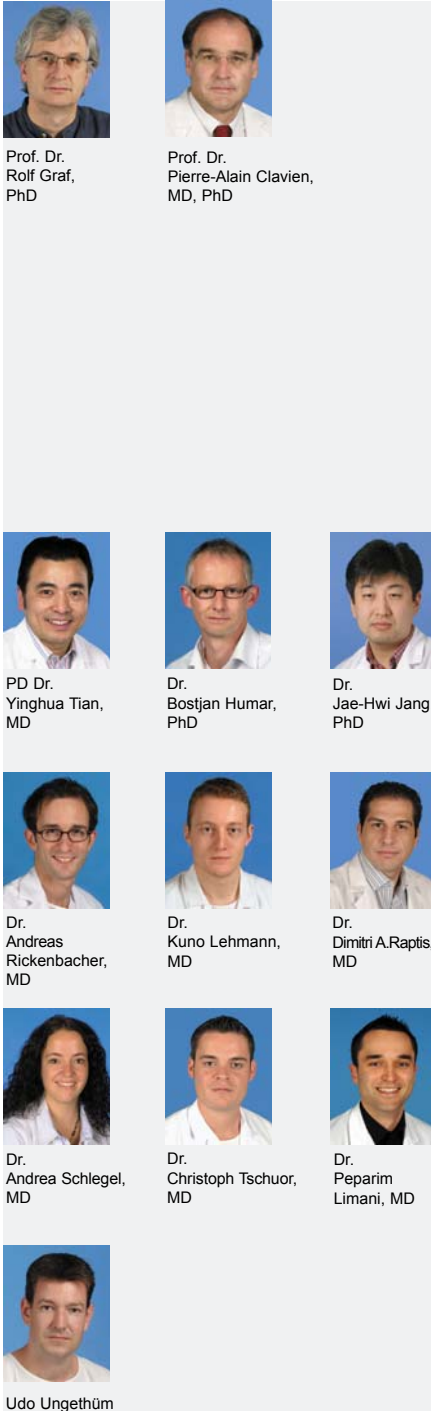


Scanning electron microscopy images of cross sections of hydrogels containing nanomagnets based on covalently crosslinked nanoparticles (Source: Fuhrer et. al.).

Collaborations:

- R. Fuhrer, Prof. W.J. Stark, Swiss Federal Institute of Technology (ETH) Zurich, Institute for Chemical and Bioengineering

2.2 Visceral & Transplant Surgery Research



2.2.1 Hepatobiliary & Transplant Surgery

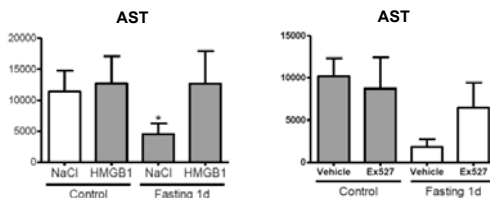
A. Rickenbacher, K. Lehmann, D. Raptis, A. Schlegel, C. Tschuor, P. Limani, U. Ungethüm, J.-H. Jang, Y. Tian, B. Humar, R. Graf, P.-A. Clavien

Strategies to protect from hepatic ischemia reperfusion injury

Hepatic surgery, particularly transplantation, exposes the liver to prolonged periods of ischemia. Subsequent reperfusion activates innate immunity leading to organ damage and hence an elevated risk of post-operative complications. Our lab has a strong interest in strategies that help to minimise ischemia reperfusion injury (IRI) and ultimately may improve the surgical outcome.

Fasting reduces serum Hmgb1 via a Sirt1-dependent mechanism to protect from IRI

Fasting is well-known to exert several beneficial health effects but is difficult to implement in a longer term (due to issues of compliance). Since short-term fasting is part of many standard pre-operative protocols, we assessed in mice the impact of a one-day fast on the levels of hepatic IRI. Fasted mice had markedly reduced levels of organ injury following ischemia and reperfusion (IR). Fasting-induced protection from IRI was due to diminished levels of serum Hmgb1, a key activator of innate immunity and a mediator of organ damage following reperfusion. Further studies revealed the Hmgb1 reduction is dependent on the histone deacetylase Sirt1, one of the central molecules implicated in the beneficial effects of fasting. These findings suggest short-term fasting may suppress innate immunity sufficiently to protect from IRI in a systemic way. Current experiments are aimed at clarifying the mechanisms through which Sirt1 acts on Hmgb1.

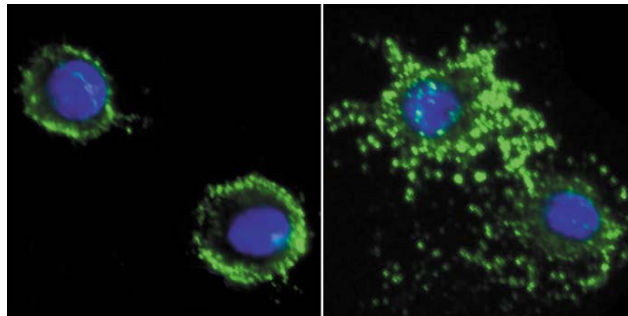


Right panel: Addition of exogenous Hmgb1 to unfasted mice has no effect on the levels of liver injury (AST) post reperfusion, whilst it aborts the protective effects of fasting.

Left panel: Treatment of fasted mice with an inhibitor of Sirt1 likewise abolishes the protection afforded by one day fasting.

ω 3-fatty acids protect from IRI through Gpr120-induced dampening of proinflammatory Kupffer cell activity

We have previously shown that ω 3-fatty acids protect steatotic liver from IRI through a reduction in the vasoconstrictive molecule thromboxane A₂. ω 3-fatty acids likewise protect lean liver from IRI, however through different, ill-defined mechanisms. Following bolus injection of concentrated ω 3-fatty acids, the fatty acid-mediated IRI protection was associated with a Kupffer cell-dependent suppression of inflammation. Within liver, these resident macrophages were the only cells to express the protein Gpr120, a recently identified receptor for unsaturated fatty acids. *In vitro* experiments demonstrated that ω 3-fatty acids activate Gpr120 to inhibit proinflammatory signalling through the Tak-NF κ B-Jnk axis. This pathway is also central for the activation of innate immunity following reperfusion (e.g. through Hmgb1), conceivably explaining the protective effects of ω 3-fatty acids. Further experiments are being performed to verify these findings *in vivo*. The establishment of Gpr120 as a mediator of the ω 3-fatty acid effects on liver may open the door to a new class of drugs for the prevention of ischemia-reperfusion injury.



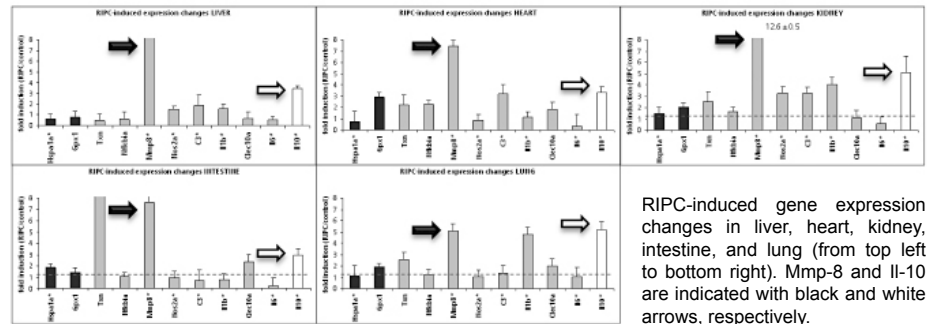
Left panel: in normal macrophages, expression of gpr120 (green) is limited to the membranes.

Right panel: upon stimulation with ω 3-fatty acids, gpr120 is internalized via vesicles to initiate anti-inflammatory signalling.

A central role for peripheral serotonin and Vegf in the mediation of IRI protection through remote ischemic preconditioning

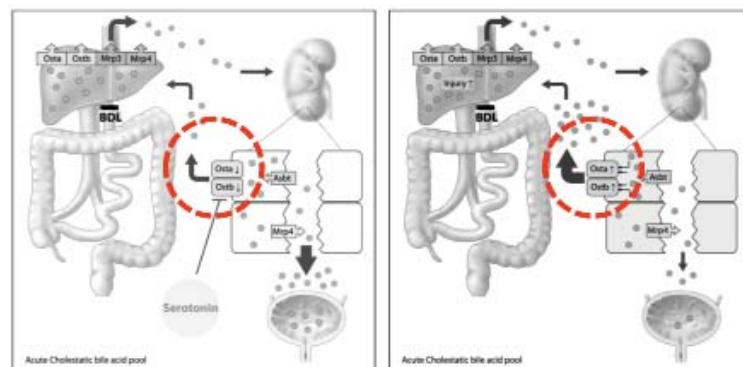
Remote ischemic preconditioning (RIPC, the repeated application of pressure to induce short periods of ischemia in limbs) has emerged as a promising tool to reduce organ injury due to IR. Whilst many molecules have been proposed to contribute to the effects of RIPC, the basic mechanism behind RIPC has not been identified so far. Using various mouse models, we could show that the application of limb pressure activates platelets in the underlying vessels, leading to the release of peripheral serotonin. The vasoactive molecule in turn appears to directly activate endothelial cells to secrete Vegf, which then is distributed via the blood to elicit a protective response in all organs that we examined. This response varied from organ to organ, however all organs reacted with an upregulation of Mmp-8 and Il-10, two molecules previously implicated in tissue protection. Indeed, inhibition of serotonin, Vegf, Mmp-8 or Il-10 blunted the protective effects of RIPC. Therefore, RIPC on limbs connects to distant organs via an axis that involves platelet activation, serotonin release and peripheral Vegf production leading to upregulation of tissue-protective molecules in the target organs.

Preliminary results suggest some decisive advantages of RIPC over existing measures such as direct ischemic preconditioning, including an efficacy also in old or fatty liver.



Endogenous peripheral serotonin acts to protect from cholestatic liver injury

In addition to the well-known actions of serotonin in the brain, the neurotransmitter has been shown to regulate a staggering variety of unrelated processes in the periphery. Cholestasis, the pathological accumulation of toxic bile salts in the liver, can have serious consequences and hence induces adaptive changes for its mitigation. Our experiments in *Tph1*^{-/-} mice (deficient in peripheral serotonin) have revealed the molecule also acts to protect from cholestatic liver injury. How serotonin would mediate such protection was unclear, but the increased levels of bile salts in the liver of *Tph1*^{-/-} mice suggested serotonin may promote hepatic bile salt disposal. Surprisingly, none of the hepatic transporters and enzymes involved in bile salt management were affected by serotonin deficiency. Instead, *Tph1*^{-/-} mice displayed an upregulation of the renal *Osta*-*Ost* β transporter, resulting in an increased transport of bile salts across the kidney into the blood, thus reducing the urinary excretion rate but leading to excess bile salts in circulation and liver. Serotonin supplementation of *Tph1*^{-/-} mice downregulated the renal *Ost* transporter, reduced peripheral/organ bile salt concentrations and normalised the levels of hepatic injury. Therefore, a novel physiological role of endogenous peripheral serotonin is to participate in the adaptive control of bile salts during cholestasis.



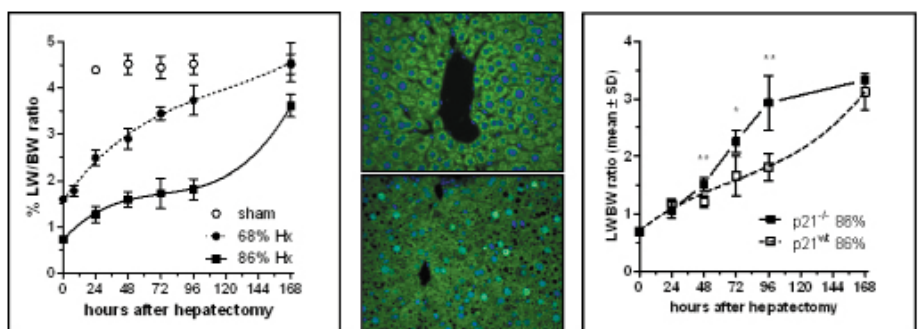
Schematic illustration of the bile flow during experimental cholestasis in wild type (left panel) and serotonin-deficient (right panel) mice. BDL = bile duct ligation to induce experimental cholestasis. The renal *Osta*-*Ost* β transporter is marked by a circle.

Liver regeneration and its promotion in the Small-for-Size Syndrome

The application of liver transplantation and resection is limited by the size of the graft or remnant, respectively. Below a certain threshold, the graft/remnant size will be too small to maintain vital function. As a consequence, the patient may develop the “Small-for-Size Syndrome” (SFSS), characterized by bilirubinemia, liver dysfunction, and a pronounced mortality. The mechanisms behind SFSS are unknown and accordingly, no treatment is available. We hence had a strong motivation in developing a valid mouse model of SFSS in order to (i) investigate its biological causes and to (ii) explore potential therapeutic approaches.

Experimental SFSS develops due to a p21-dependent delay in cell cycle progression during the regeneration of critically small liver remnants

Existing mouse models of critically small liver remnants are based on extended resection (eHx) and all feature excessive liver injury as well as mortality. However, due to the presence of confounding injury, these models are not suited to study the regenerative capacity of marginal remnants. We hence modified the surgical resection to better preserve critical structures and to minimize blood loss. Indeed, most mice survived and lacked any apparent injury following the modified eHx. Intriguingly, they also displayed classic SFSS symptoms, thus providing a model of experimental SFSS. When studying liver regeneration in experimental SFSS, we observed a marked delay in the regain of liver volume after resection. Surprisingly however, the initial regenerative response after modified eHx was stronger than after standard hepatectomy. In contrast, the progression through the cell cycle was markedly delayed and accompanied by persistent upregulation of the cell cycle inhibitor p21. Removal of p21 was sufficient to restore the regenerative capacity, and to improve liver function as well as survival, implicating p21 as a key mediator of experimental SFSS. Furthermore, we observed in our SFSS model a deficient induction of *Foxm1b*, a promoter of cell cycle progression and a repressor of p21.



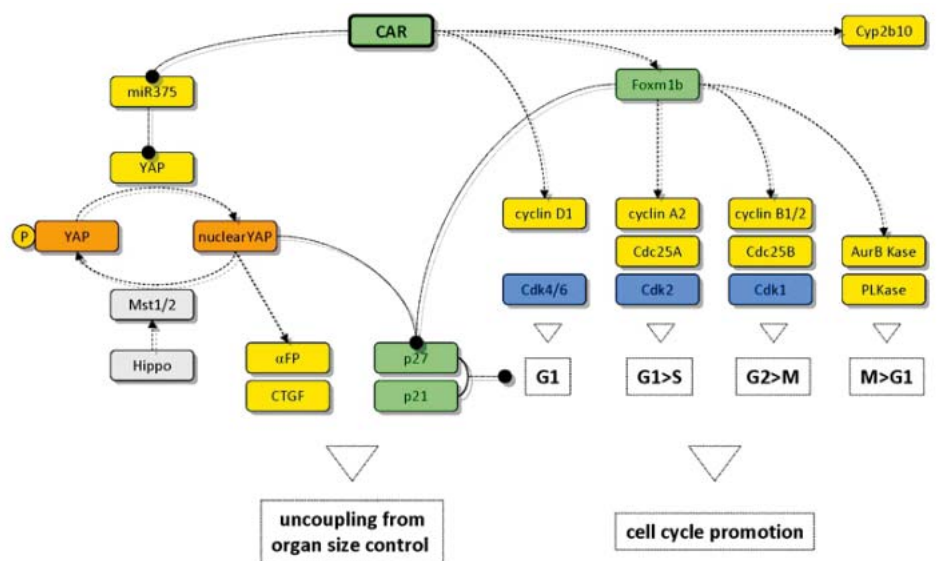
Left panel: deficient liver regeneration in mice after eHx (86%) compared to standard resection (68%).

Middle panel: upregulation of p21 (green) after eHx (bottom).

Right panel: improved regeneration after eHx in mice nil for p21.

Agonism of the constitutive androstane receptor overcomes the regenerative deficits in experimental SFSS

TCPOBOP is a chemical belonging to the peculiar class of primary mitogens, which induce liver growth without the need for resection or injury. TCPOBOP is an agonist of Car, a member of the nuclear receptor family with a liver-specific expression pattern. Notably, Car directly activates the transcription of *Foxm1b*, the p21 repressor suboptimally induced in our SFSS model. We hence tested whether Car agonism by TCPOBOP may rescue from SFSS. Indeed, TCPOBOP treatment at the time of eHx not only restored the impaired regeneration and survival, but also normalised bilirubinemia and liver function. More so, Car agonism was able to rescue from SFSS even when given 9h after surgery, indicating its potential therapeutic utility. These changes were paralleled by strong *Foxm1b* upregulation and repression of p21, emphasising the critical function of the cell cycle inhibitor in the development of SFSS. Further experiments are aimed at (i) describing the molecular network controlled by Car in SFSS and (ii) translating our findings into a humanised SFSS model.



Potential molecular pathways underlying the effects of Car agonism on experimental SFSS

Collaborations/Sponsors:

- Prof. Dr. Adriano Fontana, MD, Experimentelle Immunologie (UniversityHospital Zurich, Switzerland)
- Prof. Bruno Stieger, PhD, (UniversityHospital Zurich, Switzerland)
- Prof. Dr. Achim Weber, MD, Institut für Pathologie (UniversityHospital Zurich, Switzerland)

2.2.2 Machine Liver Perfusion



Dr.
Andrea Schlegel,
MD



Dr.
Olivier de Rougemont,
MD



Prof. Dr.
Philipp Dutkowski,
MD

Hypothermic oxygenated machine liver perfusion protects from endothelial injury in DCD pig livers via mitochondrial signaling

A. Schlegel, O. de Rougemont, JH. Jang, R. Graf, P.-A. Clavien, P. Dutkowski

Machine liver perfusion is a promising approach to protect livers exposed to warm ischemia. The mechanism of protection remains, however, unclear.

The aim of this study was to investigate the relation between mitochondrial electron transfer and liver ischemia reperfusion injury during and after machine liver perfusion.

Pig livers exposed to 60 minutes warm ischemia were either cold stored for 7 hours (WI + CS) or hypothermically perfused for 1 hour after 6 hours cold storage (HOPE). In both experimental groups pig livers were normothermically reperfused for 3 hours with diluted blood on an isolated perfusion system. Endothelial ultrastructure was analysed by electron microscopy before and after reperfusion. Mitochondrial respiration rate was measured during oxygenated machine perfusion by NADH metabolism and CO₂ production. Mitochondrial injury, apoptosis, and nuclear injury during reperfusion were measured by cytochrome c release, TUNEL staining, and HMGB1 release. Endothelial activation and inflammation were quantified by VWF and ICAM-1 staining after reperfusion.

In additional experiments, machine perfusion was performed using a deoxygenated perfusate (N₂) in the presence or absence of MPT pore inhibition by cyclosporine (HNOPE, HNOPE + cyclosporine). Livers without warm ischemia and minimal cold storage (1 h) served as controls.

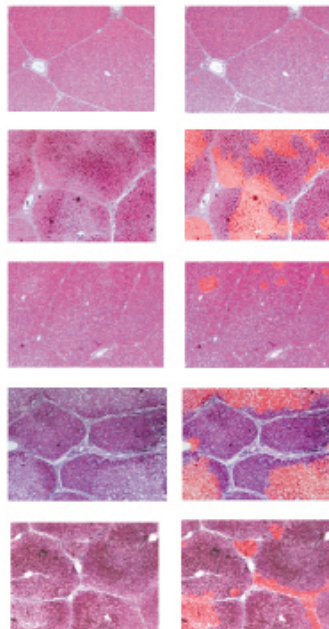
HOPE treatment led to a significant decrease in the respiration rate during one hour machine perfusion. Afterwards, mitochondrial injury in terms of cytochrome c release and TUNEL positive cells during reperfusion was significant less in HOPE treated pig livers as compared to untreated livers. Correspondingly, HMGB1 release decreased in HOPE treated DCD livers ($p < 0.001$). Finally, sinusoids were occluded with blood cells in untreated livers in contrast to machine perfused livers, along with significant endothelial injury in untreated livers in contrast to HOPE treated livers (30 % vs 5 % vWF activation, $p < 0.001$).

Importantly, machine perfusion with deoxygenated perfusate showed no protection from hepatocyte necrosis and HMGB1 release, while endothelial injury was also prevented by machine perfusion in the absence of perfusate oxygen (10 % vs 30 % vWF activation, $p < 0.001$). Vice versa, MPT pore inhibition during deoxygenated machine perfusion inhibited hepatocyte death and cytochrome c release, but led to endothelial injury.

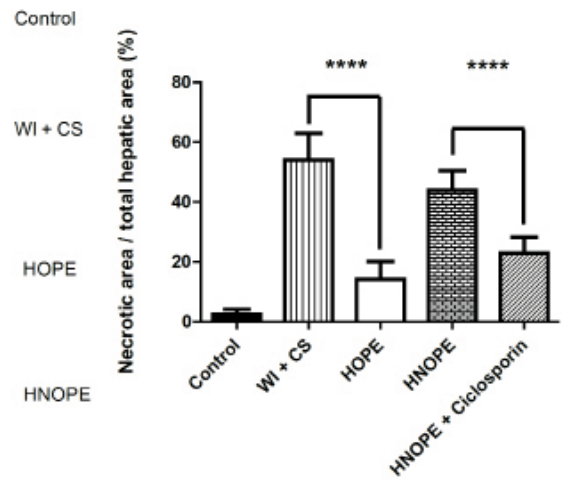
Small changes in mitochondrial electron flow before reperfusion are a precursor event for later tissue damage during hepatic ischemia reperfusion injury. Disruption of mitochondrial redox circuitry due to high electron flow rates during early reperfusion occurs in untreated DCD livers, and triggers a lethal sequence of mitochondrial, nucleic and inflammatory injury.

However, deactivation of the mitochondrial electron transfer in DCD livers before reperfusion is possible by one hour hypothermic oxygenated machine perfusion, resulting in less hepatocyte necrosis and less activation of platelets and leukocytes. In addition, DCD livers appear to be protected from endothelial injury by machine perfusion regardless of oxygenated or deoxygenated perfusate via mechanisms independent from mitochondrial injury.

Histology HE



Histology Necrosis



2.2.3 Reversible Portal Vein Embolization induces Liver Regeneration and Hypertrophy

E. Melloul, D.A. Raptis, T. Pfammatter, R. Graf, P.-A. Clavien, M. Lesurtel



Prof. Dr.
Mickael Lesurtel,
MD, PhD



Dr.
Emmanuel Melloul,
MD

Preoperative portal vein embolization (PVE) is widely used before major hepatectomy to induce hypertrophy of the future remnant liver. The goal is to prevent life threatening risk of postoperative liver failure. The selective occlusion of tributaries of the portal vein can be achieved either by permanent or absorbable agents, usually injected percutaneously. However, there is currently no general consensus regarding the ideal embolization agent to be used. Reversible PVE with absorbable agents would be safer in clinical situations where the embolized liver is not resected. The aims of this project are: (1) to develop a model of reversible PVE in mice, (2) to determine the recanalization time course following reversible PVE, (3) to confirm the efficacy of reversible PVE on hypertrophy of the non-embolized liver lobes, and (4) to observe the impact of PVE on embolized liver lobes.

Thirty BL6/male mice underwent 70% PVE using powdered absorbable material. Repeated portographies and angiographic magnetic resonance imaging (MRI) were carried out until complete recanalization of the embolized lobes (**Figure 1**). Liver regeneration was assessed by immunohistochemistry (PCNA, Ki-67, Ph-Histone 3 stainings). Liver lobe volumes were determined by small animal MRI volumetry. The preliminary results show that reversible PVE induced significant hepatocyte proliferation in the non-embolized lobes. Proximal and complete recanalization occurred 10 and 14 days after PVE, respectively. As showed in **Figure 2**, the hypertrophy ratio of the non-embolized lobes was $52 \pm 5.9\%$ at day 10 (i.e. 67% of total liver volume) and $75 \pm 19\%$ at day 14 (i.e. 63% of total liver volume). In contrast, the atrophy ratio of the embolized lobes was $55 \pm 1.4\%$ at day 10 (i.e. 33% of total liver volume) and $33 \pm 11\%$ at day 14 (i.e. 37% of total liver volume).

In conclusion, reversible PVE efficiently induces liver regeneration and hypertrophy in the non-embolized lobes. The next step will be to assess the functional and morphological recovery of the embolized liver lobes after recanalization.

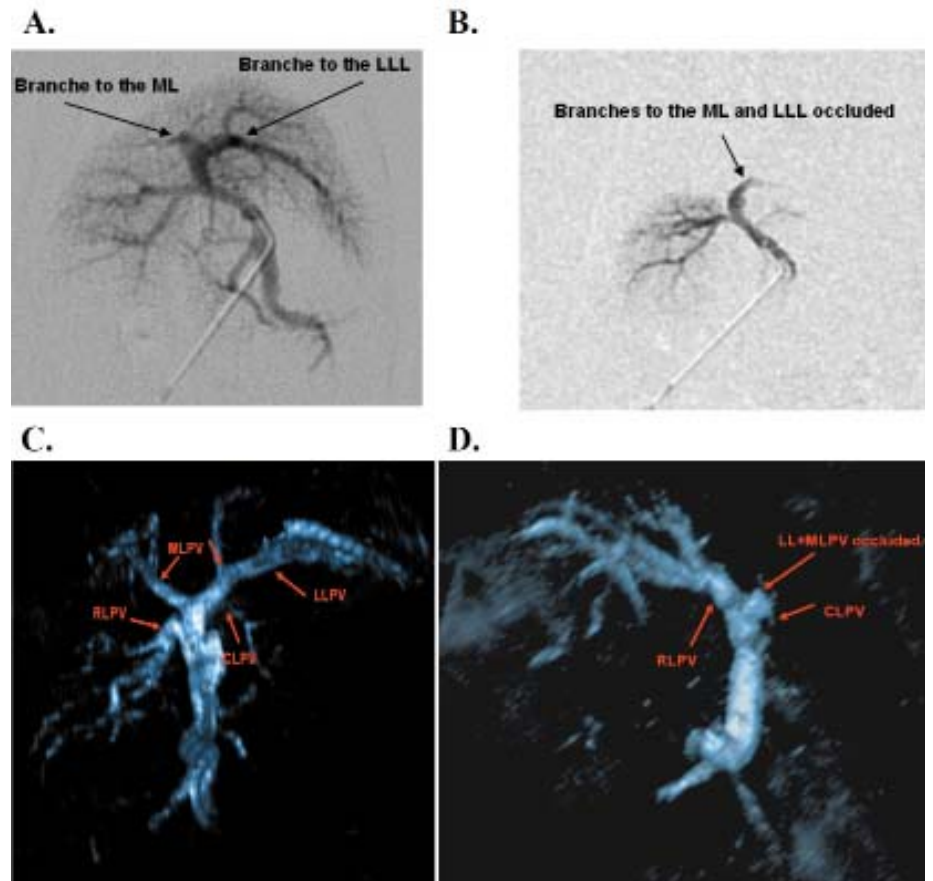


Figure 1: Portography (A, B) and MRI angiography (C, D) in a single mouse showing the portal vein anatomy before (A, C) and after (B, D) embolization. MLPV: medial lobe portal vein, RLPV: right lobe portal vein, CLPV: caudate lobe portal vein, LLPV: left lateral lobe portal vein.

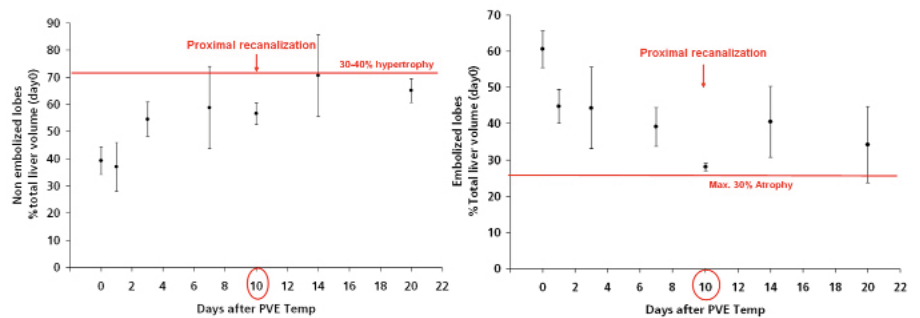


Figure 2: Kinetic of the non-embolized (A) and embolized lobes (B) after temporary embolization. Proximal and complete recanalization occur at day 10 and 14, respectively.

2.2.4 Pancreatitis Research Laboratory

S. Sonda, K. Grabliauskaite, E. Saponara, T. Reding Graf, M. Bain, R. Graf



Prof. Dr.
Rolf Graf, PhD



Dr.
Sabrina Sonda,
PhD



Dipl. phil. II
Theresia
Reding Graf



Kamile
Grabliauskaite,
M.Sc.



Martha Bain
Lab. Technician



Enrica Saponara,
M.Sc.

Pancreatitis is a debilitating inflammation of the pancreas, which in its severe form is associated with substantial morbidity and mortality. We are particularly interested in understanding the pathophysiology of the disease and the molecular mechanisms governing regeneration of the injured pancreas.

Main research projects:

- Role of serotonin in acinar cell secretion
- Role of serotonin in pancreatic regeneration
- Regulation of acinar to ductal metaplasia formation

Role of serotonin in acinar cell secretion

Alterations in acinar secretion are amongst the earlier events observed at the onset of pancreatitis and contribute to the tissue damage, indicating that acinar secretion plays a key role both in the physiological and pathological situations of the pancreas. The goal of our research was to investigate whether acinar secretion is modulated by serotonin, a well-known neurotransmitter with important biological functions outside the nervous system. Using TPH-1^{-/-} mice, which lack peripheral serotonin, and pharmacological modulators of serotonin-dependent pathways, we found that intracellular serotonin promotes zymogen secretion from acinar cells. Furthermore, we observed both *in vivo* and *in vitro* that serotonin modulates the re-localization of zymogen granules and the re-arrangement of actin cytoskeleton, critical processes for acinar secretion (**Figure 1**). In addition, absence of serotonin resulted in attenuated pro-inflammatory response after induction of pancreatitis, thus directly linking serotonin to the pathophysiology of the disease.

Role of serotonin in pancreatic regeneration

Pancreatic acinar cells are able to regenerate following tissue injury; however the extent of regeneration is limited. Serotonin is critical to promote cellular regeneration in the liver, an organ which shares the same developmental origin with the pancreas. Here we investigated whether serotonin modulates regeneration in the injured pancreas following pancreatitis. We found that reduced availability of serotonin delayed acinar cell proliferation at the G1/S-G2/M transition. This delay was characterized by accumulation of the early phase cyclins and delayed expression of growth factors in the pancreas of TPH-1^{-/-} mice. Importantly, progenitor cell markers, which are transiently expressed during acinar cell de-differentiation in the course of regeneration, failed to be up-regulated in absence of serotonin, suggesting that this molecule modulates the progression of cell cycle by regulating the de-differentiation program of pancreatic acinar cells.

Regulation of acinar to ductal metaplasia formation

One important feature observed during pancreatic regeneration is the transient de-differentiation of acinar cells to a duct-like phenotype, a process described as acinar-to-ductal metaplasia (ADM). ADM has been observed not only following pancreatitis, but also constitutes an important link to the

development of pancreatic ductal adenocarcinoma.

The molecular mechanisms that regulate ADM formation are still poorly defined and their characterization would further our knowledge of both pancreatic regeneration and the progression to malignant lesions. Here, we investigated molecular factors which can regulate ADM formation. In a model of pancreatitis-induced ADM, we found enhanced ADM formation in absence of the cyclin-dependent kinase inhibitor p21 without increased acinar cells proliferation, suggesting that p21 regulates ADM formation independently of the cell cycle. In a second model of oncogenic-induced ADM in transgenic K-Ras^{G12V} mice, we found that acinar cell-driven inflammation promoted the formation of ADM and neoplastic lesions PanIN, indicating that inflammation contributes to the development of pancreatic cancer (**Figure 2**).

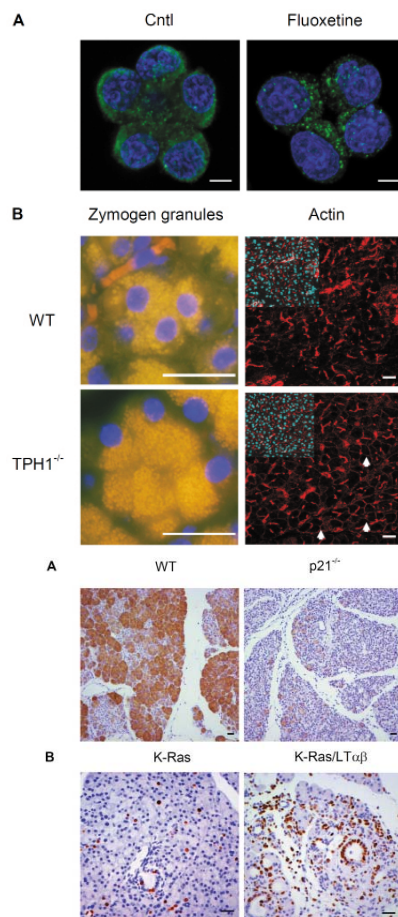


Figure 1: A. Reduction of intracellular serotonin levels with fluoxetine results in decreased amylase secretion and intracellular amylase accumulation. B. Re-localization of zymogen granules and actin dynamics are perturbed in TPH1^{-/-} mice. Arrows, baso-lateral staining. Nuclear DNA was stained with DAPI (blue). Scale bars: 10 μ m (A) and 50 μ m (B).

Figure 2: A. Increased ADM formation p21^{-/-} mice following one week of experimental pancreatitis. Amylase staining shows the loss of acinar tissue in metaplastic areas. B. Ectopic expression of lymphotoxin $\alpha\beta$ (LT $\alpha\beta$) in acinar cells accelerates the formation of PanIN in K-Ras^{G12V} mice. Ki67 staining shows the presence of highly proliferative lesions. Scale bars: 50 μ m.

Collaborations/Sponsors:

- Prof. Dr. Uwe Otten, MD, (University of Basel)
- Prof. Dr. Mathias Heikenwalder, PhD, (TUM Munich)
- Prof. Dr. Adrian. Hehl, MD, (University of Zurich)
- Prof. Dr. Achim Weber, MD, (UniversityHospital Zurich)
- Gitta Seleznik, MSc., (UniversityHospital Zurich)

2.2.5 Bariatric Surgery



Dr. Marco
Bueter,
MD, PhD



Dr.
Marc Schiesser,
MD, M.Sc.

Changes in food preferences and taste responses after Roux-en-Y Gastric Bypass

M. Bueter, K. Abegg, N. Theis, L. Asarian, M. Schiesser, CW. le Roux

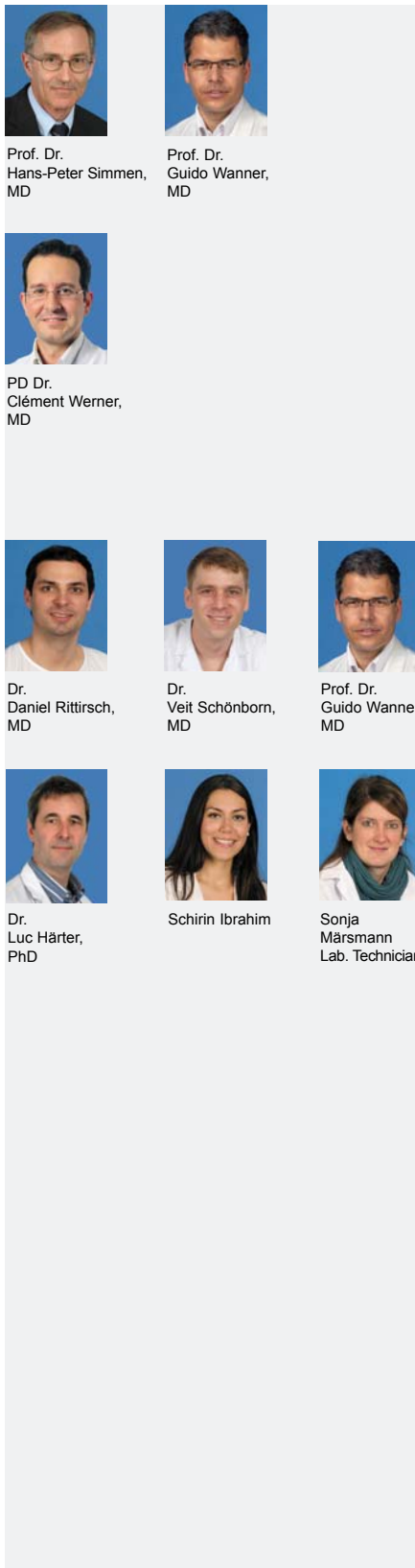
Roux-en-Y gastric bypass (RYGB) is considered by many to be the most effective treatment available for weight loss. Patients lose on average 25% of their body weight postoperatively for the long term and this is accompanied by an attenuation of appetite leading to decreased caloric intake. Importantly alterations in food selection have been reported. Indeed, there is some evidence that patients decrease their preference for and intake of high sweet and high fat foods and possibly increase their preference for fruits and vegetables. Moreover, there are many anecdotal reports from patients that they experience changes in taste sensibility. The role of taste in guiding food choices may promote a shift to a lower calorie density and potentially contribute to the weight loss. The literature reporting these effects, however, is mixed, with some studies finding changes and others not.

Against this background, we investigated fat preference after RYGB with a two bottle intake test in rats using a commercially available parenteral nutritional supplement, Intralipid[®], which is a soy-based triacylglycerol emulsion. After RYGB, rats did not show the increase in Intralipid consumption and preference that was seen in the sham-operated controls. We also investigated the ingestive behavior of rats, after RYGB, in response to sucrose. We found that sucrose consumption and preference was markedly decreased after RYGB compared with sham-operated rats when given a two-bottle intake test. This is consistent with observations in the literature that patients display decreased preference for sweets after RYGB. We therefore further examined whether changes in sugar preference after RYGB might have a sensory origin by constructing psychometric sensitivity functions for sucrose before and after surgery in humans. Our results indicated that sucrose detection thresholds (i.e., EC50) significantly decreased by 30% (i.e., increased sensitivity). These results confirm that direct measures of taste function are feasible in humans and that RYGB has complex effects engaging a variety of systems.

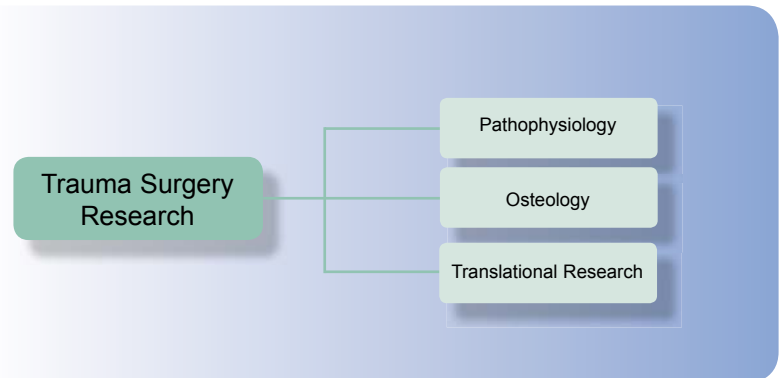
Our strategy to studying RYGB-induced taste and feeding-related motivational changes has been to take a coordinated approach to the problem by conducting parallel experiments in both our established rat model and in the established human bariatric clinical research program. Disparities in the literature could be more effectively resolved by complementing the collection of existing findings with more direct measures of target behaviors in humans that can also be applied to animal model. We have found this approach to be both feasible and instructive, offering great potential to provide a conceptual conduit between human and animal model research, the latter in which mechanism can be aggressively pursued.

Collaborations

- Prof. Dr. vet. Thomas Lutz (Institute of Veterinary Physiology, University of Zurich)
- Prof. Dr. Alan Spector, MD, (Florida State University, USA)



2.3 Trauma Surgery Research



2.3.1 Pathophysiology

Interleukin-33 and its soluble receptor ST2 – novel players in trauma-induced systemic inflammation

D. Rittirsch, V. Schoenborn, S. Märsmann, S. Ibrahim, L. Härter, GA. Wanner

The inflammatory response following trauma is highly complex and still inadequately understood. Endogenous danger signals (alarmins) play a crucial role in the initiation of the immune response. The novel cytokine interleukin-33 (IL-33) is known to act as an alarmin in various inflammatory conditions. Its soluble decoy receptor sST2 functions as an endogenous antagonist of IL-33. Aim of the study was to investigate the role of IL-33 and sST2 in systemic inflammation in patients with multiple injury.

Plasma from patients with multiple injury (n=32; injury severity score ISS \geq 17 points) was analyzed for IL-33 and sST2 at different time points (day 0, d1, d2, d3, d5, d7, d10, d14, d21) after trauma. In addition, plasma samples from trauma patients were analyzed for IL-33 by western blot analysis in order to identify the isoforms of IL-33 that are released after trauma.

Levels of IL-33 were increased in 13 of 32 patients, peaking at d0 (**Figure 1A**). While high levels of IL-33 (d0-d5) were associated with thoracic injury, there were no further correlations of IL-33 with the injury pattern. Western blot analysis revealed that full-length IL-33 (30kDa) is systemically released after trauma, but not other forms, such as caspase-cleaved IL-33 (**Figure 2**). All patients showed elevated levels of sST2 with a sharp peak on d1 (**Figure 1B**). Increased sST2 levels on d2, d3 and d5 were associated with the development of sepsis. The sST2 concentrations on d2 correlated with the ISS. Patients with abdominal or thoracic trauma showed significantly elevated levels of sST2 (d1, d2). In patients who underwent emergency splenectomy due to severe injury to the spleen, levels of sST2 were suppressed or even non-detectable during the later course (d5-d21) as compared to patients in whom the spleen was uninjured. Taken together, the results of the present study demonstrate for the first time that IL-33 and its soluble receptor sST2 are released during the early phase after multi-system injury.

While IL-33 peaks within hours after trauma, the kinetics of sST2 release differ, with peak levels on d1. Plasma concentrations of sST2 during the early phase reflect the severity of injury and are associated with the development of sepsis. Intriguingly, the data suggest that the spleen may represent a source for sST2 and/or may be involved in the regulation of sST2 release during the late phase after trauma.

In conclusion, these findings suggest that IL-33 and sST2 contribute to systemic inflammation after trauma. While the mechanisms of action and release of IL-33 are not entirely clear at present, sST2 represents a promising marker for assessment of the inflammatory response after trauma and for identification of patients at risk for complications.

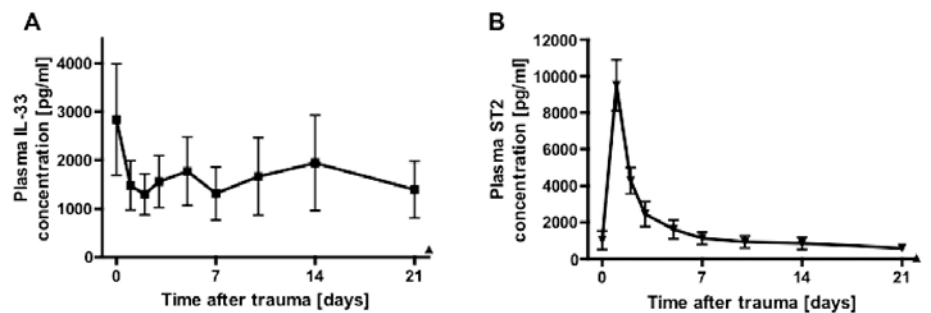


Figure 1. Time course (day 0 - 21) of interleukin-33 (IL-33) (A) and soluble ST2 (sST2) (B) in plasma from patients with multiple injury (injury severity score ISS \geq 17 points, n=32). \blacktriangle = healthy volunteers (n=10).

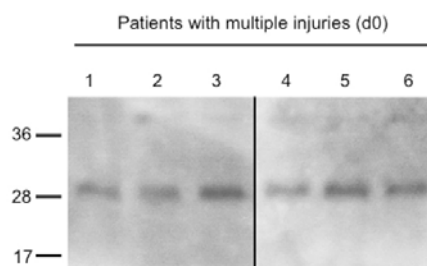


Figure 2. Western blot analysis of plasma from 6 patients with severe trauma (day 0) who showed elevated levels of IL-33 as assessed by ELISA.

Circulating receptors of the complement activation product C5a in sepsis

D. Rittirsch, S. Ibrahim, S. Märsmann, GA. Wanner

The first line of defense of innate immunity comprises the complement system and neutrophils (PMN), both of which play a crucial role in the pathogenesis of sepsis. The systemic inflammatory response in experimental and clinical sepsis is characterized by a loss over control mechanisms of complement activation. Especially excessive generation of the anaphylatoxin C5a and its interaction with PMN is considered to be crucial in the pathogenesis of sepsis since, at high concentrations, C5a exerts multiple harmful effects, eventually leading to the development of multi-organ dysfunction and impairment of cellular innate immune defenses.

Increased C5a plasma levels and decreased binding capacity of its receptor, C5aR, on PMN during sepsis are associated with a poor outcome. In this study, we sought to investigate the “fate” of C5aR during sepsis *in vitro* and *in vivo*.

Experimental sepsis was induced by cecal ligation and puncture (CLP) in rodents. In addition, isolated PMN or macrophages were incubated with C5a and/or lipopolysaccharides (LPS) *in vitro*. Soluble C5aR was detected in serum, supernatant fluids, or cell lysates, respectively, using flow cytometry, western blotting and ELISA techniques.

In experimental sepsis in rodents, increased levels of circulating C5aR were found in serum as a function of time, peaking between 12 and 24 hours after sepsis induction (**Figure 1A**). The soluble receptors were released as membrane vesicles predominantly from PMN, as indicated by co-expression with CD66e, a specific marker for PMN-derived membrane vesicles (**Figure 1B**). In contrast, macrophages did not appear to be a source for C5aR-containing membrane vesicles (**Figure 1C**). When isolated human PMN were incubated with recombinant C5a *in vitro*, C5aR, but not the second C5a receptor, C5L2, was released into supernatant fluids. Likewise, peritoneal PMN (but not macrophages) from wildtype (WT) mice released C5aR when exposed to C5a or lipopolysaccharides (LPS) *in vitro*. In the absence of C5L2, *in vitro* incubation of peritoneal PMN with C5a and/or LPS resulted in increased levels of C5aR in supernatants as compared to PMN from WT mice. In accord, in C5L2 knockout mice the signal for C5aR in serum was more intense during sepsis than in septic WT mice.

In summary, these findings indicate that C5aR-containing membrane vesicles are secreted from PMN during sepsis, which might represent a mechanism for the internal clearance of excessively generated C5a. Moreover, the concentration of circulating C5aR in serum correlates with the outcome.

Due to its kinetics of release during sepsis C5aR-membrane vesicles might represent a potential biomarker for sepsis and systemic inflammation. Studies to develop a clinical test for quantification of circulating C5aR and verification of its usability as a diagnostic marker in sepsis and systemic inflammation are currently under way.

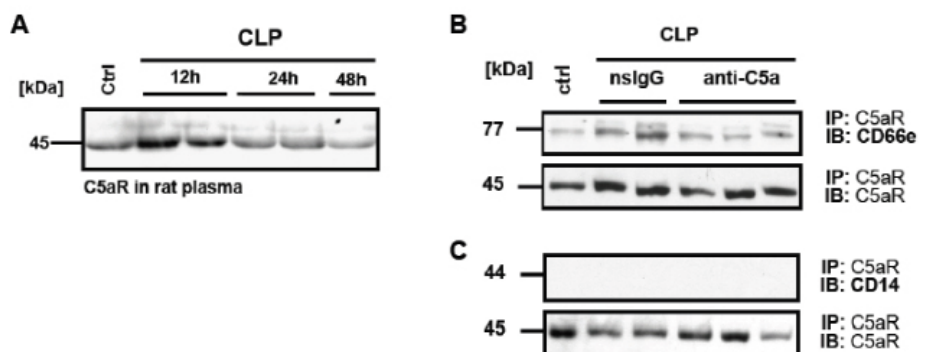


Figure 1. Detection of circulating C5aR during experimental sepsis in rodents. **(A)** Western blot analysis of rat serum for C5aR at indicated time points after cecal ligation and puncture (CLP). Co-expression of C5aR with CD66e **(B)**, known as a marker for membrane vesicles from neutrophils (PMN), or CD14 **(C)**, a marker for macrophage-derived membrane vesicles, in serum samples from septic mice treated with anti-C5a or non-specific IgG (nslgG). Ctrl = control.

2.3.2 Osteology



Dr.
Dieter Cadosch,
MD



Prof. Dr.
Hans-Peter Simmen,
MD

“The Right Implant for the Right Patient”

D. Cadosch, L. Filgueira, H-P. Simmen

In the case of patients developing complaints (such as pain, warmth, effusion and reduced range of motion) following metal implant surgery, and after having excluded common elicitors including a low-grade infection, the diagnosis of metal hypersensitivity should be made. This T-lymphocytes dominated reaction is believed to be a delayed-type hypersensitivity (DTH) predominantly to nickel, chromium, cobalt, and molybdenum ions. Additionally, we demonstrated the strong and specific antigenicity of Titanium 4+ ions suggesting the involvement of the adaptive immune system in the response towards titanium implants. Evidence supporting a causative association between metal ions released by biocorrosion and DTH reactions arises from (i) histology consistent with a DTH reaction, (ii) positive patch test reactions, (iii) positive *in vitro* test (e.g. lymphocyte transformation test, LTT) and (iiii) complete recovery following removal of the offending metals. A variety of factors and cytokines derived from the activated immune system, including the receptor activator of NF- κ B ligand (RANK-L) and TNF- α , directly and indirectly promote osteoclast activity and inhibit osteoblast function (**Figure1**).

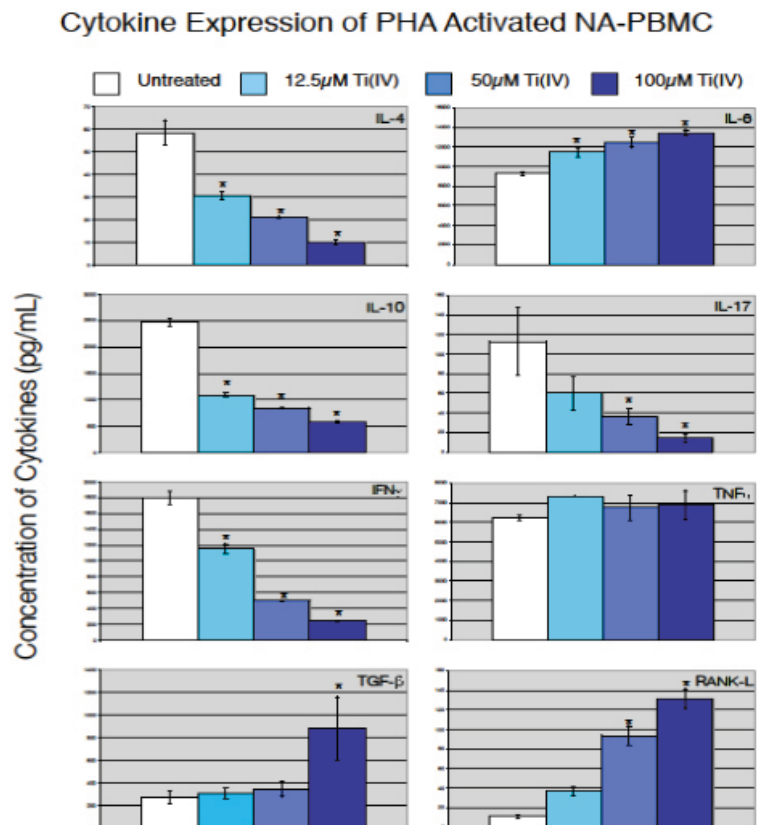


Figure 1: Histogram showing the expression levels of different cytokines in the super-natant of PHA-activated non-adherent peripheral blood mononuclear cells (NA-PBMC) after 24 hours of incubation with different Titanium (IV) concentrations (0, 12.5, 50 and 100 μ M).

Therefore it is reasonable to assume that the activation of the immune system may also lead to an enhanced osteolysis (enhanced osteoclastogenesis), a decreased osteointegration and potentially implant loosening (aseptic loosening). However, even when a specific immune response is absent, metal ions may enhance recruitment, functional maturation of osteoclast precursors towards mature osteoclasts and osteoclastic activity through direct and indirect mechanisms without the involvement of the immune system (**Figure 2**).

Titanium 4+ ions directly induce monocytic proliferation and subsequent terminal differentiation toward mature and functional osteoclasts. Cobalt 2+ and chromium 3+ stimulate human mononuclear cell to release TNF- α .

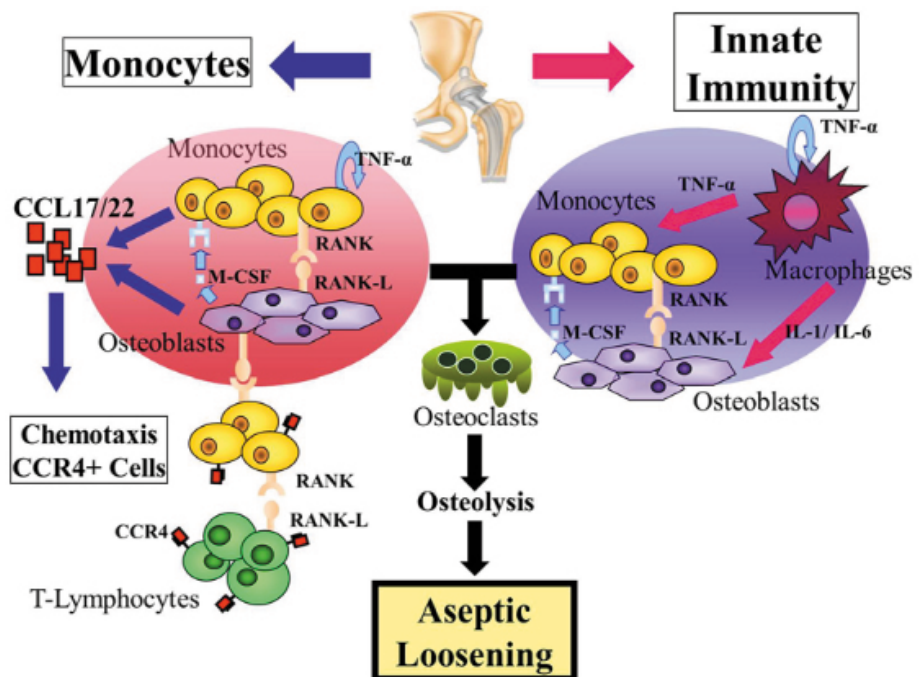


Figure 2: Postulated pathways involving metal ions leading to an increased osteolysis without a specific immune response.

Based on these results we developed an *in vitro* test based on the proliferation rates of peripheral blood mononuclear cells (PBMCs) incubated with metal ions (**Figure 3**). It is our opinion that this reflects more accurately the complexity of the pathophysiological mechanisms leading to complications after implant surgery, and takes into consideration the potential direct effects of metal ions on the monocytic cell fraction. Our preliminary data are promising and indicate a strong correlation between the *in vitro* test results and the clinical course. In patients with moderate to high proliferation rates of PBMCs exposed to metal ions the sensitizing metals should be avoided.

Ongoing studies aim to improve the test and confirm our preliminary results. Additionally, we are currently investigating the gene expression of immune and bone cells exposed to metal ions.

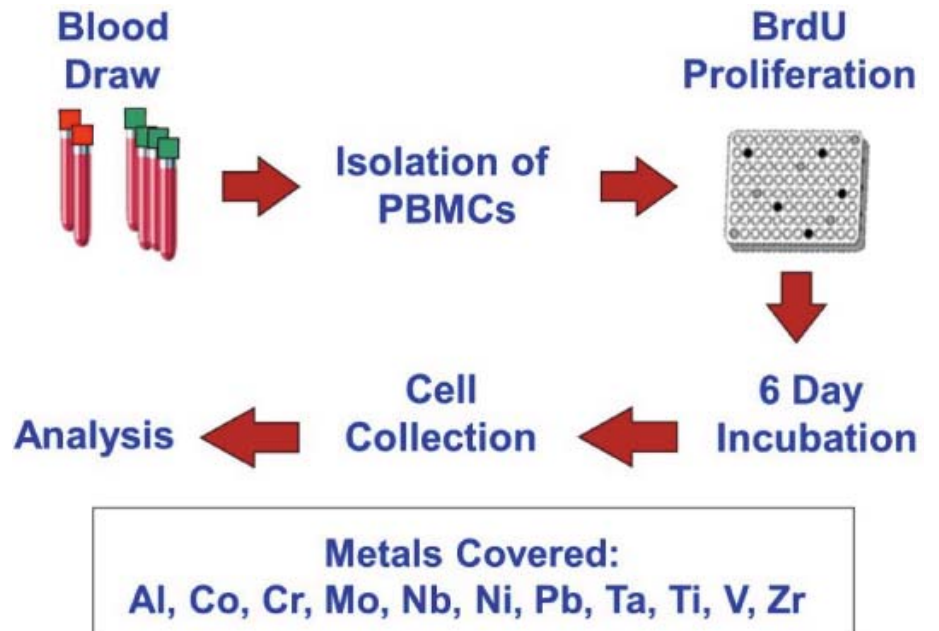
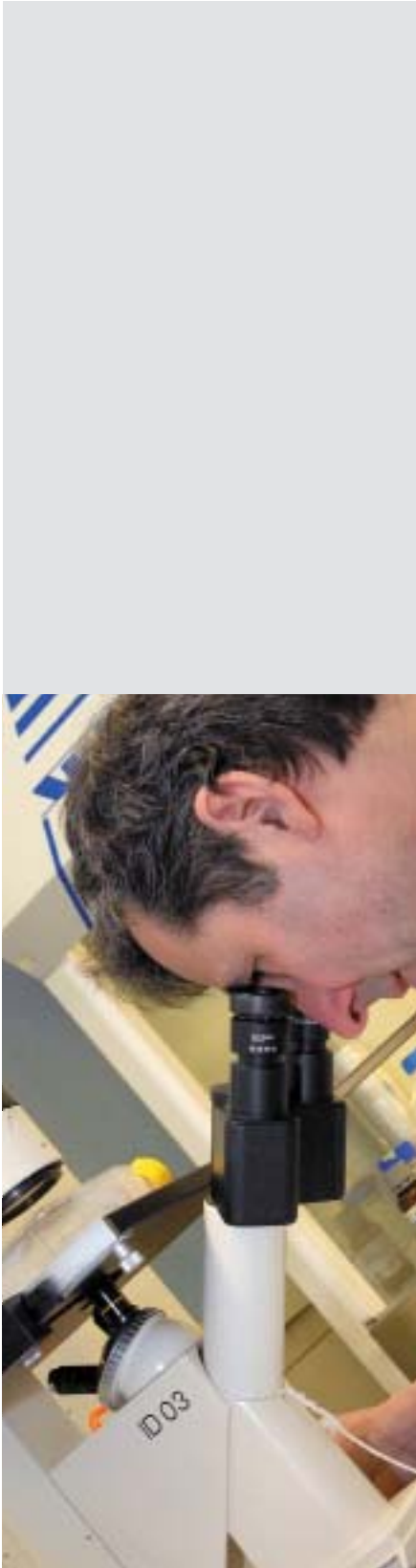


Figure 3: "Metal hypersensitivity" tested by measuring the proliferation rates of peripheral blood mononuclear cells (PBMCs) incubated with metal ions. Data are expressed as the percentage of absorbance relative to untreated (spontaneous proliferation of PBMCs in standard medium without sensitizing metal) controls. An increased cell proliferation of >35% is defined as high, >25% as moderate and >15% as low "metal hypersensitivity". In patients with moderate to high "metal hypersensitivity" the sensitizing metals should be avoided.



Dr.
Stefan
Zimmermann, MD



PD Dr.
Clément Werner,
MD



Dr.
Carola Würgler-
Hauri, MD



Dr.
Max Joseph
Scheyerer, MD



Dr.
Dieter Cadosch,
MD



Dr.
Shuping Gao,
MD



Sonja Hemmi
Lab. Technician



Dr.
Thorsten
Jentzsch, MD



Dr.
Pavel Zwolak,
MD



Flora Nicholls
Dipl. nat.

Heterotopic Ossification: New Approaches continued

SJ. Zimmermann, CC. Würgler-Hauri, M. Scheyerer, H-P. Simmen, CML. Werner

Heterotopic ossification (HO) is a problem widely encountered by orthopaedic and trauma surgeons.

HO may result in joint contracture, pain or even spasticity and neurovascular compression leading to significant disability.

Patients with high-grade ossification frequently necessitate reoperation thereby largely increasing the costs of treatment. This is why effective means of prevention are of great importance in a clinical setting.

The exact mechanism leading to HO formation is not completely understood. During bone growth, development and remodeling, angiogenesis as well as osteogenesis are closely associated processes, sharing some essential mediators ultimately leading to the replacement of avascular cartilaginous tissue by highly vascularized bone. Hypoxic stress induces angiogenic stimulators, which trigger stem cells to differentiate to chondrocytes with subsequent heterotopic bone formation.

Current standard treatment modalities with NSAIDs and or radiation therapy may not completely prevent HO from forming and have drawbacks such as impaired fracture healing and implant ingrowth.

Our goal was to find a more effective and easily applicable therapeutical approach differing from the pre-existing attempts to prevent the occurrence of heterotopic ossification. We believe that hypoxia is the core in the development of heterotopic ossification and therefore investigated the effect of inhibited neovascularization of hypoxic tissue on the development of heterotopic ossification.

A standardized animal model to produce heterotopic ossification by means of an Achilles tenotomy was chosen. All mice underwent bilateral Achilles tendon tenotomy and were divided into two groups: Control (n=10) and Imatinib (n=10). The control group underwent Achilles tenotomy only. The Imatinib group received Imatinib Mesylate orally by gavage once a day for a duration of six weeks.

After 10 weeks the limbs were harvested and Micro CT was performed. Heterotopic bone volume was then identified in 3d images and statistical analysis was performed.

Heterotopic bone developed in 83% of all cases with bone volumes ranging from 0.005-7.429mm³. The mean bone volume in the control group was 0.976mm³ and 0.221mm³ in the Imatinib. A significant reduction could be found in the Imatinib group by 85% (p=0.028). However, the dosing still needs to be optimized.

An important point for consideration is the effect of Imatinib on fracture healing, since the ultimate goal is to find a substance, which not only prevents HO development, but does not impede fracture healing. Future studies involving standardized fracture models will aim to investigate this matter.



Figure 1: Typical location and component arrangement Imatinib group (this image 0.253mm^3 /mean volume 0.221mm^3)

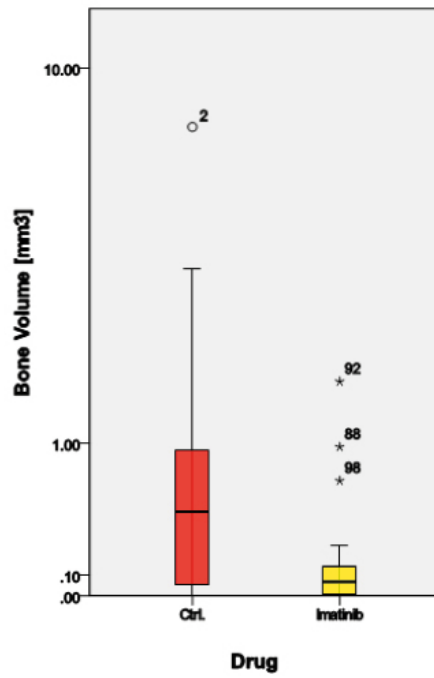


Figure 2: Typical location and component arrangement for Control group (cumulative volume of this limb 1.032mm^3 /mean volume $=0.974\text{mm}^3$)

2.3.3 Translational Research



Dr. Veit Schoenborn, MD



Prof. Dr. Guido Wanner, MD



Dr. Daniel Rittirsch, MD



Dr. Elisabeth Wanner, MD



Dr. Sebastian Günkel, MD



Dr. Max Joseph Scheyerer, MD



Dr. Kai Sprengel, MD



Dr. Stefan Zimmermann, MD



Dr. Helmut Wegmann, MD



Dr. Michael Zürcher, MD



Dr. Marius König, MD



Dr. Stefanie Hirsiger, MD

Transcriptomic profiling in severely injured patients, opening the “window of opportunity”

V. Schoenborn, D. Rittirsch, A. Billeter, S. Günkel, L. Härter, M. Bauer, G. Wanner

Most Patients with multiple trauma develop post-traumatic complications such as a systemic inflammatory response syndrome (SIRS), sepsis and severe multiple organ dysfunction or -failure (MODS/MOF). It results in a general inflammatory immune response representing an overall inflammatory reaction of the immune system which is depending of the injury severity, the initial treatment and of the individual constitution and genetic background. This cytokine storm involves many factors which have been well described e.g. IL-1, IL-6, IL-8, TNF, CRP and PCT. However, the complex pathophysiology and the mechanisms of their changes and their relation to each other during the inflammatory response are still poorly understood.

Treatment of patients with severe trauma is performed by two alternative approaches: In “Early total care” all necessary operations are carried out immediately, whereas in the “Damage control” concept the patient is stabilized first and final operations, which might present a second stress/trauma for the patient, are performed some days (4-7 days) later during the “window of opportunity”. However up to date no exact measures exist to precisely define this time point, which should be in an optimal way during a balanced phase of inflammatory and anti-inflammatory reaction.

Since RNA is the biological messenger of protein acting for the above described mediators, gene expression analysis has the potential for clarification of similar mechanisms after severe trauma. Whole-genome gene expression analysis offers the possibility to provide an insight into the complex mechanisms of the pro- and anti-inflammatory reaction followed by trauma.

A combined cross-sectional and longitudinal approach enables us to test the hypothesis that multiplexed transcriptomic signatures could allow an earlier diagnosis and risk prediction of SIRS related sepsis with better sensitivity and specificity, and would enable to define more precisely the optimal time point for the “window of opportunity”.

More than 100 severely injured patients with an injury severity score (ISS) >16 are enrolled in the study until today. As pilot study a whole-genome gene expression profiling was performed in 12 Patients on 9 different time points using the Illumina HumanHT-12 Expression BeadChip platform that contains more than 47,000 probes. By means of the gene expression profiling it was possible to distinguish between the SIRS and the Sepsis patients, in some cases up to 24 hours before clinical symptoms appeared.

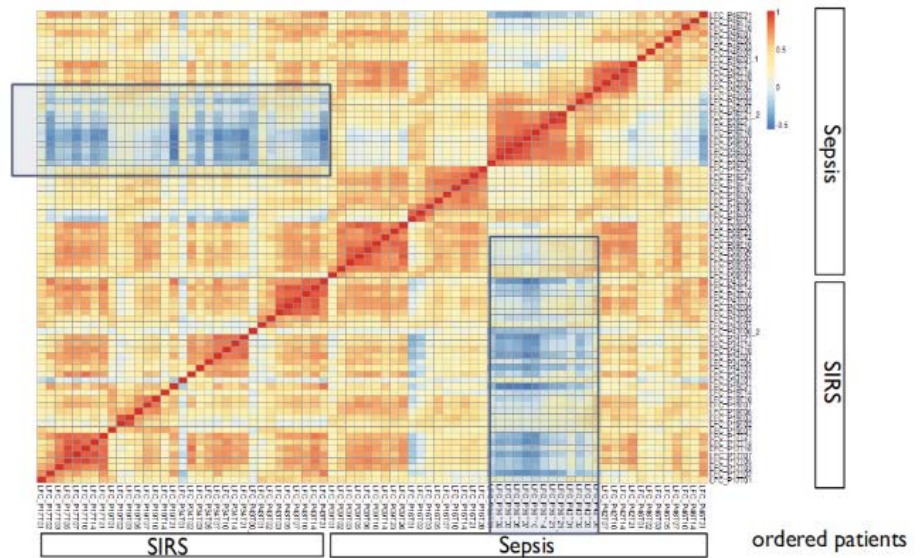


Figure 1: Heat map with patterns of different expressed genes, which shows remarkable differences between sepsis and SIRS patients

Furthermore, preliminary studies using gene expression pathway analysis software showed promising results in regard to changes in expression of not yet described genes which might play an important role in the inflammatory response (**Figure 2**).

We are confident that expanding our pilot study with the analysis of the remaining patients will allow us to identify a set of genes suitable for the development of a robust diagnostic test.

Data will be validated by quantitative RT-PCR and will then be used for designing a QRT-PCR based clinical diagnostic test for sepsis/SIRS for the evaluation of our patients. We believe that by monitoring the changes of expression of the identified genes it will be possible to perform an earlier diagnosis and risk prediction of SIRS related sepsis with better sensitivity and specificity. This will finally enable us to define the optimal time point to open the “window of opportunity” at peak time.

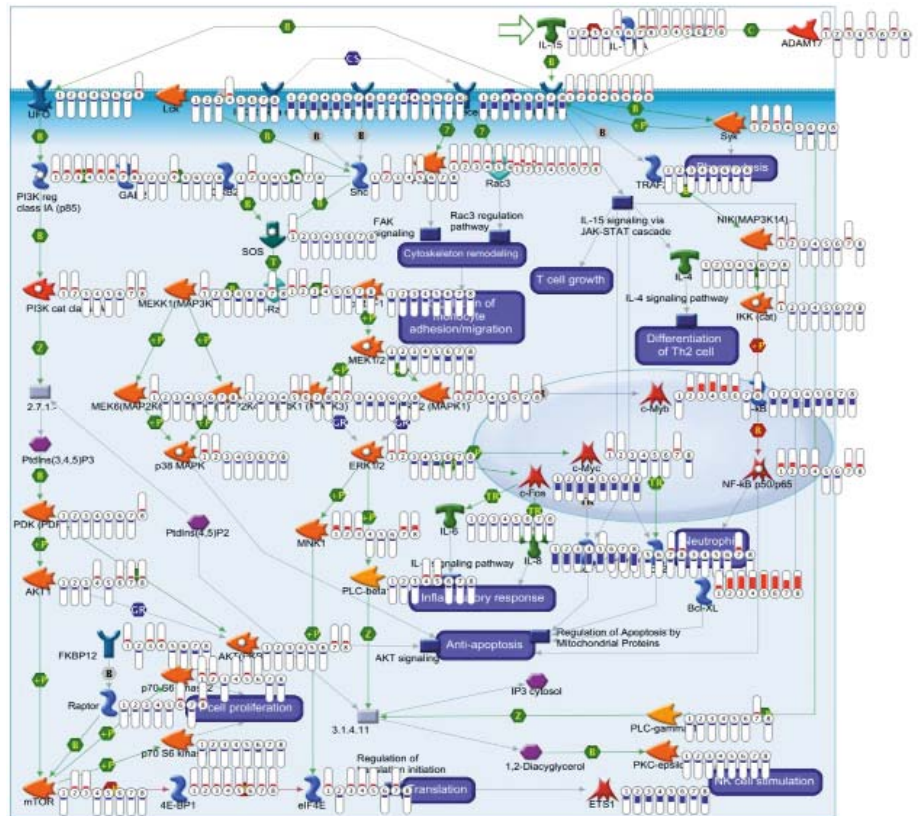


Figure 2: Representative expression changes of a patient in the IL-15 mediated inflammatory response pathway at different time points upon injury.

Collaborations:

- Clinical Trials Center, UniversityHospital Zurich
- Institute for Biomechanics, Federal Institute of Technology, Zurich
- Orthopedic Research Laboratory, Biomechanics, University Hospital Balgrist, Zurich
- Beatrice Beck-Schimmer, Institute of Anesthesiology, UniversityHospital Zurich
- Michael Bauer, Institute for Anesthesiology and Intensive Care Medicine, University Hospital Jena, Germany
- Markus Huber-Lang, Dept. of Traumatology, Hand-, Plastic and Reconstructive Surgery, University Hospital Ulm, Germany
- Michael Flierl, Philip Stahel, Dept. of Orthopedic Surgery, Denver Health Medical Center, USA
- Peter A. Ward, Dept. of Pathology, University of Michigan Medical School Ann Arbor, USA
- Alessio Fasano, Mucosal Biology Research Center, University of Maryland, Baltimore, USA

2.4 Cooperation Trauma Surgery and Plastic, Hand & Reconstructive Surgery Research



PD Dr.
Maurizio Calcagni,
MD



Prof. Dr.
Guido Wanner,
MD



Dr.
Johanna
Buschmann, PhD



Dr.
Shuping Gao,
PhD



PD Dr.
Nicole Lindenblatt,
MD



Dr.
Luc Härter,
PhD



Manfred Welti,
Laboratory
Technician



Sonja Hemmi,
Laboratory
Technician

Isolation, Cultivation and Differentiation of Human Adipose-Derived Stem Cells (ADSC)

S. Gao, J. Buschmann, L. Härter, S. Hemmi, M. Welti, H-P. Simmen, P. Giovanoli, M. Calcagni, G. Wanner

Human fat tissue has been found to be a suitable and easy source for mesenchymal stem cells, called adipose-derived stem cells (ADSC). Under proper cultivation conditions, these cells can be differentiated into human osteoblasts, endothelial cells, chondrocytes and adipocytes. In our joint project: "Development of Bone Grafts using adipose-derived stem cells and different scaffolds" (Clin. Trials Gov ID NCT01218945) we plan to develop an autologous bone graft from human ADSC and scaffold material for patients with critical size bone defects.

Up to now, we have collected fat tissue from 20 different donors and have isolated the ADSC. In most cases the fat was excised surgically (n=18), in two cases fat-tissue was obtained by liposuction method. The amount of isolated fat tissue varied (mean: 124.8g ± 60g), as well as the amount of isolated cells (mean 51.9x10⁶ ± 39.5x10⁶) resulting in a mean number of 4.3x10⁵ ± 3.4x10⁵ isolated ADSC per 100g fat tissue. Primary isolates from fat tissue were cultivated and expanded in D-MEM (high Glucose) medium until confluency, passaged and analysed by immunohistochemical and flowcytometric (FACS) methods. Isolated cells exhibited a typical ADSC morphology (**Figure 1**) and surface protein expression profile (**Table 1**). Growth rates over seven days varied between 1.5 and 6.4 times (mean 3.0±1.1 times) resulting in doubling times from 1.1 to 4.6 days (n=7). After passage 3 to 7 ADSC were subjected to differentiation into osteoblasts or endothelial cells by transferring cells into suitable differentiation medium. Over the following two to five weeks the cells were monitored for surface protein expression and RNA expression (**Figure 2**). Osteoblasts were also subjected to AlizarinRed and von Kossa staining. These differentiated cells are then used for cultivation on different scaffolds (see following report).

Table 1 Surface antigen expression on ADSC and ADSC-derived cells

Antigen	ADSC	Osteoblasts	Endothelial cells
CD13	+	-	-
CD44	+	-	++
CD105	+	-	-
CD31	-	+	+
Osteocalcin	-	+	-
RUNX-2	-	+	-

Expression of surface antigen was measured in FACS after staining with PE-labeled antibodies. + = high expression, ++ increased expression, - reduced expression

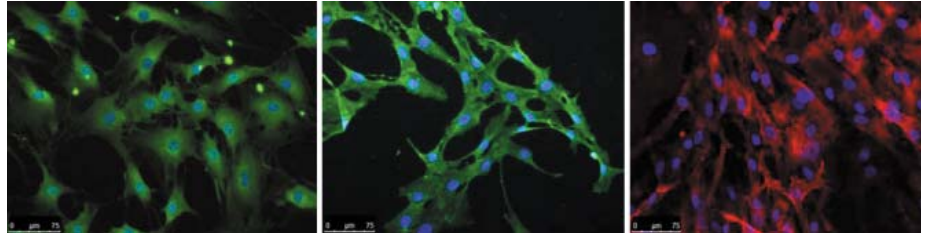


Figure 1. Immunohistochemical staining of ADSC differentiated into Osteoblasts or endothelial cells.

ADSC were cultured in respective Osteoblast-differentiation medium for 4week and then stained with antibodies against Osteocalcin-FITC (left) or RUNX-2-FITC (middle). ADSC cultured in endothelial differentiation medium were stained with antibody against CD31-PE (right).

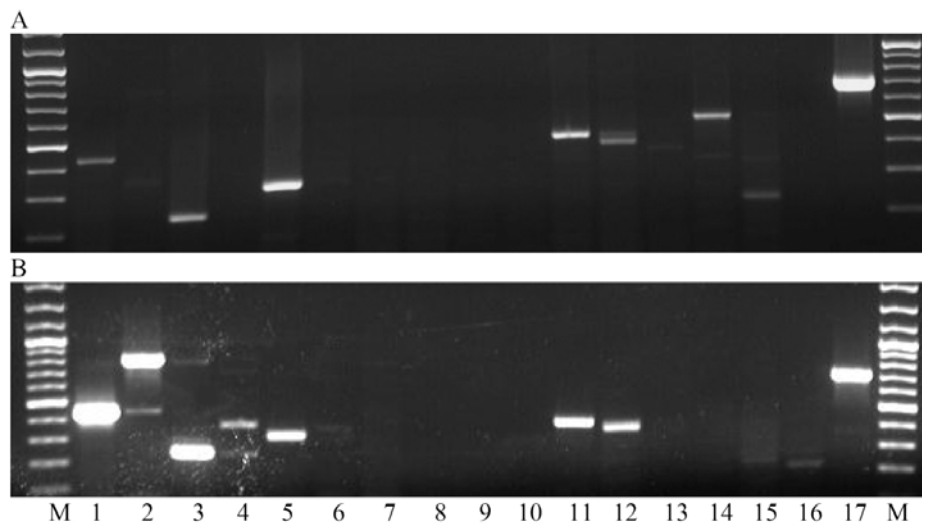


Figure 2. RNA expression in ADSC cultured with or without endothelial differentiation medium

ADSC cultured in endothelial differentiation medium (**A**), or in normal medium (**B**) were harvested and RNA isolated. PCR was performed with respective primers 1 vWF, 2 VEGFR-1, 3 Cadherin, 4 Flt4, 5 Jagged1, 6 EphrinB2, 7 EphB4, 8 Notch-1, 9 Dll4, 10 Ang2, 11 Tie2, 12 CD31, 13 Ang1, 14 Vezrf1, 15 Flk1, 16 Flt1, 17 gapdh. Positive bands were visualized after electrophoresis on a 1% agarose gel stained with ethidium bromide under UV light. 100Bp ladder are shown on the left and right side.

Tissue Engineered Bone Grafts Based on Biomimetic Nanocomposite PLGA/Amorphous Calcium Phosphate Scaffold and Human Adipose-Derived Stem Cells

J. Buschmann, L. Härter, S. Gao, S. Hemmi, M. Welti, N. Hild, O. Schneider, W. Stark, N. Lindenblatt, C. Werner, G. Wanner, M. Calcagni

Bone tissue engineering is a field of research where improvements are still welcome up to date. In this study, we used a recently developed electrospun scaffold consisting of PLGA and amorphous calcium phosphate nanoparticles (PLGA/aCaP) (Schneider *et al.* 2008; Hild *et al.* 2011) and seeded it with human Adipose-derived stem cells (ADSC) (for isolation of ADSC, see previous report). In **Figure 1A**, a SEM image of the scaffold material is shown and the aCaP nanoparticles can be seen well. The nanoparticles without PLGA can be seen in a TEM image (**Figure 1B**). Within one week, human ADSC grew well into the scaffold material and were evenly distributed over the whole scaffold width of $\sim 200 \mu\text{m}$ as shown in a histological cross-section stained with Hemalaun-Sudan in **Figure 1C**. Human ADSC exposed to $50 \mu\text{g mL}^{-1}$ of cultivation medium have an osteocalcin expression after one week of cultivation, as depicted in **Figure 1D** (immunohistochemistry).

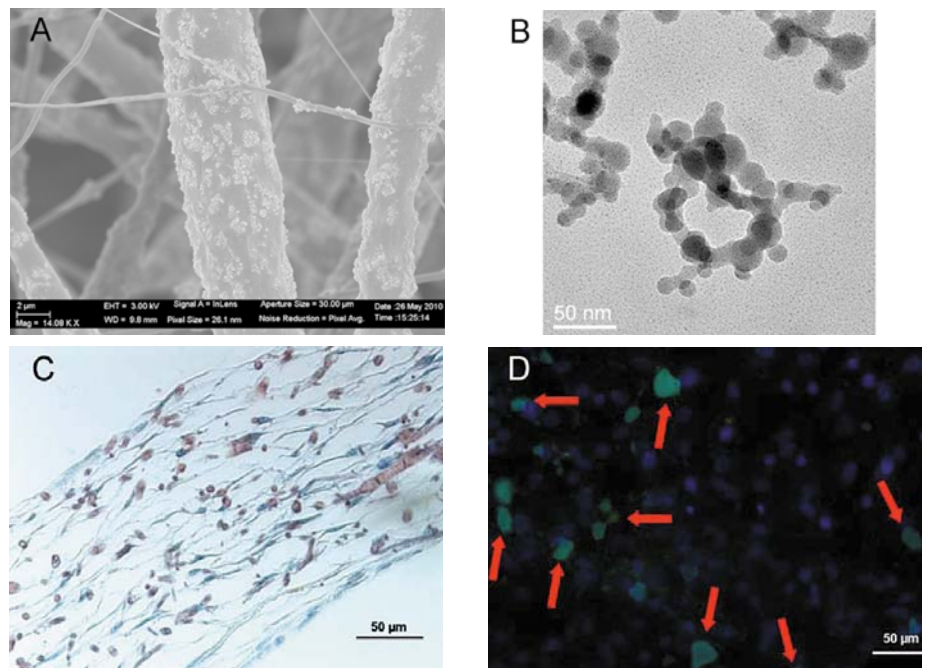


Figure 1: SEM image of PLGA/aCaP scaffold material (A) and TEM image of aCaP nanoparticles (B). In (C) the PLGA/aCaP material is stained red and the human ADSC are shown in blue (Hemalaun-Sudan staining). Immunohistochemistry of osteocalcin expression is shown in (D). Red arrows depict osteocalcin (green) and the cell nuclei are blue (DAPI staining).

Collaborations:

- Thorax Surgery, University Hospital Zurich
- N. Hild, O. Schneider, W. Stark, ETHZ, Functional Materials Laboratory, Institute for Chemical and Bioengineering



Dr. Shuping Gao, PhD



Dr. Johanna Buschmann, PhD



Dr. Luc Härter, PhD



Manfred Welti, Lab. Technician



Sonja Hemmi, Lab. Technician



PD Dr. Nicole Lindenblatt, MD



Prof. Dr. Hans-Peter Simmen, MD



Prof. Dr. Pietro Giovanoli, MD

The Endothelial differentiation potential of Human Adipose-Derived Stem Cells (hASC)

S. Gao, J. Buschmann, L. Härter, S. Hemmi, M. Welti, H-P. Simmen, N. Lindenblatt, P. Giovanoli, M. Calcagni, G. Wanner

Human adipose-derived stem cells (hASC) are routinely isolated from the stromal vascular fraction (SVF) of homogenized fat tissue. They have been found to be a suitable and an easily accessible source for adipose-derived mesenchymal stem cell (MSC) isolation. In the past years the use of MSC in tissue engineering has gained importance and has opened new possibilities for the reconstruction of large bone defects. An important hurdle for the successful application of MSC in bone regeneration is to obtain an appropriate vascularisation of the tissue. Endothelial cells (EC) are involved in the processes of angiogenesis and vasculogenesis. The capability of MSC to contribute to the formation of endothelial cells during bone regeneration is not yet completely clarified.

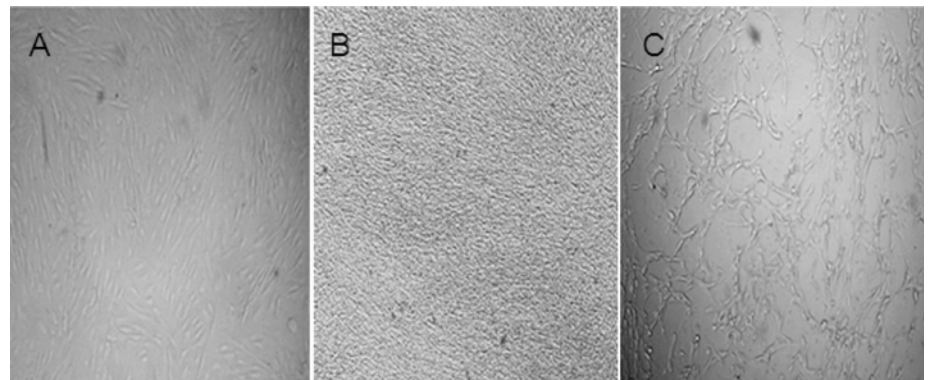


Figure 1: hASC endothelial differentiation. A. undifferentiated hASC morphology; B. Morphology of hASC after 3 weeks differentiation EC-medium; C. Morphology of hASC after differentiation in EC-medium for 4 weeks re-plated on Matrigel and subsequently cultured for 24 h. 100x

The main goals of this study were (I) to evaluate and to characterize the capacity of adipose-derived stem cells to differentiate into EC. (II) To identify characteristic EC markers for the identification of hASC derived EC.

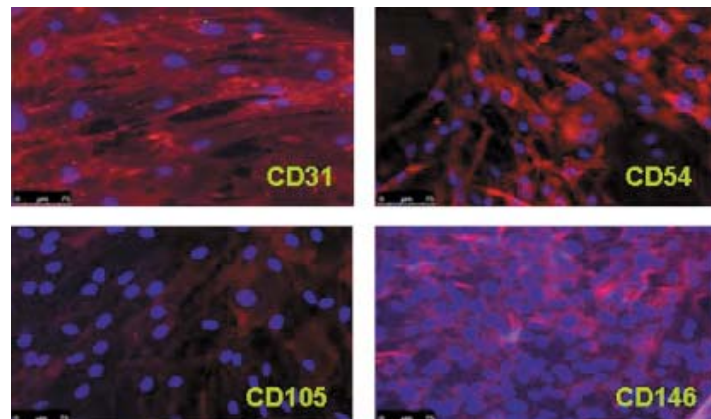


Figure 2: hASC endothelial differentiation characterization by immunofluorescence. Immunofluorescence characterization of EC differentiated ASC. Red (PE) blue (DAPI) 200x

31 hASC were harvested from subcutaneous fat tissues samples. hASC were characterized by FACS and immunohistochemistry. 22 hASC to EC differentiation experiments were performed and hADSC were cultured in endothelial cells differentiation medium for up to 3-4 weeks. We analyzed the differentiation potential and messenger RNA expression of selected genes. We further monitored vasculogenesis and expression changes of endothelial markers during the differentiation process.

The obtained EC showed cobblestone morphology (**Figure 1**) and expressed EC markers including CD31, CD146, and CD54 (**Figure 2**). Flowcytometry, FACS result showed that the MFI increased with CD31, CD105 and CD146 decreased and the obtained cells were positive for the endothelial markers CD31, CD54 and CD146 (**Figure 3**). We examined the expression of EC-specific genes by semi-quantitative PCR analysis after 3-4 weeks of induction. PCR showed expression and up-regulation of other typical EC markers, such as vWF, Tie2, Angiopoietin 1, and VE-cadherin. Differentiation experiments *in vitro* by using Matrigel indicated that the cells formed tubes and capillary-like structures, an indication that vasculogenesis is occurring under these culture conditions.

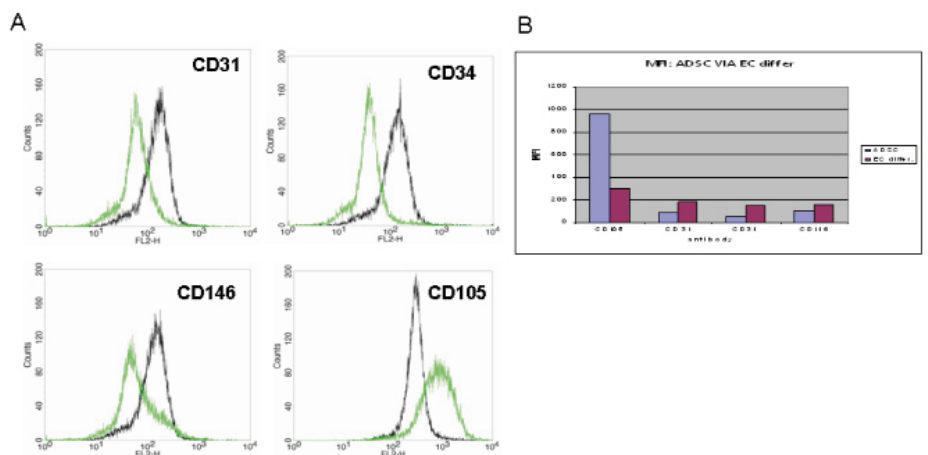


Figure 3: The FACS analysis of differentiated hASC. A. overlay of the mean fluorescence intensity (MFI) upon 4 weeks of endothelial differentiation. Green: hASC, Black: EC induction from hASC. B. MFI analysis

In conclusion, our experiments demonstrate that hADSC have endothelial cells differentiation ability and that CD31 and von Willebrand factor represent good markers for monitoring the hASC to EC conversion.

2.5 Plastic, Hand & Reconstructive Surgery Research



PD Dr.
Maurizio Calcagni,
MD



Prof. Dr.
Pietro Giovanoli,
MD

Plastic, Hand & Reconstructive Surgery Research

Motion analysis
laboratory

Connective tissue healing

Microcirculation

Protein profiling

2.5.1 Motion Analysis Laboratory



Dr.
Johanna
Buschmann, PhD



Angela Müller,
M.Sc.



Flora Nicholls
Dipl. nat.

Rabbits having one or both hind legs operated: Can we spare animals according to the 3R principle? A motion analysis.

J. Buschmann, A. Müller, F. Nicholls, R. Achermann, M. Calcagni,
P. Giovanoli

While planning the experimental design for a new technique of repairing Achilles tendon ruptures in rabbits, we were forced to decide whether only one hind leg per rabbit could be operated while a second rabbit would act as a control - or whether both hind legs would meet our claims (one hind leg operated with a new technique; the other treated by a conventional suture serving as internal control). If the outcome is identical, the second way will be preferred because only half of the number of the rabbits is used (saving animals and costs). We refer to the theoretical framework of the 3R principle, originally proposed by Russell and Burch (*Russell, W.M.S., Burch, R.L., 1959. The Principles of Humane Experimental Technique. Universities Federation for Animal Welfare Wheathampstead, England (reprinted in 1992)*).

By 2D motion analysis during the 12 week post-op phase, rabbits with both, with one and with none hind legs operated are videotaped and maximum as well as minimum angles as a function of hopping length is determined. Three markers are set on the leg by black felt pen after shaving the corresponding spots. In **Figure 1**, maximum and minimum angles for the four groups are shown as a function of time.

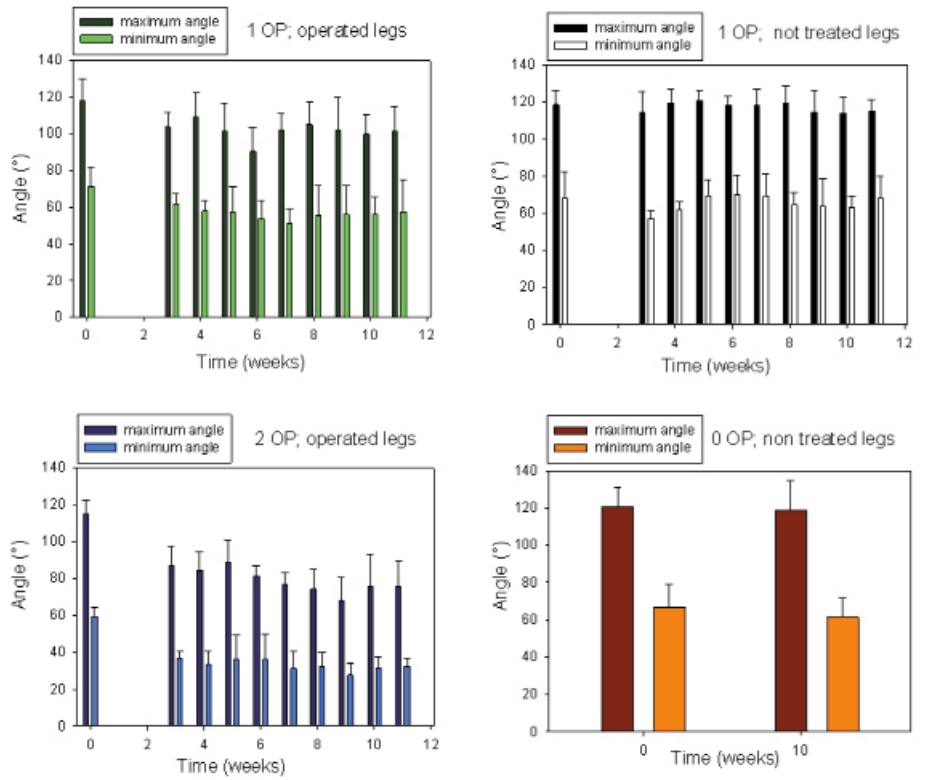


Figure 1: Maximum and minimum hopping angles, average and standard deviation ($n = 9$ steps), as a function of time for the four groups with $n = 6$ legs for each group.

Collaborations:

- R. Achermann, Health Research, Institute for Clinical Epidemiology and Biostatistics, University Hospital Basel, Switzerland

2.5.2 Connective Tissue Healing



Dr.
Johanna
Buschmann, PhD



PD Dr.
Maurizio Calcagni,
MD



Angela Müller
M.Sc.



Gabriella
Meier-Bürgisser

Cellular response of healing tissue to DegraPol tube implantation in rabbit Achilles tendon rupture repair: an *in vivo* histomorphometric study

J. Buschmann, G. Meier-Bürgisser, E. Bonavoglia, P. Neuenschwander, V. Milleret, P. Giovanoli, M. Calcagni

In (flexor) tendon rupture repair, there are still open problems up-to-date: adhesion and rupture in the early healing phase with a reoperation rate of 7 – 15 % leading to increased work disability and costs. On the one hand side, the repaired tendons should have high primary repair strength for early active post-operative motion, and on the other hand side, the repair site should be flat in order to allow the tendon to glide smoothly in the tendon sheath (*Buschmann et al. 2011*). According to *Kuwata et al.*, optimum primary repair strength requires multi-strand locking loops and cross-stitch epitendinous sutures (*Kuwata et al. 2007*). However, such repair techniques lead to bulging at the repair site and thus to adhesion during the healing process (*Khanna et al. 2009*).

Considering these problems, a polymer device which bags the repaired tendon tightly and has a flat outer surface would probably help to reduce the adhesion caused by a rough and large primary cross-sectional area at the repair site. In addition, such a flattening tube may act as a potential carrier device and be supplemented with bioactive substances (*Ehrbar et al. 2007*) or stem cells (*Yao et al. 2011*) in order to stimulate the healing process *in situ*.

As a consequence, we developed a potential carrier system which is able to do both; flatten the repair site and deliver growth factors, cytokines or other stimuli to the repair site. DegraPol® tubes were implanted around transected and conventionally sutured rabbit Achilles tendons and we determined their effects 12 weeks post-operatively. Number and morphology of tenocytes, collagen structure and inflammation zones were explored on a histomorphometric basis. The study is funded by the *Hartmann-Müller Stiftung*, the *Fonds für Medizinische Forschung* and the *Wolferrmann-Nägeli Foundation*. The study has been published in *Journal of Tissue Engineering and Regenerative Medicine* (2012).

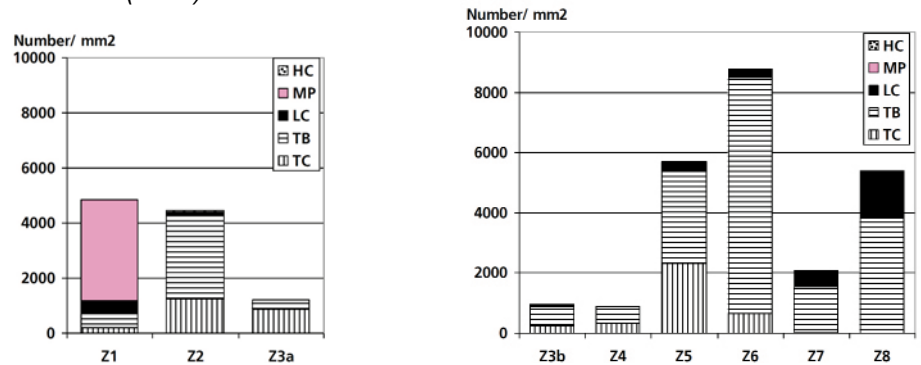
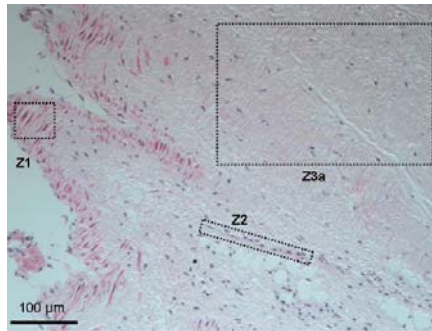
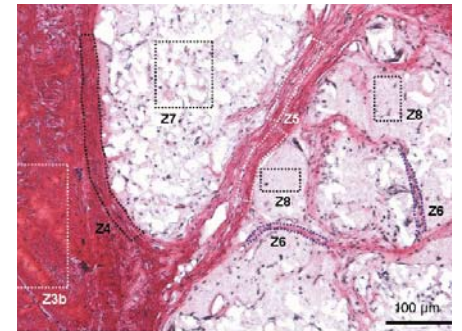


Figure 1: Analysis of inflammation. **Left:** Density of different cell types as a function of zone type in tissue at least 1 mm away from DP area (at the periphery of the reconstructed tissue). Averages of 5 FOV (200 x or 400 x magnification) of one selected specimen (DP, 4-str, 1 OP); the other specimen having similar distributions. Key: HC = heterophiles, MP = macrophages, LC = lymphocytes, TB = tenoblasts and TC = tenocytes. Z1 = inflammation zone, Z2 = endotenon and Z3a = tendon tissue near inflammation zone.

Right: Density of different cell types as a function of zone type near or in DP area. Averages of 5 FOV (200 x or 400 x magnification) of one selected specimen (DP, 4-str, 1 OP); the other specimen having similar distributions. Key: Z3b = tendon tissue near DP, Z4 = reactive zone at the margin of DP, Z5 = reactive zone at the boundary of DP, Z6 = reactive zone of cell immigration into DP, Z7 = DP area, Z8 = amorphous zone of DP.



655 x 492 μm



655 x 492 μm

Figure 2:

Left: Zones Z1, Z2 and Z3a in a representative H&E stained longitudinal section (100 x magnification).

Right: Zones Z3b to Z8 in a representative Picosirius Red stained histological cross-section (100 x magnification). Partially degraded DP is white.

Collaborations:

- K. Feldmann, T. Tervoort, Swiss Federal Institute of Technology (ETH-Hönggerberg), Department of Materials
- P. Neuenschwander, E. Bonavoglia, ab medica, Italy
- G. Fessel, J. G. Snedeker, Balgrist University Hospital, Department of Orthopedics

2.5.3 Microcirculation



PD Dr.
Claudio Contaldo,
MD



PD Dr.
Nicole Lindenblatt,
MD



Alicia Knapik
M.Sc.



Dominik Högger
cand. med.

Radial pressure waves mediate apoptosis and functional angiogenesis during wound repair in ApoE deficient mice

C. Contaldo, D. C. Högger, M. Khorrami, M. Stotz, U. Platz, N. Forster, N. Lindenblatt, P. Giovanoli

This study aims to quantify by intravital microscopy and histological wound scoring the effect of radial pressure wave treatment (RPWT) on murine incisional wound healing. The dorsal skinfold chamber in mice (**Figure 1**) was used for intravital microscopy, whereby an incisional wound was created within the chamber. RPWT to the wound was carried out using a ballistic shockwave source (EMS Swiss DolorClast). Animals received a dose of 500 pulses at an energy flux rate of 0.1 mJ/mm^2 and a frequency of 3 Hz at day 1, 3, 5, 7, 9, and 11 post wounding. RPWT treated and untreated ApoE depleted mice (ApoE^{-/-}) were compared to normal healing wild type animals (WT). The microcirculation of the wound was analyzed quantitatively *in vivo* using epi-illumination intravital fluorescence microscopy (**Figure 2**). Tissue samples were examined *ex vivo* for wound scoring and immunohistochemistry. Upon RPWT total wound score in ApoE^{-/-} mice was increased by 13% (not significant) on day 3, by 37% on day 7 ($P < 0.05$), and by 39% on day 13 ($P < 0.05$) when compared to untreated ApoE^{-/-} mice (**Figure 3**). Improved wound healing was associated with an increase of functional angiogenic density by 23% (not significant) on day 5, by 36% on day 7 ($P < 0.05$), and by 41% on day 9 ($P < 0.05$) (**Figure 2**). Following RPWT, on day three we observed enhanced expression of caspase-3 (2-fold), proliferating cell nuclear antibody (PCNA, 1.6-fold), and endothelial nitric oxide synthase (eNOS, 2.6-fold), all $P < 0.05$ (**Figure 4 und 5**). In conclusion repetitive RPWT accelerated wound healing in ApoE^{-/-} mice by increasing functional neovascular density. In addition our findings strongly suggest that radial pressure waves may facilitate the linear progression of wound healing phases by fostering apoptosis.

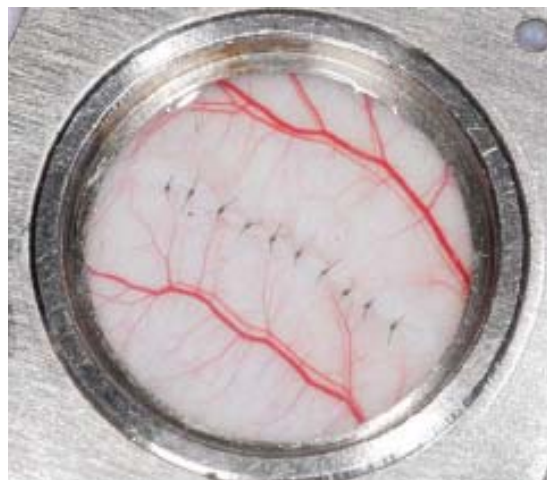


Figure 1: Murine dorsal skinfold chamber model. An incisional wound is created whereafter the wound edges are adapted with Nylon sutures. The chamber is covered with a glass coverslip allowing for intravital microscopy.

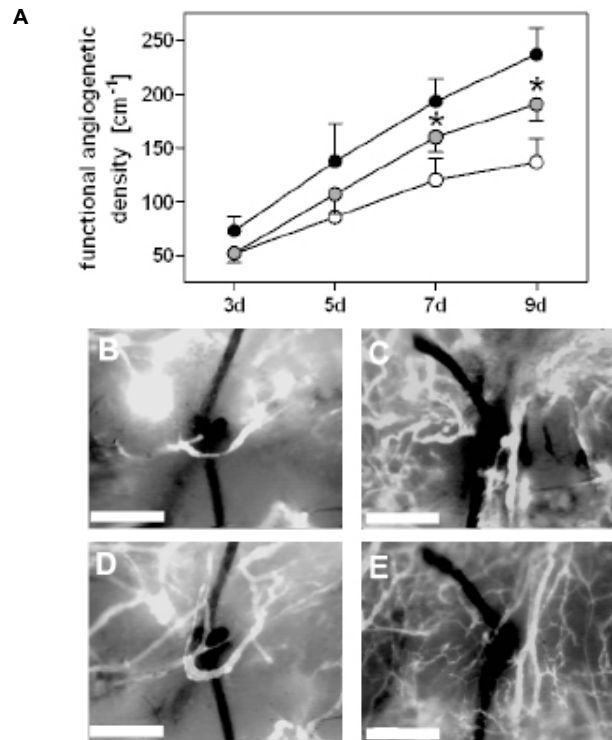


Figure 2: (A) Functional angiogenic density (FAD) of wild type mice (●) compared to ApoE knockout mice (○), and ApoE^{-/-} mice after RPWT (⊖) with 500 pulses on day 1, 3, 5, 7, 9 and 11 after incisional wounding in the dorsal skinfold. Data represent means \pm SEM (n=6). * $P < 0.05$ vs. ApoE^{-/-}. **(B-E)** Intravital fluorescence microscopy (contrast enhancement by 5% FITC-dextran) in wounds. Representative pictures 5 **(B, C)**, and 9 **(D, E)** days post-wounding are shown. Note the more dense capillary system after RPWT **(C, E)** compared to nontreated **(B, D)** animals (scale bars = 100 μ m; 9-0 Nylon suture is shown).

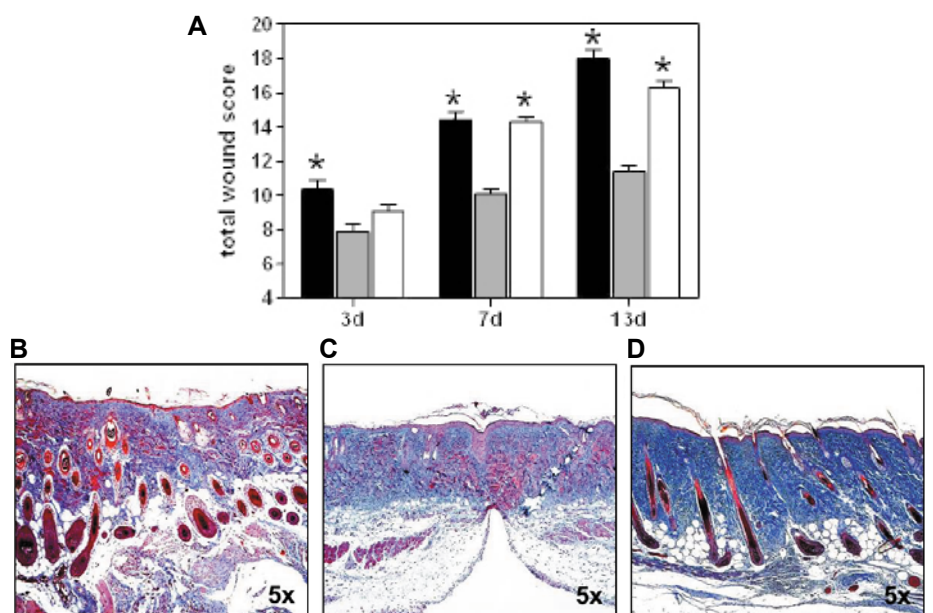


Figure 3: Total histological wound score of normal healing wild type (WT) mice (A) (●) compared to ApoE knockout mice (○), and ApoE^{-/-} mice after RPWT (⊖) with 500 pulses on day 1, 3, 5, 7, 9 and 11. Data represent means \pm SEM (n=6). * $P < 0.05$ vs. ApoE^{-/-}. **(B, C, D) Masson trichrome stained paraffin sections from the center of 13-day wounds. Note that ApoE^{-/-} mice **(C)** show substantial better healing after RPWT **(B)**, comparable to that of WT mice **(D)**.**

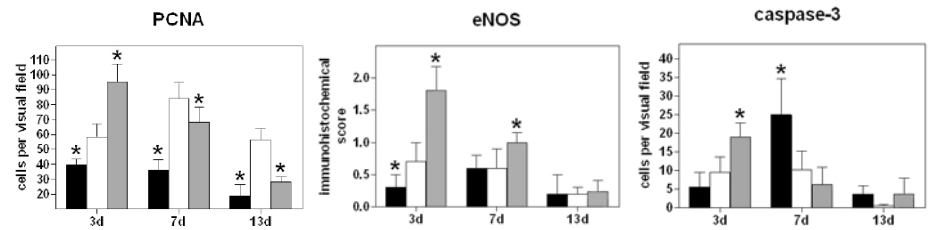


Figure 4: Staining intensity of eNOS expression (A), as well as number of PCNA (B), and caspase-3 (C) stained cells of normal healing wild type mice (black bars) compared to ApoE knockout mice (white bars), and ApoE^{-/-} mice after RPWT (grey bars) with 500 pulses on day 1, 3, 5, 7, 9 and 11 after incisional wounding. Data represent means \pm SEM (n = 5 per group); *P < 0.05 vs. ApoE^{-/-}.

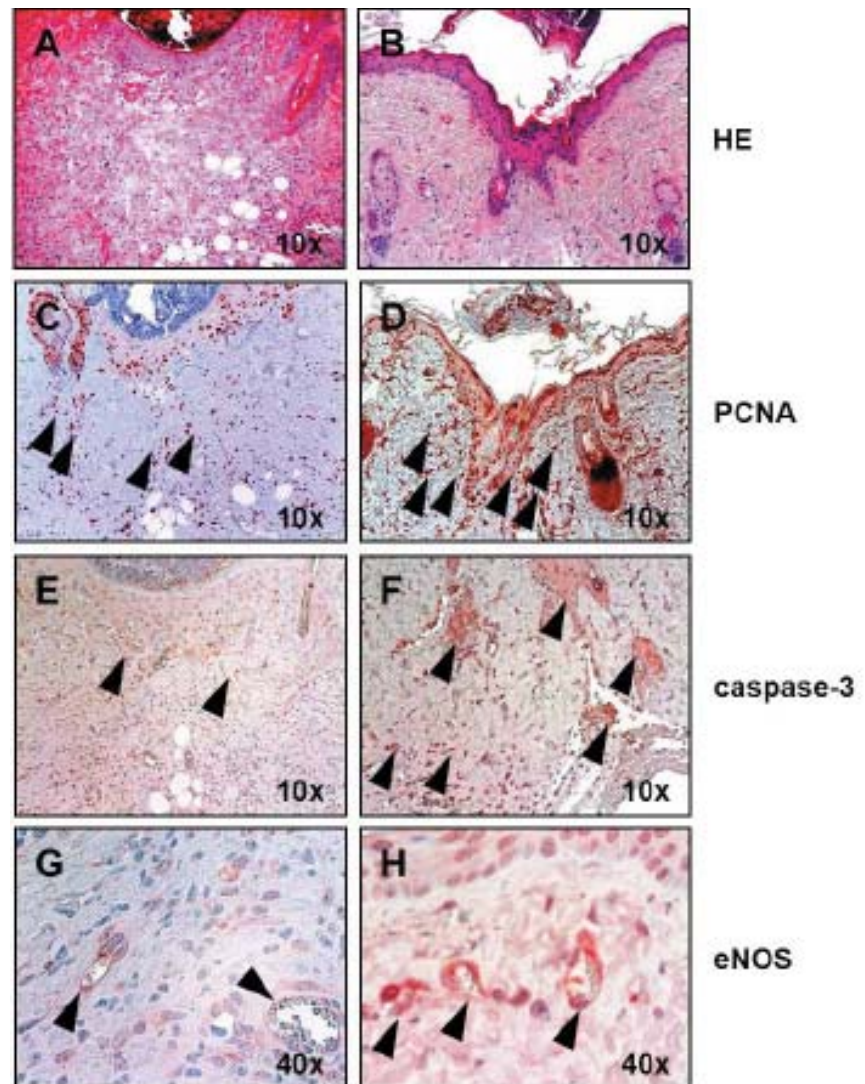


Figure 5: Immunohistological demonstration (arrow heads, red staining) of PCNA (C, D), caspase-3 (E, F), and endothelial eNOS (G, H) in endothelial cells (arrows) in serial paraffin sections from the center of 7-day wounds in untreated ApoE^{+/+} mice (A, C, E, G), and ApoE^{-/-} mice after RPWT (B, D, F, H) with 500 pulses on day 1, 3, 5 after incisional wounding in the dorsal skinfold.

Revascularisation of skin grafts – vascular transformations and proteolytic activity

N. Lindenblatt, A. Knapik, K. Kornmann, M. Calcagni, N. Hegland, M. Althaus, C. Contaldo, P. Giovanoli

Successful revascularisation represents the crucial step in skin graft taking. A better understanding of physiological skin graft incorporation has regained interest in the field of skin tissue engineering. Clinical studies with take rates of 10-90 % show that the vascularisation of full-thickness skin substitutes today is far from being satisfactory. Therefore, major efforts are put into the improvement of vascularisation strategies, e.g. the construction of a tissue-engineered microvascular network within skin substitutes. Angiogenic research usually concentrates on mechanisms of endothelial cell sprouting, lumenogenesis and tubulogenesis. However, only little is known about the process of capillary inosculation with a pre-existing vascular network and the expression of vascular factors in this context. An *in vivo* crossover design between wild type C57BL6J und transgenic GFP mice was established allowing for the tracking of GFP (green fluorescent protein) positive cells both originating from the wound bed and the skin graft. By means of this, the origination of cells and vascular structures during skin graft revascularization was intended to be identified. With the beginning of graft reperfusion 48-72 hours after transplantation GFP-positive structures from the wound bed were visible in the graft capillaries with predominantly in the centre of the graft. Overall, we observed a replacement of existing graft capillaries with vessels from the wound bed in 68% of the vessels (**Figure 1**). Of note, vessel replacement occurred in almost 100% of graft vessels in the periphery. In a next step we questioned which molecular and cellular mechanisms actually take place at the wound bed/graft interface. Therefore we performed additional *in vitro* experiments. Proteases like MMP (matrix metalloproteinases), ADAM (a disintegrin and metalloproteinase) and ADAMTS (a disintegrin and metalloproteinase with thrombospondin motif) are zinc-containing endopeptidases produced by endothelial cells that are capable of degrading ECM proteins. They are currently seen as crucial regulators of angiogenesis and have been found to be activated in capillary sprouts. In line with this immunohistochemistry at day 3 revealed the expression of MT1-MMP at the tip cells making these proteases a potentially important factor in vessel migration and eventually connection to the existing graft. The modified dorsal skinfold chamber with autologous skin grafting was prepared in C57BL/6J mice and intravital microscopy was performed. The expression of proteases and vascular factors was quantified by immunohistochemistry. Wound bed bud formation appeared after 24 to 48 hours representing starting points for capillary sprouting. In the reperfused skin graft larger buds developed over several days without transformation into angiogenic sprouts, instead pruning took place. MT1-MMP was detected at sprout tips of in-growing vessels. MMP-2 expression was located at the wound bed/graft connection sites (**Figure 2**). Pericytes were found to withdraw from the angiogenic vessel in order to facilitate sprouting. Since intravital fluorescence microscopy is somewhat limited concerning the penetration depth into the tissue, we intended to improve this method by using a multi photon microscope.

In cooperation with Prof. Urs Ziegler and Claudia Domröse animals were scanned after transplantation of full-thickness grafts. Capillaries were traced up to a penetration depth of 400 μm without damage to the tissues by the laser light. IMARIS software served to localize blood flow and collagen fibres (**Figure 3**). Further studies in transgenic mice are planned for spring 2012 to differentiate graft and host vessels.

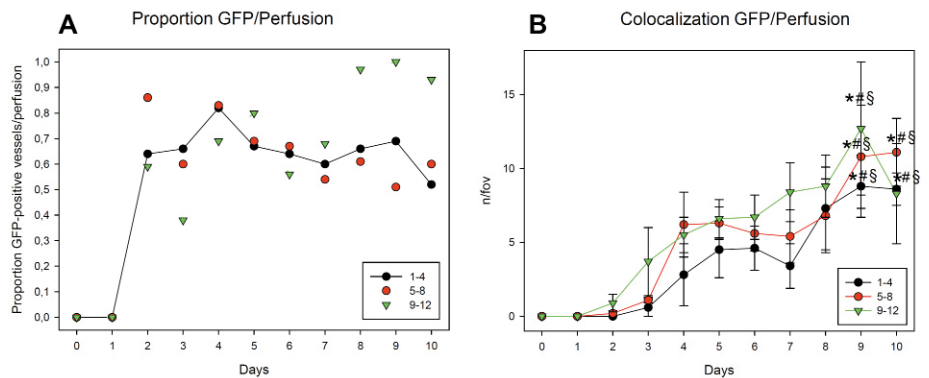


Figure 1: (A) Proportion of GFP-positive vessels in relation to perfused vessels with respect to capillary density (calculated from Fig. 4) in centre (1-4), inner periphery (5-8) and outer periphery (9-12) of the WT skin graft. (B) Co-localisation of vessel perfusion and green-fluorescent structures in different areas of the graft: centre (1-4), inner periphery (5-8) and outer periphery (9-12). Mean \pm SEM; * p <0.05 vs. day 0; # p <0.05 vs. day 1; \$ p <0.05 vs. day 2.

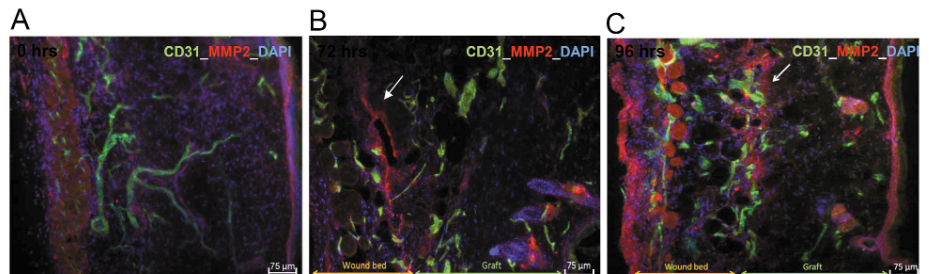


Figure 2: Immunofluorescence of MMP-2 expression over time on cross sections. CD31 (AlexaFluor 488), MMP-2 (Cy3) and DAPI nuclear staining. (A) Skin before transplantation. (B) 72 hours after transplantation MMP-2 expression at the wound bed adjacent to the skin graft (C) 96 hours after transplantation MMP-2 expression is predominantly located in the deep dermis of the skin graft. Bar represents 75 μm .

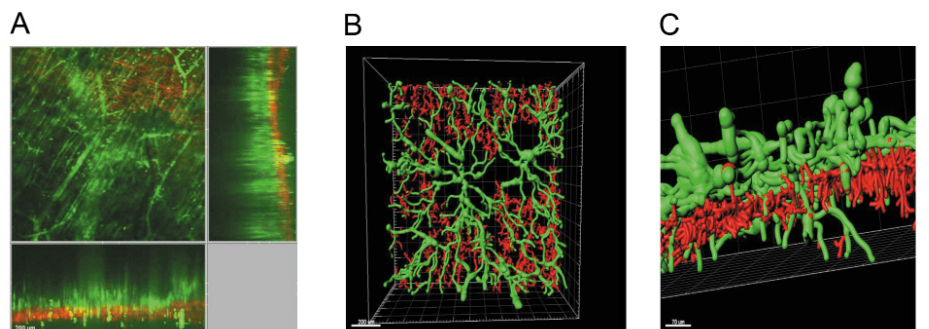
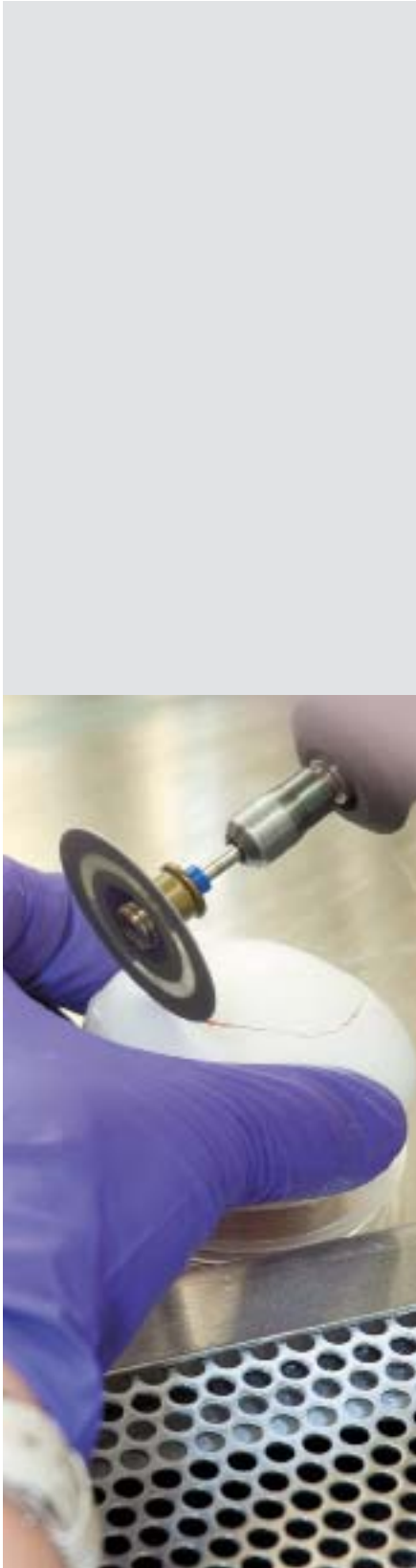


Figure 3: (A) Tracking of capillaries of the modified dorsal skinfold chamber by multiphoton microscopy (MPM). Perfused capillaries are stained with green dye (FITC-dextran), collagen is stained in red. (B) 3D reconstruction of the vascular structures using IMARIS software. (C) Cross-section of the wound bed showing angiogenic vascular structures (green) and collagen (red).



Collaborations:

- Prof. Dr. Simon P. Hoerstrup, MD, PhD, Department of Surgical Research and Clinic for Cardiovascular Surgery, UniversityHospital Zurich
- PD Dr. Ernst Reichmann, MD, Tissue Biology Research Unit, Children's Hospital Zurich
- Dr. Christian A. Schmidt, MD, Clinic for Cardiovascular Surgery, UniversityHospital Zurich
- Ina Kalus, PhD, Rok Humer, PhD, Department of Internal Medicine, UniversityHospital Zurich
- Dr. Deon Bezuidenhout, MD, Cardiovascular Research Unit, University of Cape Town, South Africa
- Dr. Eric P. Meyer, MD, Institute of Zoology, University of Zurich
- Prof. Urs Ziegler, Claudia Domröse, Klaus Marquardt, Center for Microscopy and Image Analysis, University of Zurich
- Prof. Dr. Brigitte Vollmar, MD, Institute for Experimental Surgery, University of Rostock, Germany
- Prof. Dr. Martin Glocker, MD, Proteom Center, University of Rostock, Germany
- Prof. Dr. Michael D. Menger, MD, Institute for Clinical and Experimental Surgery, University of Saarland, Germany

2.5.4 Protein profiling



Dr.
Juliane C. Finke,
MD



Dr.
Tatjana Lanaras,
MD



PD Dr.
Nicole Lindenblatt,
MD



Dr. dent.
Marius Bredell,
MD



PD Dr.
Maurizio Calcagni,
MD



Prof. Dr.
Pietro Giovanoli,
MD

Proteome Signatures of Free Flaps - Protein Profile Changes During Ischemia and Reperfusion

J. C. Finke, T. Lanaras, N. Lindenblatt, M. Bredell, M. O. Glocker, M. Calcagni, P. Giovanoli

Transfer of tissue transplants (free flaps) has become the method of choice to cover and reconstruct major wounds and defects in specialized plastic surgery and head and neck surgery centers. However, the consequences of a transplant failure are devastating for the individual patient including long duration of hospitalization, infections, functional deficits, and high costs for the health care system. Currently, only clinical examination of the transplanted tissue is available for gaining information about the status of the flap. But the information that is obtained by such examinations is considered not reliable enough and time of detection based on clinical parameters could be too late for transplant rescue. By contrast, monitoring ischemic processes on the molecular level shall enable estimations on the individual transplant quality at a much earlier time, when clinical signs are not yet visible. Plasma protein profiles in free flaps hold information about the overall clinical quality of the transplant, specific for the type of transplanted tissue (skin, bone, muscle). Thus, in order to obtain a molecular signature that is capable to describe the ischemic status of the transplant, proteome research approaches shall be applied in a differential manner. The goal is to gain monitoring factors and possibly prognostic profiles for free flap healing and development. Ultimately, molecular marker signatures shall enable to detect problems earlier than manifestations on vascular insufficiencies, opening the way to increases in flap salvage and decreases in flap failures, and to guide future therapy optimization strategies.

Differential analysis of plasma proteins shall be applied to learn about the ischemic proteome profiles in individual free flap transplants. Plasma samples from three groups of transplants (osteocutaneous flaps, muscle flaps, and skin flaps) shall be analyzed. From each transplant three blood / plasma samples are available, one from the tributary artery and two from the effluent vein (at two points in time: t1 and t2).

Two general avenues shall be taken for molecular profiling. The first one applies global proteome profiling in order to screen for differences of the plasma profiles without previous knowledge of mutual differences. The second one focuses on abundance differences of cytokines and chemokines, respectively, in a targeted fashion. Information from both independent data sets will be brought together in order to generate a molecular profile of the ischemic status of free flap tissue, shedding light on the molecular mechanisms of these processes. As a consequence, proteome profiles shall be applied to estimate the individual transplant quality.

In the future, this knowledge shall be transferred into an assay that will be made available to the surgeon who then will be enabled to optimize the transplantation process, i.e. to decide at an early time point - prior to the appearance of clinical signs of vascular problems - whether a free flap needs to be taken back for salvage procedure.

Three groups of free flap transfers were included in the study: (i) muscle flaps, e.g. gracilis flap, latissimus dorsi flap, serratus anterior flap, (ii) fasciocutaneous flaps, e.g. radialis flap, antero lateral thigh flap, and (iii) osteocutaneous flaps, i.e. fibula flaps. Clinical measurements include the ischemia time, flap weight, length of bone (in fibula flaps) and the dimension of the skin island. Very strict exclusion criteria have been defined. Patients qualified for the study had to be between 30 and 70 years old, with normal weight (BMI 20 – 25), non-diabetics, in no infection situation, and of good health with no essential diseases besides the main diagnosis. Samples were provided by the Division of Cranio-Maxillo-Facial and Oral Surgery and by the Division of Plastic Surgery and Hand Surgery of the University Hospital Zurich. Blood samples were taken intraoperatively prior to arterial anastomosis (t1) from the arterial flap inflow and after arterial anastomosis (t2) from the venous flap outflow to investigate protein profile changes during time of ischemia and reperfusion in the flap tissue. In total, nineteen blood sample pairs were collected, six in muscle flaps, four in fasciocutaneous flaps, and nine in osteocutaneous flaps. The osteocutaneous flaps (n = 9) were free fibula flaps for head and neck reconstructions in tumour diseases, the ischemia time ranged from 90 to 220 minutes. The muscle flaps (n = 6) were mostly latissimus dorsi muscle flaps (n = 4), one gracilis muscle flap, and one serratus anterior muscle flap. All muscle flaps were needed for lower limb reconstruction. The ischemia time varied from 60 to 120 minutes. The fasciocutaneous flaps (n = 4) were radialis flaps that were used to cover defects in the head and neck area, the ischemia time ranged from 80 to 150 minutes.

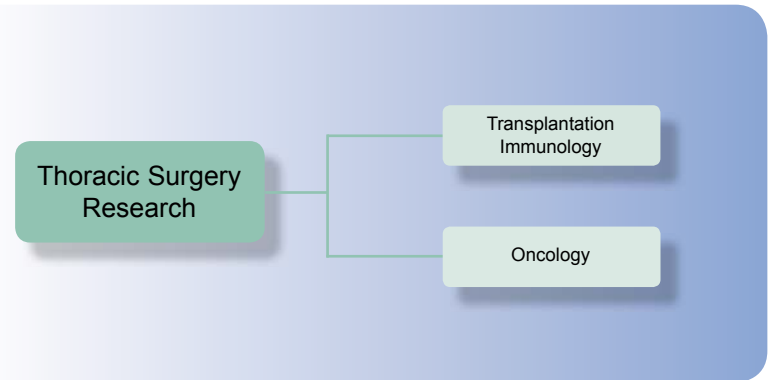
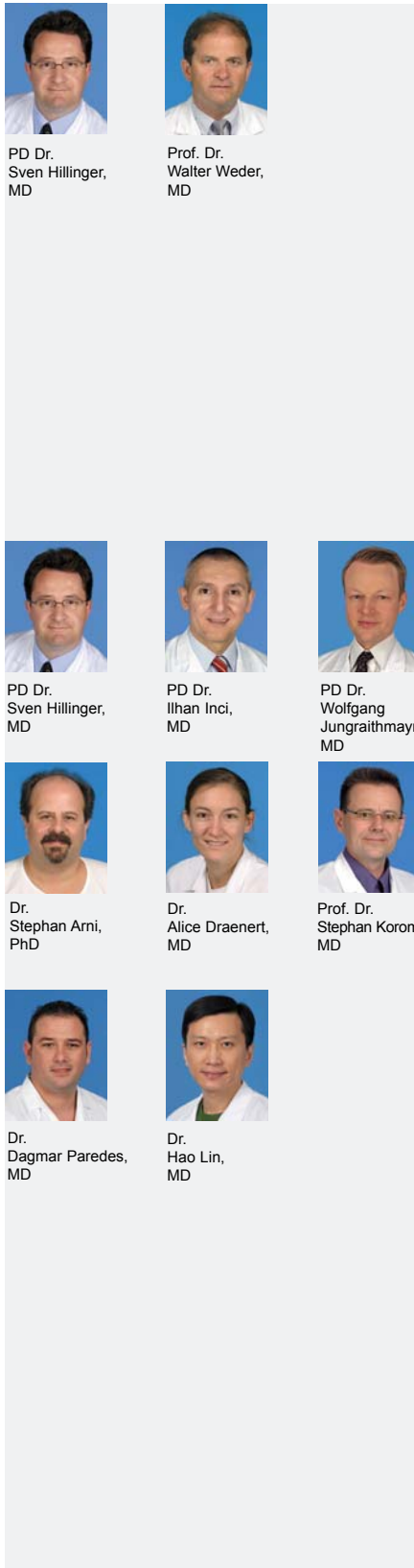
Blood samples (1.5 ml each) were taken using monovette syringes (Monovette®, Sarstedt, Germany) during the operation. Blood samples were immediately subjected to sedimentation of blood cells by centrifugation at 2000 g (1000 rpm) at room temperature for 15 min. Plasma was aspirated, sterile filtered (0.2 µm pore size) and divided into aliquots (100 µl each) which were stored at – 80 °C. Altogether, time between blood sample collection and storage of plasma aliquots averaged below one hour.

The sample taking will be completed this year, the samples are going to be transferred to the collaborating Proteome Center of the University of Rostock, Germany, for the systematic proteome analyses.

References

1. Koy C, Heitner (Finke) JC, Woisch R, Kreutzer M, Serrano-Fernandez P, Gohlke R, Reimer T, Glocker MO. Cryodetector mass spectrometry profiling of plasma samples for HELLP diagnosis: An exploratory study. *Proteomics* 5(2005): 3079-3087.
2. Heitner (Finke) JC, Koy C, Kreutzer M, Gerber B, Reimer T, Glocker MO. Differentiation of HELLP patients from healthy pregnant women by proteome analysis – On the way towards a clinical marker set. *J Chrom B* 840(2006): 10-19.
3. Doctoral thesis Juliane C. Finke 15.12.2008 „Protein – Profiling beim HELLP-Syndrom“:
http://rosdok.uni-rostock.de/metadata/rosdok_disshab_000000000204

2.6 Thoracic Surgery Research



2.6.1 Transplantation Immunology

Magnetic resonance imaging using ultra-short echo-time sequences in syngeneic mouse lung transplantation

W. Jungraithmayr, A. Boss, W. Weder

Here, we tested the *in-vivo* feasibility of magnetic-resonance imaging (MRI) for the detection of ischemia reperfusion (I/R) injury in syngeneic mouse lung transplants and to characterize tissue relaxation properties using ultra-short echo-time sequences at 4.7T.

To address this objective, mice (C57BL/6) underwent MRI 24 hours after syngeneic orthotopic left lung transplantation (Tx) (n=6). A small animal MR imager equipped with a circular polarized 1H mouse whole body RF coil was used. In addition to a conventional T1w spoiled gradient-echo and a T2w fast-spin-echo sequence, 3D ultra-short echo-time (UTE) sequences with echo-times TE=50µs-5000µs were acquired (**Figure 2**). Colour-encoded parametrical maps of T2* transverse relaxation time were calculated on a pixel-by-pixel manner. Quantitative T2* values of lung transplant parenchyma and relative spin density were compared by region-of-interest analysis using the two-sided paired student's t-test. After MRI, Tx lungs were processed for histology.

All mice revealed a ventilated Tx lung with similar low signal intensity in the conventional T1w and T2w sequences. The UTE sequence exhibited signal yield in the lung higher than the noise level. Increased spin density (50.8±26.9%, p=0.006) and longer T2* relaxation time (1041±424µs, p=0.016) were found in the Tx lung (**Figure 1**). Best visualization was possible using colour-encoded log-transformed parametrical T2* maps. Conventional T2w sequences revealed small pleural effusion. Histology revealed I/R injury with an either predominance of cell influx or edema.

We could conclude that I/R injury after syngeneic lung Tx can be visualized and characterized with UTE sequences showing different MRI relaxation properties when compared to normal lung parenchyma.

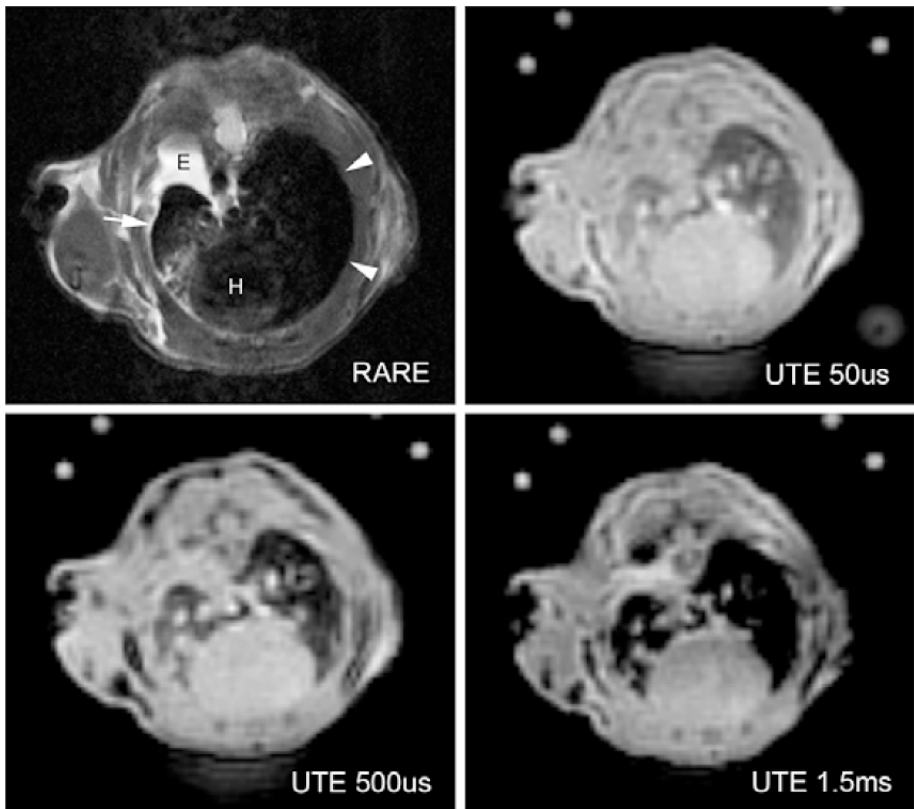


Figure 1: Conventional T2w fast-spin echo (RARE) image (TR/TE 2500 ms/33ms) and ultra-short echo-time sequence images with echo-times TE of 50 μ s, 500 μ s, and 1.5 ms are displayed. In the conventional T2w image, no MRI signal is visible neither in the normal lung (arrow heads) nor the transplanted lung (arrow). Little effusion (E) is visible with high signal intensity; low signal in the heart (H). In the UTE sequence, in both, normal and transplanted lung MRI signal is visible (higher signal in the transplanted lung). Increasing the echo-time results in signal loss in the lung at TE of 1.5 ms, thereby giving an image impression similar to the conventional T2w sequence.

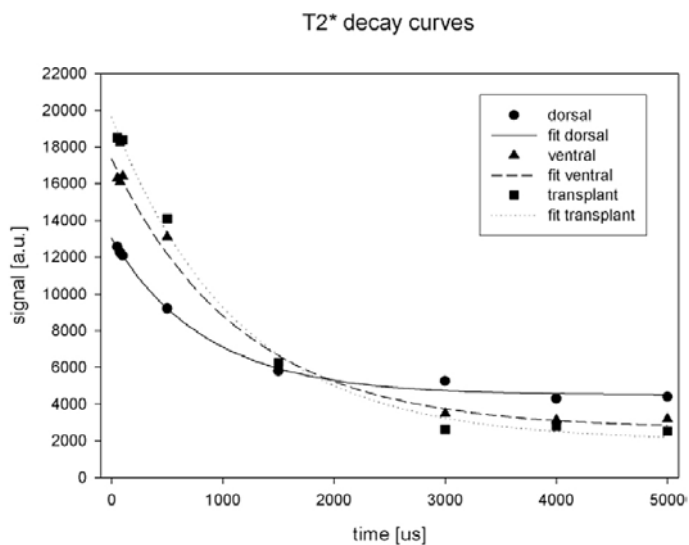


Figure 2: Typical T2* decay curves with measurement points between 50 μ s up to 5ms. Lowest spin density and fastest signal decay can be found in the dorsal part of the normal lung.

CD26/DPP4 – inhibition recruits regenerative stem cells via stromal cell-derived factor - 1 and beneficially influences ischemia-reperfusion injury in mouse lung transplantation

W. Jungraithmayr, I. De Meester, W. Weder

The CD26 antigen is a transmembrane glycoprotein that is constitutively expressed on activated lymphocytes and in pulmonary parenchyma. This molecule is also identified as dipeptidyl peptidase 4 (DPP-4) that cleaves a host of biologically active peptides. Here, we aimed to identify an important substrate of CD26/DPP-4 – stromal cell-derived factor 1 (SDF-1/CXCL12) – as a key modulator for stem cell homing together with its receptor CXCR4 in response to ischemic injury of the lung.

In order to elucidate this issue, orthotopic single lung transplantation (Tx) was performed between syngeneic C57BL/6 mice. Inhibition of CD26/DPP-4 activity in recipients was achieved using vildagliptin (10 mg/kg, every 12 hrs) subcutaneously, and 6 hours ischemia time was applied prior to implantation. Forty-eight hours after Tx, lung histology, SDF-1 levels (ELISA) in lung, spleen and plasma, and expression of the SDF-1 receptor CXCR4 in blood and lung were assessed. Homing of regenerative progenitor cells to the transplanted lung was evaluated using Fluorescent Activated Cell Sorting (FACS).

Compared to untreated lung transplanted mice, systemic DPP-4 inhibition of Tx recipients resulted in an increase in protein concentration of SDF-1 in plasma, spleen and lung. Concordantly, the frequency of cells bearing the SDF-1 receptor CXCR4 rose significantly in the circulation (**Figure 1**) and also in the lungs of DPP-4 inhibited recipients. We found co-expression of CXCR4/CD34 in the grafts of animals treated with vildagliptin, and the regenerative stem cell markers Flt-3 and c-kit were present on a significantly increased number of cells. The histological morphology of grafts from DPP-4 inhibitor treated recipients revealed less alveolar edema when compared to untreated recipients (**Figure 2**).

We could conclude that by targeting the SDF-1 – CXCR4 axis through CD26/DPP-4 inhibition, the intragraft number of progenitor cells contributing to the recovery from I/R lung injury was increased. Stabilization of endogenous SDF-1 is achievable and may be a promising strategy to intensify sequestration of regenerative stem cells and thus emerges as a novel therapeutic concept.

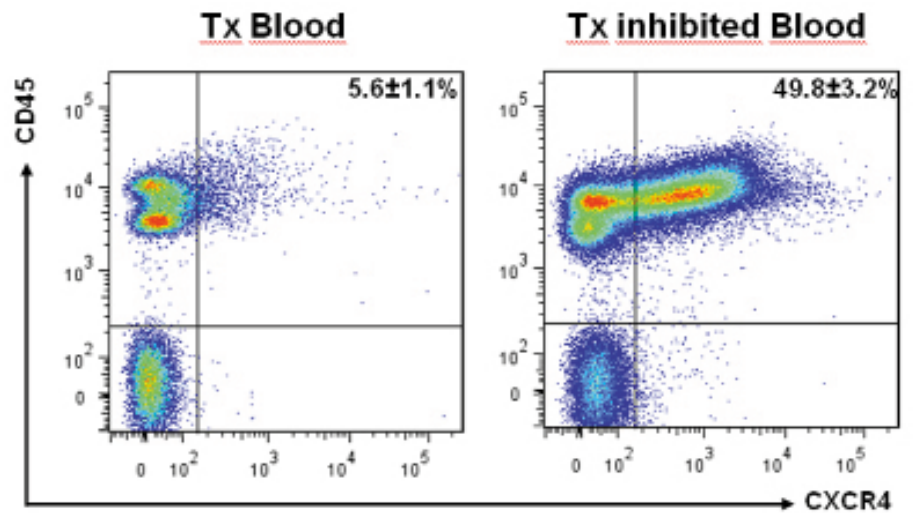


Figure 1: Representative FACS analysis showing the mean percentages of CD45+CXCR4+ cells in peripheral blood of transplanted (Tx) and Tx inhibited animals taken 48 hours post Tx, the latter showing a significantly higher cell frequency (* p < .05); data represent mean ± SEM (n=4).

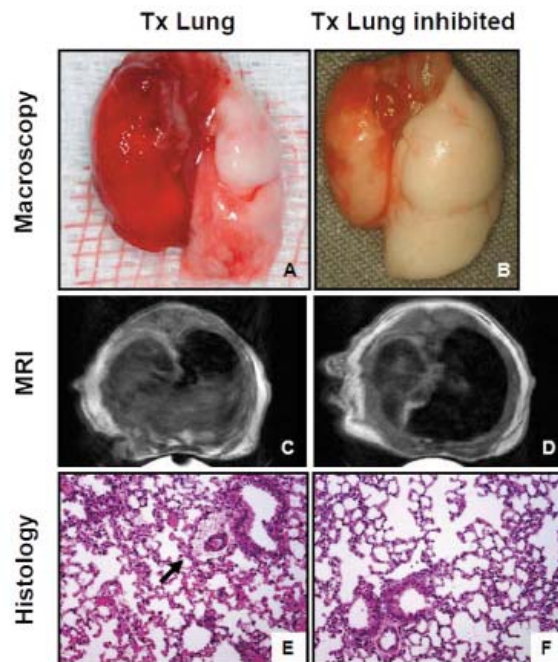


Figure 2: Representative syngrafts from transplanted (Tx) lungs (**Fig. 8A**) and Tx lung from animals that were inhibited (**Fig. 8B**), macroscopically appeared less inflamed and less edematous (n=4). MRI images showed a lower transparency in transplanted (Tx) lungs (**Fig. 8C**) when compared to Tx lung from animals that were inhibited (**Fig. 8D**) (n=4). H&E sections from transplanted (Tx) lungs (**Fig. 8E**) show more perivascular (arrow) and also interstitial edema and edema of the alveolar wall (**Fig. 8E**) when compared to Tx lung from animals that were inhibited (**Fig. 8F**) (n=6) (magnification: ×100).

Chest Surgical Disorders in Ancient Egypt

Evidence of Advanced Knowledge

W. Jungraithmayr, W. Weder

The autonomy of the ancient Egyptians ensured a freedom from foreign intrusions that favored the development of medical advances. The invention of writing and papyrus paper provided the basis for propagating medical practice. For a culture achieving enormous feats such as the erection of pyramids, together with having a high level of inventive and technical skills that characterized this nation, it is not surprising that this era of old Egyptian culture contributed significantly to the early development of medicine. Among many medical specialties such as gynecology, neurosurgery, and ophthalmology, also chest surgery was subject to diagnosis followed by an appropriate treatment. Here, we elucidate the remarkable level of their knowledge and understanding of anatomy and physiology in the field of chest medicine. Furthermore, we look at how ancient Egyptian physicians came to a diagnosis and treatment based on the thoracic cases in the Edwin Smith papyrus.



Figure 1: This hieroglyph represents the trachea and most likely the right and left lungs attached at the lower part of the symbol (A). The falcon representing the God Horus was thought to protect the lung within the canopic jars (B), and the symbol of a piece of flesh was often added to distinguish between homophones with different meanings (C). The word *sma* is presented in (D) and means "unite".



Figure 2: The hieroglyphic symbol of the heart reveals some impressive similarities to human anatomy. Although the origin of the drainage was not clearly differentiated between esophagus, jugular veins or air (trachea), the upper part is suggestive as being the influx drainage part whereas the protrusion at each side could represent the right and the left pulmonary arteries.

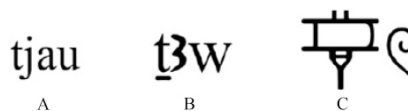


Figure 3: Different representations of breath and air: pronunciation (A), transliteration (B), and hieroglyph (C).

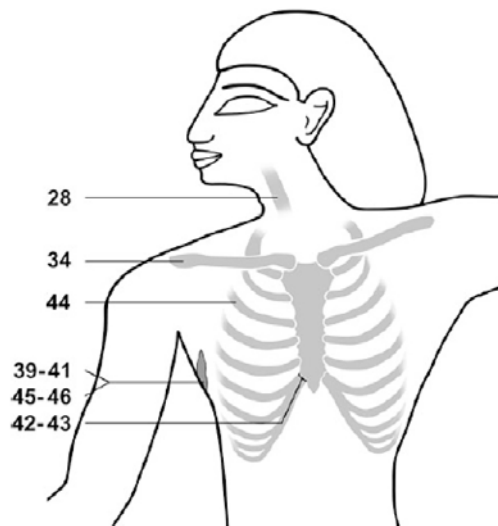


Figure 4: Anatomical location of injuries and diseases that are described in the cases of the Edwin Smith papyrus with the respective numbers, adapted from Nunn.



Figure 5: The hieroglyphic symbol for the rib that describes the curved form of the bone with a slope, possibly being a vessel or nerve that lies closely adjacent to the rib.

Collaborations:

- Prof. Dr. Christian Münz, Prof. Dr. Burkhard Becher, Dr. Laura Codarri, (Institute of Experimental Immunology, University Irchel, Zurich)
- PD Dr. Alex Soltermann, Dr. Peter Vogt (Institute of Surgical Pathology, UniversityHospital Zurich)
- PD Dr. Dr. Andreas Boss, PD Dr. Thomas Frauenfelder, Dr. Natalie Chuck (Institute of Diagnostic Radiology, UniversityHospital Zurich)
- PD Dr. Stefan Breitenstein (Department of Viszeral and Transplantation Surgery, UniversityHospital Zurich)
- Dr. Johanna Buschmann (UniversityHospital Zurich)
- Prof. Dr. Ingrid De Meester, Dr. Veerle Mattheussen (Institute of Biochemistry, University of Antwerp, Belgium)
- Dr. Stefanie de Vleeschauwer (Institute of Pulmonary Research, University Leuven, Belgium)
- Dr. Jeffrey O'Dodd (Institute of Anesthesiology, John's Hopkins University, Baltimore, USA)
- Dr. Ruedi Braun (Children Hospital, University of Madison, Wisconsin, USA)
- Dr. Johannes Schwarz (Experimental Pneumology, Helmholtz Zentrum München, Germany)

Reconditioning of category 3 non-heart beating donor lungs insulted to gastric aspiration: Utilization of ex vivo lung perfusion system

I. Inci, S. Hillinger, S. Arni, W. Weder

We tested whether an injured lung graft from category 3 DCD donor could be reconditioned in an ex vivo lung perfusion (EVLP) system with intratracheal surfactant instillation prior to transplantation.

In a pig model cardiac arrest was induced by de-connecting from the ventilator. Injury was done by intratracheal instillation of 1 ml/kg Pepsin+HCl (Oroacid®). After retrieval the heart-lung block was stored at 4° C for 2 hours. In the treated group the lung grafts were transplanted after reconditioning with intratracheal diluted surfactant lavage in EVLP system. In the control group left lung transplantation was performed without any reconditioning in EVLP system. Respiratory, hemodynamic and blood gas analysis recorded every hour during four-hour observation period. Extravascular lung water index was measured using transpulmonary thermo-dilution technique which uses single (cold saline) indicator. At the end of the experiment bronchoalveolar lavage was performed and lung tissue samples were taken for further assessments.

During EVLP evaluation surfactant group showed better oxygenation and lower pulmonary vascular resistance. During the observation period following transplantation better oxygenation, lower mean pulmonary artery pressure and lower lung edema were observed in surfactant group compared to control (**Figures 1, 2**). Lower blood IL-1 beta and IL-6 cytokine levels were obtained in the surfactant group. Neutrophil infiltration in the lung tissue, percentage of neutrophils, IL-1 beta and IL-6 cytokine levels in bronchoalveolar lavage at the end of experiment were significantly lower in the surfactant group (**Figure 3**).

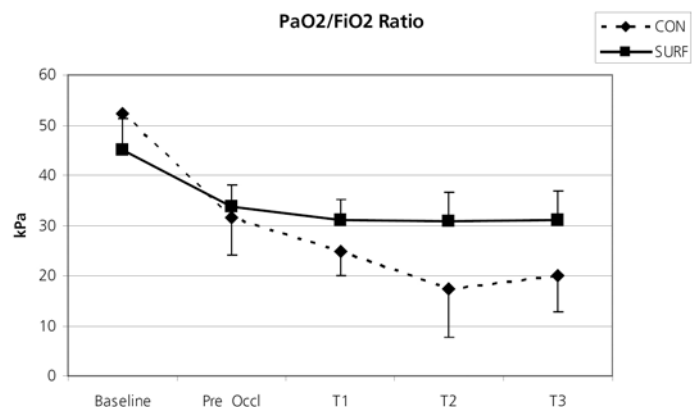


Figure 1. Analysis of variance (ANOVA) for repeated measures which consists of all measurements made during the reperfusion period for oxygenation did not differ between the groups ($p > 0.05$). Oxygenation: Partial arterial oxygen pressure/Fraction of inspired oxygen ($\text{PaO}_2/\text{FiO}_2$ ratio). Time points: Baseline, Pre_Occl: 10 min. before occlusion of the right lung, T1: 1 h after occlusion of the right side, T2: 2 h after occlusion of the right side, T3: 3 h after occlusion of the right side. $\text{kPa} = 7.5 \text{ mmHg}$. CON: Control group, SURF: Surfactant group

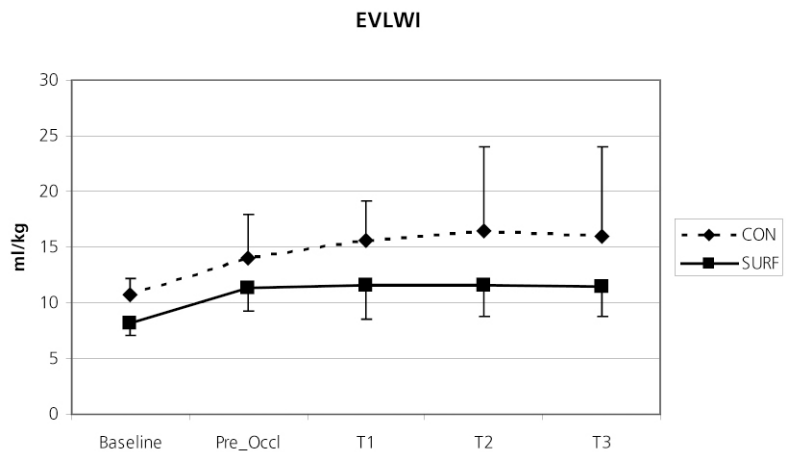


Figure 2. Extravascular lung water index (EVLWI) was higher at all time points during the reperfusion for the CON group. EVLWI, however was not significantly different between the groups. Time points: Baseline, Pre_Occl: 10 min. Before occlusion of the right lung, T1: 1 h after occlusion of the right side, T2: 2 h after occlusion of the right side, T3: 3 h after occlusion of the right side. kPa=7.5 mmHg. CON: Control group, SURF: Surfactant group

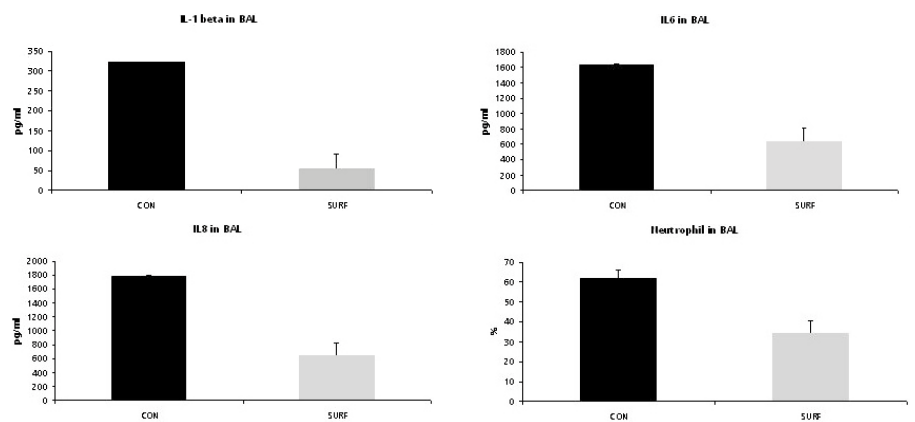


Figure 3. BAL IL-6, IL-8, IL1-beta und percentage of neutrophils were significantly higher ($p < 0.05$) in the control group compared to surfactant group at the end of experiment.

Due to our data it may be possible to recondition and transplant an acutely damaged lung graft due to acid aspiration from a category 3 DCD donor. Utilization of an EVLP system is an important tool to resuscitate and assess a questionable graft before transplantation.

Collaborations:

- Christa Acevedo, Rau Gunnar, Prof. Gesine Hansen, Medical School, Hannover, Germany
- University of Antwerp, Belgium: CD26/DPP IV
- University of Leuven, Belgium

2.6.2 Oncology

Lung Cancer



PD Dr.
Sven Hillinger,
MD



Prof. Dr.
Isabelle Opitz,
MD



Dr.
Stephan Arni,
PhD



Thomas Wiedl
PhD Student



Dr. Nhung Le,
PhD Student



Dr. Byron
Bitanihirwe, PhD



Dr. Mayura Meerang,
Postdoctoral Fellow



Dr.
Stephane Collaud,
MD



Manfred Welti,
Lab. Technician

Activity-based proteomics: identification of ABHD11 and ESD activities as potential biomarkers for human lung adenocarcinoma

T. Wiedl, S. Arni, B. Roschitzki, J. Grossmann, S. Collaud, A. Soltermann, S. Hillinger, R. Aebersold and W. Weder

Lung cancer is the leading cause of all cancer-related deaths and treatment options are still suboptimal. It has become evident that predicted and real survival times and treatment responses can vary significantly, even for patients at the same stage of disease. The establishment of prognostic molecular markers which may additionally represent therapeutic targets is therefore of utmost importance. In the post genomic era biomarker studies typically compare RNA or protein abundances in normal versus disease states. However, crucial changes in enzymatic activities remain undetected. Activity-based proteomics became a promising option to circumvent this limitation. In summary, chemical structures termed Activity Based Probes (ABPs) are employed to covalently target active enzymes. Tagged proteins are subsequently affinity purified and qualitatively and relative-quantitatively analyzed with mass spectrometry (**Figure 1A**). Since inactive enzymes remain unlabeled, this approach represents a valid strategy to determine activity profiles even in complex proteomes. Within this study activity profiles of serine hydrolases (SHs) are investigated in human lung adenocarcinoma biopsies, a non-small cell lung cancer (NSCLC) subtype. The serine hydrolase superfamily represents a large and highly diverse class of enzymes, members of which have been linked to lung cancer development. This study aims to establish an activity-based proteomics platform and to investigate the potential role of serine hydrolase activity profiles as prognostic biomarkers in lung cancer.

A directed mass spectrometry (MS) based approach was used for qualitative and quantitative analysis of Activity Based Probe (ABP) labeled proteomes. A fluorophosphate derivative linked to biotin served as an Activity Based Probe. In summary, proteomes were incubated with the ABP and enriched enzymes were digested with trypsin, followed by analysis on an FTICR mass spectrometer. MS/MS data were searched against a recently updated human database (UniProtKB/Swiss-Prot) using the Mascot 2.2 search engine. False Discovery Rates (FDRs) for protein identification were <5%. After initial experiments in data-dependent acquisition (DDA) mode, inclusion/exclusion lists were generated and MS/MS spectra were recorded according to these lists. For relative quantitation MS data were analyzed with Progenesis LC-MS version 2.5 (Nonlinear Dynamics). All experiments were carried out in biological triplicates. The three most intense peptides matching to a protein were considered for analysis. To validate this an ABP labeled enzyme (murine plasmin) was spiked at various amounts into a complex proteome.

Serine hydrolase activity profiles of 40 human lung adenocarcinoma biopsies (TNM stage: I to IV) and corresponding normal lung tissues were compared. On average, 30 serine hydrolases – mostly esterases and proteases – were identified per investigated proteome.

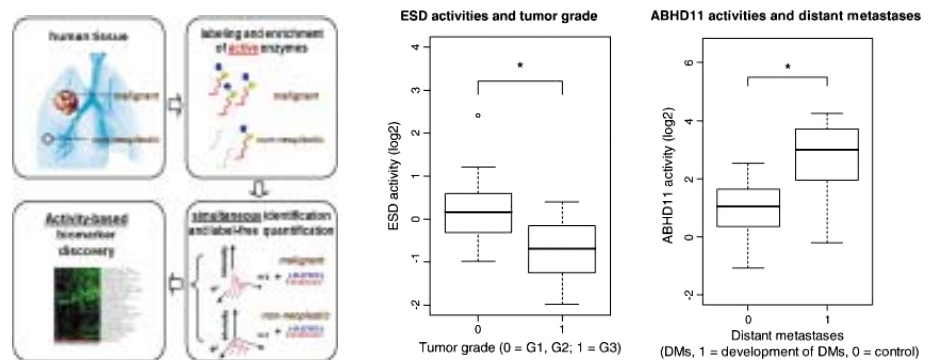


Figure 1:

A) Experimental workflow.

B) Esterase D significantly predicts the presence of poorly differentiated tumors (G3).

C) Abhydrolase domain-containing protein 11 significantly predicts the development of DMs of patients with lymph node metastases (N1, N2) at diagnosis.

With logistic regression we found that the activity of S-formylglutathione hydrolase, also known as Esterase D (ESD) (UniProtKB/Swiss-Prot ID: P10768) significantly predicts the presence of poorly differentiated tumors (G3) in malignant vs. normal tissue ($n(\text{G3})=14$, $n(\text{G2, G1})=15$, $p<0.05$) (**Figure 1B**). The activity of ESD discriminated poorly differentiated (G3) tumors (cut-off value: $p=0.55$) with a misclassification rate of 31%, a specificity of 73% and a sensitivity of 64% as determined by leave-one-out cross-validation (AUC: 0.76). Statistical analysis revealed that the activity of the previously uncharacterized protein Abhydrolase domain-containing protein 11 (ABHD11) (UniProtKB / Swiss-Prot ID: Q8NFV4) significantly predicts the development of distant metastases (DMs) of patients with lymph node metastases (N1, N2) at diagnosis before undergoing radical surgery in malignant vs. normal tissue ($n(\text{DM})=7$, $n(\text{Control})=12$, $p<0.05$) (**Figure 1C**). The activity of ABHD11 discriminated patients (cut-off value: $p=0.4$) with a misclassification rate of 21%, a specificity of 83% and a sensitivity of 71% as determined by leave-one-out cross-validation (AUC: 0.77).

An active-site directed and mass spectrometry based platform for the identification and quantification of biomarker candidates has been established. Activity based proteomics holds great promise in the expanding field of biomarker discovery due to the unique properties of this technology, i.e. isoform specific activity readouts of any given proteome. Investigation of a first cohort of human lung adenocarcinoma biopsies and corresponding normal tissues revealed that the activities of ESD predict the presence of high-grade tumors and the activities of ABHD11 predict the development of distant metastases, both in a statistically significant model.

Selective reaction monitoring for activity-based proteomics in human lung cancer biopsies

N. Le, M. Matondo, S. Hillinger, T. Wiedl, W. Weder, R. Aebersold, S. Arni

Our long-term goal is the use of the activity profile of the serine hydrolase (SH) enzyme superfamily as potential biomarker candidates in human lung adenocarcinoma (LA). In the discovery phase, we could demonstrate that the SH activities of ESD and ABHD11 as potential biomarker candidates for LA, both in a statistically significant model. Now we validate ABHD11, ESD and other SHs activity profiles with a larger cohort of patient tissues and with the selected reaction monitoring (SRM) methodology.

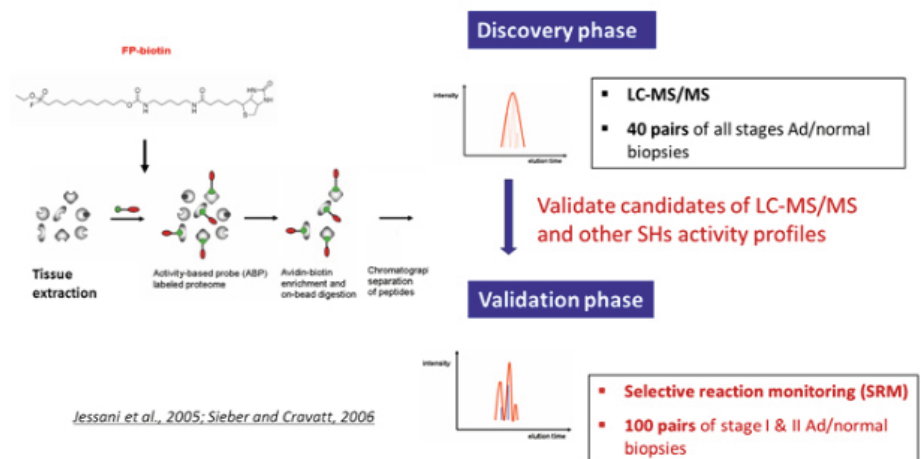


Figure 1. The discovery phase and validation phase of our studies

In this study, a set of 100 adenocarcinomas stage I and II biopsies with 100 matching non-neoplastic biopsies will be analyzed by using quantitative proteomics approach, selected reaction monitoring (SRM). The lysates from 200 biopsies will be labelled with FP-probe to target functional members of the SH superfamily before measuring collected peptides by SRM.

We will also spike in our SILAC labeled peptides to get the relative quantification and use AQUA peptides for absolute quantification during each Mass spectrometry run.

Unlike in other MS-based proteomic techniques, no full mass spectra are recorded in QQQ-based SRM analysis. This leads to an increased sensitivity compared with conventional 'full scan' techniques. The methodology also enables the detection of low-abundance proteins in highly complex mixtures, which is crucial for systematic quantitative studies.

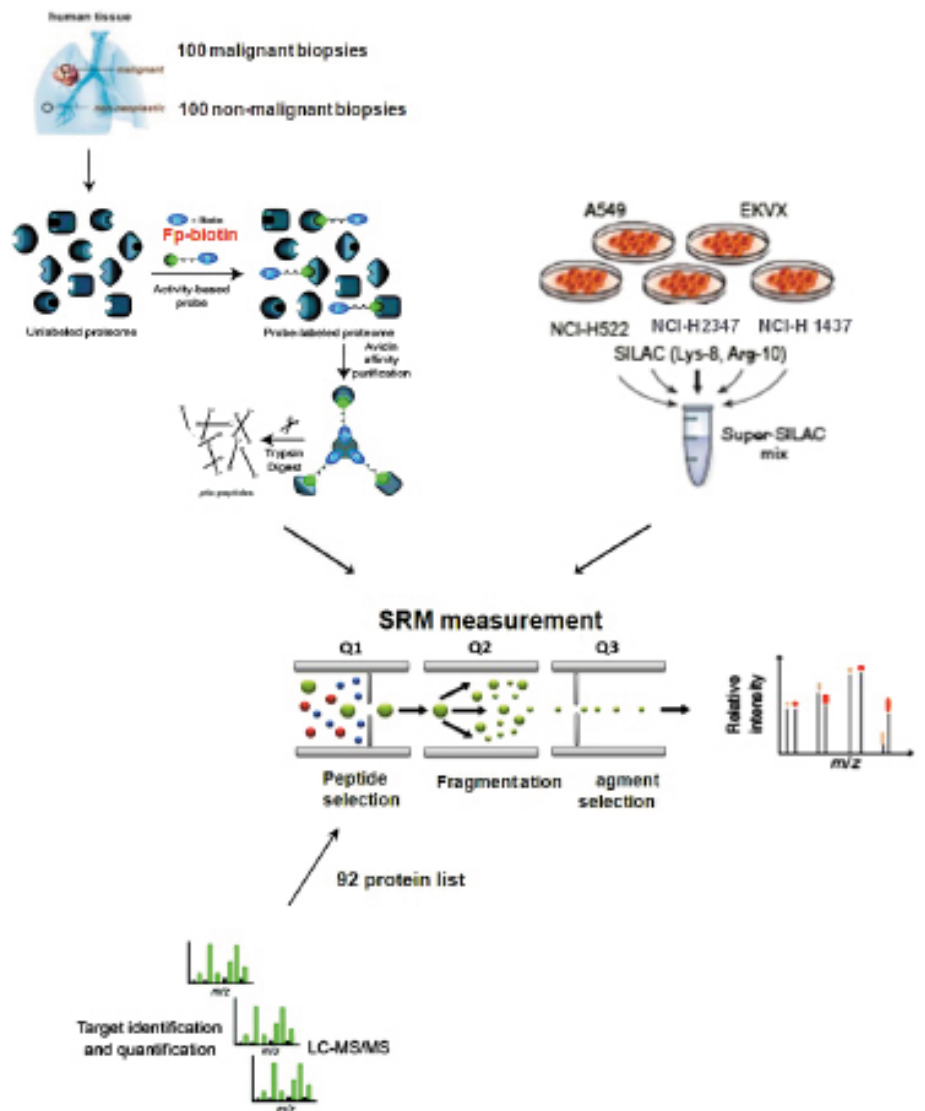


Figure 2. Workflow of SRM-based proteomic experiments for the validation phase

From the list of 121 serine hydrolase enzymes defined by our previous LC-MS/MS, other publications and databases, we detected 92 SH enzymes by SRM experiments, including our 2 candidates ESD and ABDH11. In the next step, assays for measuring 92 proteins will be applied to 200 SH-probe labeled samples. The final goal is to validate the activity changes of ESD and ABDH 11, even other SHs.

We anticipate that ESD and / or ABHD11 activities have the potential to develop into molecular predictors with a reliable clinical significance. The implemented activity-based proteomics platform represents a powerful tool in the search for novel disease biomarkers.

Kras mutation is associated with elevated myeloblastin activity in human lung adenocarcinoma

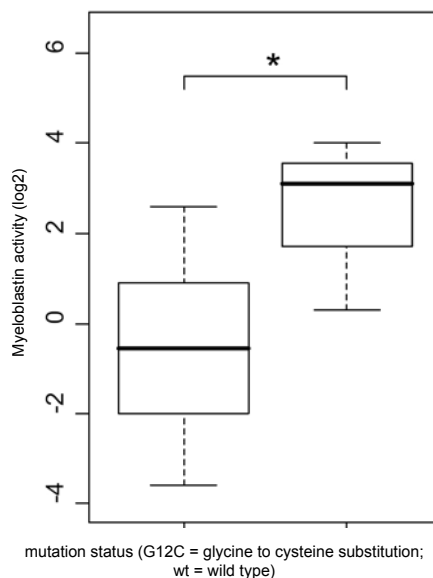
T. Wiedl, S. Collaud, S. Hillinger, S. Arni, P. Schraml, A. Soltermann, H. Moch, W. Weder

Lung cancer is the leading cause of all cancer deaths worldwide with suboptimal prognosis and treatment options. Therefore we aimed to identify molecular characteristics with a predictive clinical utility that at the same time might represent novel therapeutic targets for human lung adenocarcinoma. Within this study we investigated KRAS mutations, a gene frequently mutated in lung adenocarcinoma and their association with enzymatic activities of members of the serine hydrolase superfamily, a large class of enzymes that have previously been linked to cancer.

Participating individuals underwent surgery for lung adenocarcinoma at the University Hospital Zurich between 2003 and 2006. Formalin fixed, paraffin embedded as well as snap-frozen lung adenocarcinoma samples were histologically reviewed by a pathologist. Mutation detection was performed via a custom service by Sequenom. Cell extracts derived from human snap-frozen biopsies were processed prior to mass spectrometric analysis as previously described to analyze serine hydrolase activities.

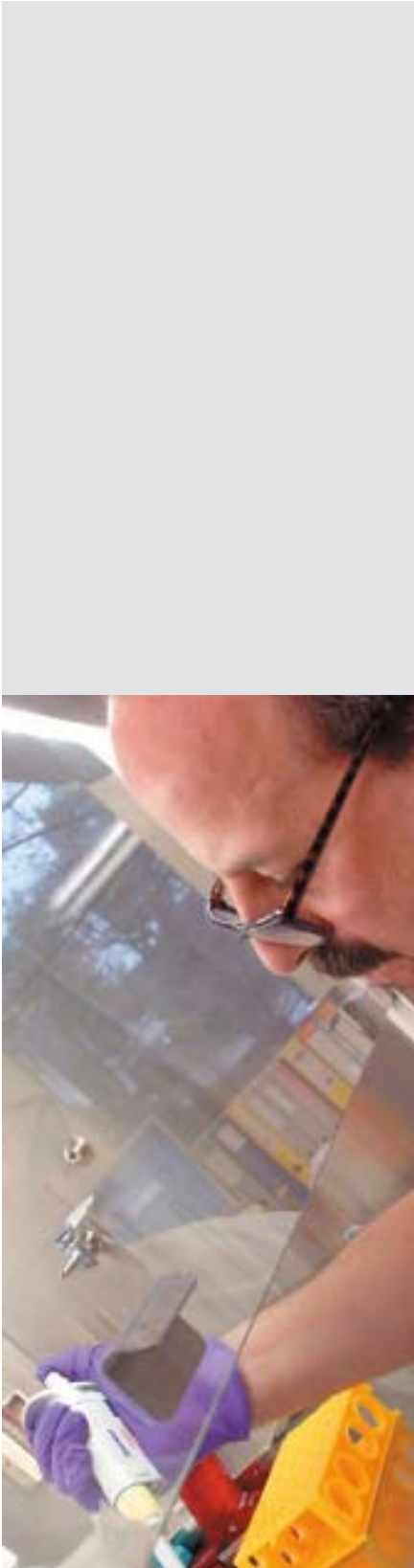
Mutation analysis of 40 human lung adenocarcinoma specimens identified 4 patients (10%) harbouring a cysteine for glycine substitution at position 12 (G12C) in the KRAS gene. By employing two-sided unpaired t-test we found a statistical significant ($p = 0.01$) activity difference of the enzyme myeloblastin between patients harbouring a G12C mutation in the KRAS gene and patients harbouring no KRAS mutation.

Myeloblastin activity and KRAS mutation status



Enzymatic activities of myeloblastin and the corresponding KRAS mutation status.

Myeloblastin (UniProtKB/Swiss-Prot ID: P24158) activities are statistically significant elevated in human lung adenocarcinoma biopsies harbouring a G12C substitution compared to KRAS wild type biopsies ($p = 0.01$, two-sided unpaired t-test, $N(\text{wild type}) = 34$, $N(\text{G12C}) = 3$).



The results of this study revealed that the activity of myeloblastin is significantly altered in lung adenocarcinoma biopsies harboring a KRAS gene mutation. Based on the results of this study we conclude that the combination of activity-based proteomics with mutational analysis is a valid approach for the discovery of novel biomarkers for human lung adenocarcinoma.

Immunotherapy for lung cancer

S. Hillinger, S. Arni

We previously reported an efficient treatment based on the injection of both the commercially available chemokine CCL19 and cytokine IL7 to eradicate lung tumors in murine models. We now produced murine myeloid dendritic cells (mDC) expressing both the chemokine CCL19 and IL7 via adenoviruses. Our final goal is to inject therapeutically transformed mDC in lung tumour bearing mice.

In the previous report we presented one weakness of our orthotopic model. Since then we asked the Zurich veterinarian authorities to perform modifications of our protocol.

In this modified application we are meanwhile approved to do the three following modifications:

- 1) We expected our experiments to last 21 days with an endpoint at day 27. Nonetheless, we reported in our last year report that the orthotopic tumour model with 3LL lung adenocarcinoma cells in C57BL/6 mice was very aggressive. The 500 cells injected in the right lung of mice killed both the control and treated groups in about 10-12 days, which was not long enough to perform our immuno-therapeutical treatment. Now we are allowed to inject the 3LL lung adenocarcinoma cells in the left lung instead of the right lung. We reasoned that the right lung with 4 lobes is more critical for breathing and that the single lobe of the left lung with a reduced air exchange capacity would cause better quality of life to the animal without reducing the impact of our results. We will now perform a small series of 20 mice with a left lung injection of 500 3LL cells.
- 2) We will obtain another clone of the 3LL lung adenocarcinoma encoding the luciferase protein (LL/2-luc-M38 from Caliper bioscience ref cat 119.267). This clone is described to be less aggressive than the parental 3LL clone we are using and we will switch to this less aggressive clone for our future experiment.
- 3) We also do have some problems with the dendritic cells we are using for treatment. Until now we used ex-vivo non-activated dendritic cells. In fact, TNF alpha added in the culture media cause maturation and we will now use dendritic cells activated ex-vivo by TNF alpha as a pilot experiment in a set of mice bearing a subcutaneous tumour. Briefly in a set of 20 mice we will inject 1×10^5 LL/2-luc-M38 cells on the right scapular area of C57BL/6 mice and after 5 days we would start treatment with ex vivo TNF alpha activated mDC directly injected into the subcutaneous tumour.

We are now in the process to obtain the LL/2-luc-M38 from Caliper bioscience ref cat 119.267 and start the experiment described above.

Collaborations:

- Prof. S. M. Dubinett, Director of the UCLA Lung Cancer Program, Dr. S. Sharma, Associate Research Professor, University of California Los Angeles
- Prof B. Cravatt, Scripps Institute, San Diego
- Prof R. Aebersold, Institute of Molecular Systems Biology, Federal Institute of Technology, Zurich, Switzerland
- Prof. H. Moch and Dr. A. Soltermann, Department of Pathology, UniversityHospital Zurich



Prof. Dr. Isabelle Opitz, MD



Dr. Mayura Meerang, Postdoctoral Fellow



Dr. Byron Bitanihirwe, PhD



Martina Friess

Malignant pleural mesothelioma

I. Opitz

Towards the identification of prognostic and predictive markers for malignant pleural mesothelioma

B. Bitanihirwe, I. Opitz

Malignant pleural mesothelioma (MPM) is an aggressive neoplastic proliferation derived from cells lining the lungs. The leading cause of MPM is unprotected contact with asbestos. No cure currently exists for patients afflicted by MPM and as such it remains a significant therapeutic challenge. The identification of novel biomarkers with a reliable prognostic significance therefore represents an ideal means to develop molecular targeted drugs against this malignancy. The phosphoinositide 3-kinase (PI3-K) pathway provides a potential therapeutic target which is activated in various cancers. This pathway is frequently activated in human mesotheliomas where it can be targeted to inhibit mesothelioma cell growth. Several tumor suppressor genes directly implicated in the PI3-K signaling pathway have been identified including phosphatase and tensin homologue (PTEN) and neurofibromatosis 2 (NF2). Indeed, by using a TMA (Tissue Microarray) with biopsies from patients with MPM we discovered that loss of PTEN expression served as an independent predictor for shorter overall survival (*Opitz, Soltermann et al. 2008*). In a similar vein, the NF2 gene has been shown to be frequently inactivated in MPM. The NF2 gene encodes the merlin protein which once activated by de-phosphorylation, translocates to the nucleus and inhibits cell growth and differentiation. Moreover, the inactivation of NF2 has been correlated with an up-regulation of stem cell signaling pathways. Nonetheless, NF2 expression has not been associated with any specific MPM subtype or specific characteristics and has not been linked to prognosis. This study therefore aims to investigate the correlation between functional nuclear NF2 status in addition to key molecules within the PI3-K and stem cell signaling pathways and clinical outcome (overall and progression free survival) in patients treated within a multimodal concept.

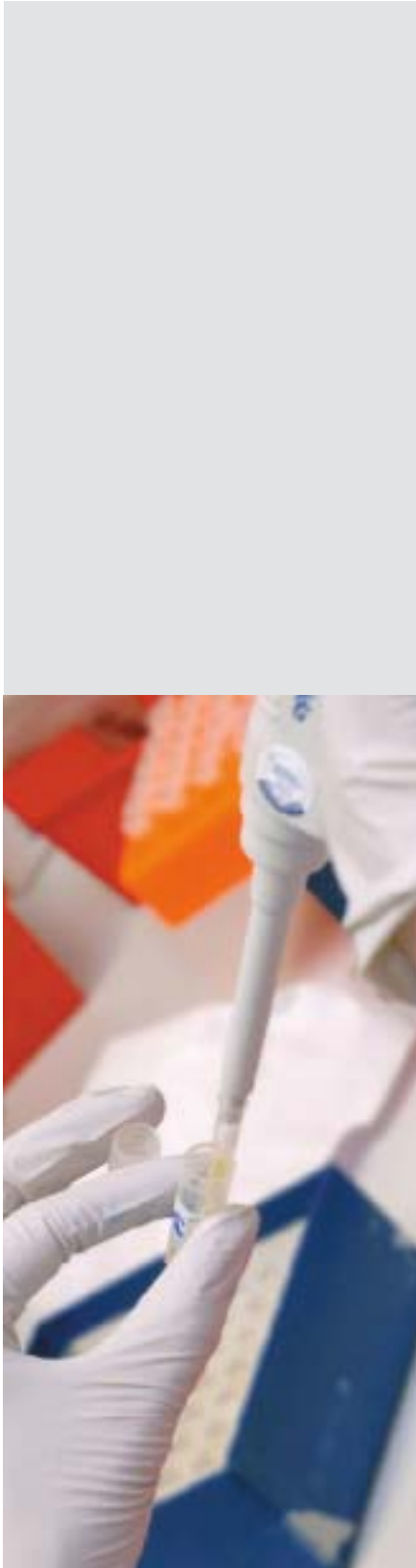
Besides assessing the functional significance of the PI3-K and stem cell signaling pathways in MPM, the expression of the excision repair cross-complementation group 1 (ERCC1) protein will be evaluated and its role as a predictive marker for chemotherapy response will be assessed. The function of the ERCC1 protein is predominantly in nucleotide excision repair of damaged DNA. Measuring ERCC1 expression level may have utility in clinical cancer medicine because one mechanism of resistance to platinum chemotherapy drugs correlates with ERCC1 activity.

A tissue microarray (TMA) containing pre- and post-chemotherapy tumor biopsies and surgical specimens of more than 300 MPM patients has been constructed in collaboration with the Institute of Pathology (historical cohort). All malignant mesotheliomas, diagnosed between 1975 and 2004, were retrieved from the archives of the Zurich Pneumoconiosis Research Group, Switzerland. The tissue specimens were mainly derived from post-mortem examination (77% autopsy). The TMA was classified for the histological subtype (epithelial, sarcomatoid or biphasic) by two lung pathologists.

Clinical data was collected retrospectively. In addition, a prospectively documented patient cohort clinically well-defined comprising 270 patients treated for the diagnosis of MPM has been assembled. A separate Toronto (Canada) TMA consisting of tumor biopsies from clinically well-defined patients has also been constructed during a fellowship in Toronto supported by a Swiss National Foundation travel grant and a Max Cloetta grant awarded to the PI. Both patient cohorts had undergone multimodal treatment and the TMA contains biopsies before and after chemotherapy. The TMAs will be processed for immunohistochemistry using specific antibodies against potential markers. Specifically, the expression of nuclear NF2, PTEN, phosphorylated mammalian target of rapamycin (p-mTOR) and other key molecules in the PI3-K-pathway including phosphorylated AKT (pAKT) will be evaluated. Similarly, the expression of molecules that play an integral role in stem cell signalling pathways (e.g. nuclear YAP) and DNA repair (ERCC1) will be evaluated. After immunostaining, semiquantitative scoring of the nuclear and cytoplasmic intensity of the different markers will be performed by two independent observers as follows: 0 (negative), 1 (mild), 2 (moderate) and 3 (strong). Following the scoring process statistical analyses will be conducted with clinical and pathological variables of patients.

Successful immunostaining of PTEN has been performed in both the Zurich and Toronto perspective cohort TMAs. Statistical analyses will subsequently be conducted on the collected data by including the clinical and pathological variables of patients in to the final analysis. Regarding the NF2 nuclear staining, a protocol has to be established.

Outlook: We are in the process of adapting an established protocol for nuclear NF2 staining (*Li, You et al. 2010*) to formalin fixed, paraffin embedded cells, tissue sections and subsequently TMAs.



Collaborations:

- Toronto General Hospital, University of Toronto
(Dr. Ghassan Allo and Prof. Marc de Perrot)
- Laboratory of Molecular Oncology, University Hospital Zurich
(Prof. Rolf Stahel, Dr. Emanuela Felley-Bosco)
- Department of Pathology, University Hospital Zurich
(Dr. Alex Soltermann, Dr. Svenja Thies and Lukas Frischknecht)

Investigation of the role of hedgehog signaling on malignant pleural mesothelioma recurrence by intracavitary treatment with a hedgehog inhibitor, GDC-0449

M. Meerang, I. Opitz

Localized multimodal treatment currently provides the best survival outcome for malignant pleural mesothelioma; however, local tumor recurrence remains a significant problem. In collaboration with the Laboratory of Molecular Oncology, we have identified the MPM chemoresistant side population cells which maintain precursor properties (*Frei, Opitz et al. 2011*). Moreover, the up-regulation of the stem cell signalling pathway namely, hedgehog signalling pathway could be detected in MPM (*Shi, Y., et al, submitted*). As stem cell signalling plays an important role in tumor recurrence and metastasis, we therefore hypothesized that hedgehog stem cell activation is an important factor in MPM recurrence. We currently aim to determine whether the inhibition of hedgehog signaling is efficient to prevent the tumor recurrence often observed in MPM. We used a potent hedgehog pathway inhibitor, GDC-0449 which inhibits the hedgehog ligand cell surface receptor, smoothened (SMO). GDC-0449 has already been utilised in several clinical trials including medulloblastoma, advanced basal cell carcinoma and in-combination with cisplatin/etoposide in small cell lung cancer. Our studies on localized chemotherapy (cisplatin) with fibrin sealant carrier have been shown to sustain local drug concentration and reduce systemic toxicity (*Opitz, Lardinois et al. 2007; Opitz, Erne et al. 2011*). Based on this previous accomplishment, we aim to apply GDC-0449 intracavitarily in combination with cisplatin-fibrin sealant to a rat bioluminescent MPM recurrence model, following surgical resection of the tumor. This tumor recurrence model developed in our laboratory allows us to perform non-invasive and repetitive observation of tumor growth as bioluminescent signal produced from tumor cells has been shown to correlate with the actual tumor volume. (*Shi, Hollenstein et al. 2011*). The molecular mechanisms of the hedgehog signalling pathway in MPM will also be investigated.

Collaborations:

- Laboratory of Molecular Oncology, University Hospital Zurich
(Prof. Rolf Stahel, Dr. Emanuela Felley-Bosco)

Clinical Staging for malignant pleural mesothelioma

I. Opitz, W. Weder

In this project, we aim to assess the value of different modalities for a better clinical staging and assessment of therapy response of malignant pleural mesothelioma (MPM) including computed tomography (CT)-scan, positron emission tomography-CT (PET-CT), PET-magnetic resonance (MR) (*Frauenfelder, Tutic et al. 2011*).

Patients with proven MPM will undergo chest CT scan and PET-CT before and after chemotherapy. Tumour response will be measured and classified with modified RECIST criteria and compared to tumour volumetric approach in CT-scans, the metabolic response will be defined in PET-CT. Clinical staging will be obtained using TNM classification and IMIG-stages with the help of CT- and PET-CT. Furthermore, the maximum SUV, the total glycolytic volume will be assessed for every patient (70 patients with pre-induction CTX CT and PET-CT). In a separate project, patients will be staged retrospectively based on CT and PET-CT by 2 independent observers (2 radiologists and 2 thoracic surgeons) and inter-observer correlation in clinical staging will be assessed. PET-MR will be assessed for specific patient groups with focus on comparison of chest wall invasion (separate protocol).

Outlook: Improvement of the diagnostic tools would help to select patients for treatment of MPM.

Collaborations:

- Laboratory of Molecular Oncology (Prof. Rolf Stahel), UniversityHospital Zurich
- Institute of Biostatistics (Prof. Burkhard Seifert), University of Zurich
- Institute of Radiology (Dr. Thomas Frauenfelder and Dr. Roger Hunziker) UniversityHospital Zurich
- Division of Nuclear Medicine (Prof. Hans Steinert), UniversityHospital Zurich

Localized intracavitary therapy for MPM – from bench to bedside

I. Opitz, W. Weder

Our newly developed intracavitary chemotherapy with cisplatin loaded in to a fibrin carrier for MPM will be applied into clinical application (*Lardinois, Jung et al. 2006; Opitz, Lardinois et al. 2007; Opitz, Erne et al. 2011*). Safety and tolerability, and later efficacy will be assessed in mesothelioma patients who underwent prior surgery. This study comprises of Phase I-dose-escalation trial and Phase II trial for the confirmation of safety and tolerability of intracavitary cisplatin-fibrin after Pleurectomy/Decortication (P/D).

The primary objective of the phase I is to determine the maximally tolerated dose (MTD) of intracavitary cisplatin-fibrin in patients with MPM. The secondary objectives of the phase I are the safety and tolerability of intracavitary cisplatin-fibrin. Furthermore, the recommended dose of intracavitary cisplatin-fibrin for exploration in a phase II study will be assessed. Patients' outcome will be measured by assessment of overall (OAS) - and progression free survival (PFS) in order to determine the efficacy of the treatment. Moreover, the pharmacokinetics for the use of intracavitary cisplatin-fibrin in humans will be studied.

In order to gain more information about the intracavitary application of cisplatin-fibrin at the MTD, a phase II study with 20 more patients will be conducted. Primary Endpoint will be to study the safety and tolerability of intracavitary cisplatin-fibrin after radical P/D at the MTD in 20 patients. Secondary Endpoints will be to study the efficacy of intracavitary cisplatin-fibrin by assessment of OAS and PFS. Further studies of the pharmacokinetics of intracavitary cisplatin-fibrin in humans will be performed. The effect of cisplatin-fibrin on mechanisms of resistance to cisplatin will be assessed by determination of marker for senescence and apoptosis.

Outlook: With this study, we expect to transfer local tumor control for predominantly locally recurring MPM by introduction of intracavitary application of cisplatin-fibrin after radical surgery into clinic.

Collaborations:

- Division of Pharmacology and Toxicology (Dr. Alexander Jetter)
UniversityHospital Zurich
- Laboratory of Organic Chemistry (Prof. Detlef Günther), Swiss Federal
Institute of Technology
- Laboratory of Molecular Oncology (Prof. Rolf Stahel, Dr. Emanuela
Felley-Bosco), UniversityHospital Zurich
- Guillaume Wuilleret (Dissertation)

2.7 Urological Research



Prof. Dr.
Tullio Sulser, MD



PD Dr.
Maurizio
Provenzano,
MD, PhD



Damina Balmer
Scientific Coordinator



PD Dr.
Maurizio
Provenzano,
MD, PhD



Irina Banzola,
M.Sc.



Dr. Boris Fischer,
MD



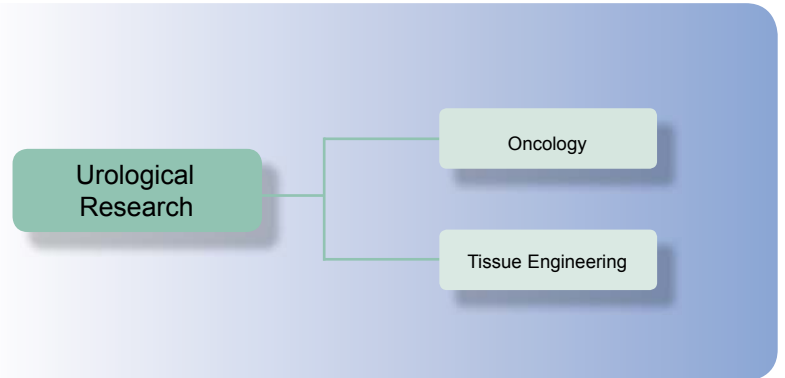
Dr. Cédric Poyet,
MD



Dr.
Mohammad Pooya,
MD, PhD



Giovanni Sais,
M.Sc.

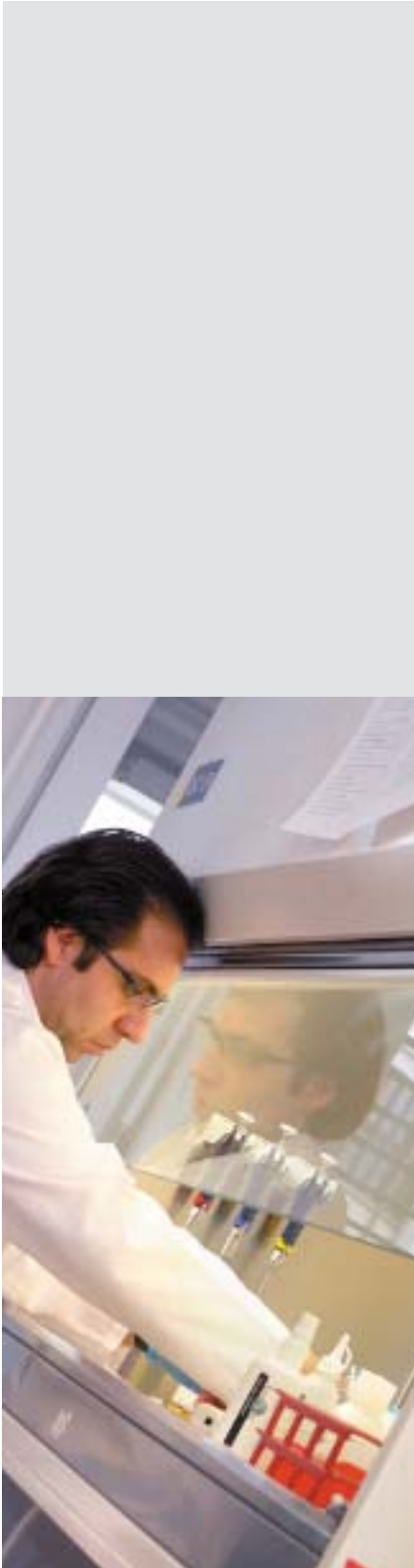


2.7.1 Oncology

Prostate cancer (PCa) is one of the most common solid cancers and one of the most important causes of morbidity and mortality worldwide in men. It is of relevance that prostate tissues appear to be characterized by features consistent with an immunosuppressive microenvironment. Infiltrating CD4+ and CD8+ T lymphocytes (TIL) are predominantly characterized by regulatory and functionally exhausted (PD-1+, B7-H1+) phenotypes, respectively. Furthermore, enhanced suppressive function of adaptive CD4+ Treg has been observed in the peripheral blood of patients with PCa and found to correlate with metastatic behavior. Indeed, factors orchestrating chronic inflammation and immune suppressions, such as IDO and TGF- β 1, and most likely mediators for PCa morbidity, also including IL-1 β , IL-6 and MMP9, might be considered positively associated to prostate cancer and thus their detection in urine might contribute to discrimination between indolent and aggressive cancer. Indeed, we were able to identify and/or to confirm eight tumor derived factors (TDFs) involved in PCa onset and progression, such as IL-1 β , IL-6, IL-7, IL-10, TGF- β 1, IDO-1, IDO-2 and MMP-9, either at a constitutive level or prevalently over-expressed within a pro-inflammatory environment (upon IFN- γ and/or TNF- α stimulation). In addition, we demonstrated that tumor cells featuring low grade prostate cancer (i.e. CAHPV-10 cells), more than those characterized by high migration potential (i.e. PC3), retain an epithelial phenotype through the expression of E-cadherin and that a mesenchymal transition, as represented by a higher expression of vimentin, is observed upon pro-inflammatory stimuli (in particular TNF- α). This finding was also sustained by functional analysis regarding cell proliferation and cell invasion/migration of both cell lines upon inflammatory stimuli. Among inflammatory agents, Polyomavirus BK infection has been postulated to contribute to the genesis of proliferative inflammatory atrophy (PIA) in the prostate and the virus has repeatedly been suggested to be associated with cancer of the genitourinary tract. However, possibly due to conflicting results regarding detection of specific sequences and proteins in human cancers, its oncogenic role is controversial.

The expression and detection of the BKV main regulatory protein Large tumor antigen (L-Tag) in pre-neoplastic prostate tissues prompted us to investigate the role of this viral antigen as target of cellular immune response in patients bearing PCa. We have analyzed the immunological profile exerted by L-Tag peptide-specific induction in newly diagnosed PCa patients by means of BKV L-Tag serology and local molecular testing, and compared it to age-matched benign prostatic hyperplasia (BPH) patients. Data were correlated to 5-year follow-up clinical information. We have identified a positive correlation between BKV L-Tag specific IgG activity and immune responsiveness with a regulatory pattern (a higher expression/production of IL-10 and TGF β -1 and a low expression/production of IFN- γ and TNF- α genes/proteins) unique to BKV L-Tag induction in patients bearing PCa with BKV L-Tag positive lesions and with evidence of biochemical recurrence (BR). Furthermore, in these PCa patients, the L-Tag derived peptides significantly boosted IL-10 secreting CD4⁺CD25^{+(high)}/FoxP3⁺/CD103⁺ T cells exerting suppressive functions of autologous CD4⁺,CD25⁻ fractions. Based on this finding, we were thus interested in identifying cellular immune responses to antigenic portions of the L-Tag in BKV seropositive PCa patients. Four HLA class I and II restricted 15mer peptides were able to exert a specific immune response characterized by high IFN- γ and TNF- α gene expression and protein production from cytotoxic T cells, both CD4⁺ and CD8⁺, with a CD107⁺, PD-1⁻ effector-memory phenotype. A systemic boosting of memory T cells from BKV seropositive prostate cancer patients using immunogenic domains within BKV L-Tag would thus implement an effector T cell response possibly favoring an active immune surveillance against immune regulatory patterns constitutively expressed in PCa patients and, as reported by us, sustained by BKV L-Tag. Our data provide important novel contributions to the analysis of the increasingly puzzling relationship between BKV infection and PCa by identifying subpopulations of patients deserving major attention in translational research and, most importantly, by highlighting subtle peculiarities of immune responses against BKV L-Tag in patients with PCa, with previously unsuspected associations with the clinical course of this disease.

Bladder cancer is the fifth most common type of cancer (following lung, colon, prostate and breast cancers), the fourth for incidence among men and the eighth among women and it has been the cause of death in approximately 150,000 patients worldwide in 2008. Bladder cancer is generally classified into non-muscle invasive (NMIBC; 80%), thereafter referred as to superficial, and muscle-invasive cancer (MIBC) based on the natural history of the tumors. Among superficial tumors, almost 70% recur after transurethral resection and 10-20% of them show progression into MIBC. Due to the worse prognosis of MIBC, there is a high interest in identifying treatment that can clear superficial cancers with a high risk of progression. It has been seen that administration of psoralen metabolites (photoreactive chemical substances, such as the 8-methoxypsoralen; 8-MOP) followed by UVA irradiation (PUVA treatment) has the capacity of reducing viability and proliferation of treated cells, also leading them to apoptosis. However, PUVA might bear toxic effects. Thus, the selection of



treatments combining low doses of UVA with better effect in bladder cancer patients is the main interest of our investigation. Our preliminary data state that the administration of standard doses of 8-MOP (250 or 500ng/ml) followed by the exposition to low doses of UVA, such as 0.5 J/cm², over 96 hours (PUVA treatment) has a significant anti-growth effect on human bladder cancer cells by blocking cell proliferation, metabolic activity and by triggering apoptosis, particularly in those cells featuring grade III. These results suggest a possible relevant use of PUVA therapy for the treatment of NMIBC, thus combining lower doses of UVA with positive clinical outcomes. In addition, approximately 25% of patients undergoing surgery for bladder cancer show lymph nodal metastases (LN+). Indeed, there is a high interest in studying the role of lymph-angiogenic factors in patients that bear superficial cancers (NMIBC) with high risk of disease progression (LN+), in order to redirect treatment options. Our data, aimed at defining the relevance of lymph-angiogenesis in bladder cancer progression, showed that the expression of vascular endothelial growth factor A, C, and D varies among bladder cancer cell-lines at constitutive level and correlates with bladder cancer cell-line grading. Moreover, we also observed that such variation might differently modulate the expression of lymph-angiogenic-related receptors (such as VEGFR-2 and 3) and factors expressed by lymphatic endothelial cells (LECs) when co-cultured with bladder cancer cells. LEC gene modulation upon co-cultures with different bladder cancer cell lines showed a relevant over-expression of genes involved in LECs migration and maturation (SLP-76, Ang-2, PDPN). This modulation seems to be VEGF-C dependent, since microenvironments generated by low grade bladder cancer and characterized by higher expression of VEGF-A do not induce same LEC gene expression profiling. In addition, VEGF-C and, to a lesser extent, VEGF-A but not VEGF-D, can directly enhance the migration potential of LECs. Furthermore, our data suggest for a paradoxical expression in LECs of signalling proteins, such as SLP-76, that have been reported to be expressed by different cells, such as platelets. It is thus tempting to speculate that the generation of new lymphatic vasculature, mainly sprouting from pre-existing blood vessels and typically enhanced by PDPN triggering to platelets, could be also possible in areas where sprouting from pre-existing lymphatic vessel occur, a frequent event in cancer.

Collaborations:

- Molecular Tumour Pathology, Department for Surgical Pathology, University Hospital Zurich.
- Institute of Pharmaceutical Sciences, Federal Institute of Technology, Zurich, Switzerland
- Institute for Surgical Research and Hospital Management, Oncology section, University Hospital of Basel.
- Institute for Medical Microbiology and Division of Infectious Diseases, University of Basel.

2.7.2 Tissue Engineering for Urologic Tissues



PD Dr.
Daniel Eberli,
MD, PhD



Dr.
Meline Stölting,
MD, PhD Student



Dr.
Fahd Azzabi,
PhD



Dr.
Souzan Salemi,
PhD



Dr.
Srinivas Madduri,
PhD



Dr.
Lukas Brügger,
MD



Dr.
Lukas
Hefermehl, MD



Dr.
Maya Horst,
MD



Dr.
Remo Largo,
MD



Dr.
Roman Inglin,
MD



Dr.
Mathias Tremp,
MD



Fatma Kivrak,
M.Sc.



Sarah Nötzli,
M.Sc.



Virginija Jovaisaite,
Master Student



Venkat
Ramakrishnan,
Fulbright Fellow



Jakub Smolar

Optimization of Minimal Invasive Injection Technique for the Urethral Sphincter Using Imaging Technologies

L. Hefermehl, T. Sulser, D. Eberli

Currently our laboratory is focusing its research efforts on a treatment for urinary incontinence using adult muscle stem cells. These cells in a collagen solution will be injected precisely into the patients urinary sphincter muscle. Still, there is no established injection technique for precise stem cell injection. The optimal visualization of the sphincter and the injection technique in humans remains to be found. The ultimate goal of this research step is to develop an optimal injection device as well as to assess its precision prior to clinical trials.

In a combined effort of the Department of Urology, Radiology and Anatomy of the University of Zurich and together with the Department of Gynecology of the Medical University in Graz, Austria, as well as together with engineers from B-K Medical we have performed several promising experiments.

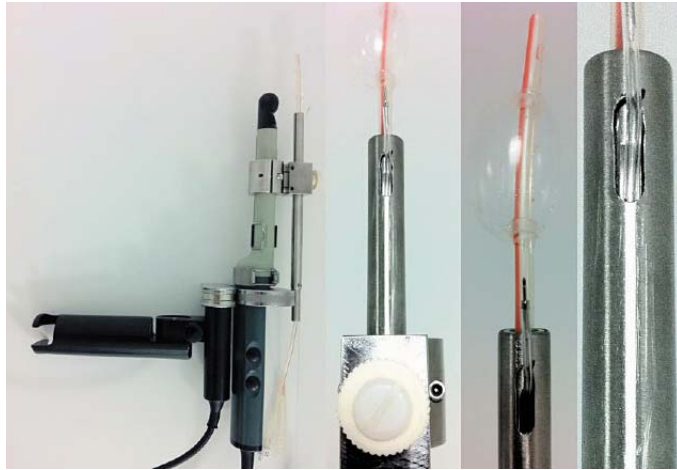
After we have spent much effort in determining the imaging modality in 2010 (MRI vs. ultrasound) we have then chosen ultrasound for our further investigations, due to its superior qualities particularly the possibility of real time guidance.

In 2011 we now focused on ultrasound guided injections techniques. We compared to different injection options: transurethral and transvaginal injections. Therefore we performed transvaginal ultrasound (*BK 8848, BK Medical, Denmark*) guided injections of fluid polymer compounds (liquid polymer which hardens after application) into urinary sphincter muscles of Thiel fixated human cadavers. The sphincter was then analyzed by MRI and histology of whole mount sections. Both methods showed good and comparable accuracy in hitting the rhabdosphincter. However, the transurethral approach seemed to be superior in means of simplicity primarily due to handling and shorter learning curve. As announced in our 2010 report, we have now developed a sophisticated tool for needle guidance, which allows standardized injections into the sphincter muscle of female patient. It is composed of stainless steel, which offers the option of sterilization and pursues international requirements for medical instruments.

Summary and outlook

We have now moved forward from choosing an imaging modality (MRI vs. ultrasound) and choosing an injection option (transvaginal vs. transurethral) to a now final prototype of an distinguished needle guidance device which seems feasible for human application. We will perform several injection experiments on human cadavers with this prototype. Once we have gained enough expertise in detecting an hitting the urinary sphincter muscle in Thiel fixated bodies we will proceed to our clinical trials.

The development of this key tool would not have been possible without the significant support of the Swiss National Foundation.



Injection device for transurethral injections.

The tip of the tube can be introduced into the urethra. A 10 Fr balloon catheter is placed through the device. This allows a steady distance to the bladder neck. The needle is pushed through the device leading to an optimal injection angle. A plastic knob enables continuous rotation of the device, which allows 360° injection into the urinary sphincter muscle.

Tracking of human Muscle Precursor Cells by MRI and Muscle regeneration *in vivo*

F. Azzabi Zouraq, V. Jovaisaite, L. Hefermehl, A. Boss, M. Rudin, T. Sulser, D. Eberli

Stress Urinary Incontinence (SUI), the involuntary loss of urine, is a medical problem that affects millions of people worldwide. Recent research suggests stem cell therapy as a potential solution to restore a normal sphincter function. Clinical trials to treat SUI by autologous Muscle Precursor Cells (MPC) transplantation are currently in preparation. In addition to functional follow-up, evaluation of cell survival and tissue formation is essential for understanding and improvement of cell therapies. Unfortunately, a biopsy of the newly engineered muscle would counteract the anticipated treatment. Therefore, tracking transplanted stem cell populations by a non-invasive manner, such as Magnetic Resonance Imaging (MRI), is desirable. One of the methods to render the cells clearly visible by MRI is intracellular incorporation of Superparamagnetic Iron Oxide Nanoparticles (SPION) prior to transplantation. In this study we explored detrimental effects of increasing intracellular levels of SPIO *in vitro* and aimed to define a safe concentration in which human MPCs can be easily detected by MRI, without altering their cellular functions.

Human MPCs were harvested following standard protocols and then labelled with increasing concentration of SPION (Endorem[®], 100 – 1600 µg/mL). In the following passage labelling efficiency, cell viability, growth, molecular characteristics and differentiation were examined *in vitro*. MPCs labelled with 400 µg/mL SPIO were then injected into the subcutaneous space of nude mice and followed for 4 weeks by MRI imaging. At harvest muscle tissue formation was assessed macroscopically and by immunohistochemistry.

Majority of cells were labelled, when 200 $\mu\text{g}/\text{mL}$ or more of SPIO was used. Labelling with more than 800 $\mu\text{g}/\text{mL}$ of iron oxide reduced the viability of cells by 15-25%. In the long term, 800-1600 $\mu\text{g}/\text{mL}$ SPIO activated cell growth while it decreased MPC differentiation ratio by 10%. Using SPIO concentration of 400 $\mu\text{g}/\text{mL}$, no effects on cell viability, growth, differentiation and muscle - specific marker expression were detected, while labelling allowed the cells to be detected by MRI. Labelled human MPCs were then injected into the subcutaneous space of nude mice. Transplanted cells formed a muscle tissue, as confirmed by histological analysis.

Location of the muscle was detectable by MRI for at least 4 weeks.

Our data concludes that the optimized conditions of MPC labelling can be safely used in clinics to track sphincter muscle regeneration in patients under SUI treatment by cell therapy.

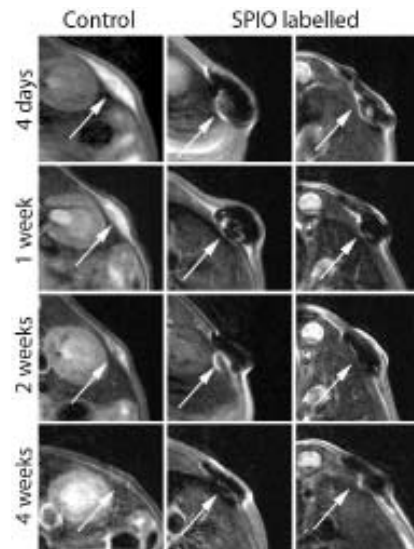


Figure 1: MRI scanning of injected human MPCs without and with iron oxide particles (control). Cultured MPCs from biopsy were labelled with iron oxide particles (SPIO) one day prior to injection subcutaneously in nude mice. The cells could be tracked for as far as for 4 weeks by MRI scanning.

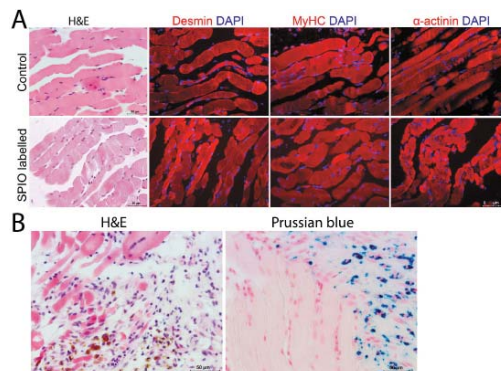


Figure 2: Fiber formation and immunohistochemistry of tissue engineered muscle after MPCs injection in nude mice. Human cultured MPCs and labelled with iron oxide particles were injected subcutaneously in nude mice. After 4 weeks, the tissue engineered muscle were harvested and stained with different technics (H&E, Prussian blue and specific marker of muscle as desmin, Myosin heavy chain and alpha-actinin). The injected SPIO labelled MPCs were capable in forming fibers and possess specific characterisation of muscles.

Xeno-free culturing of human Muscle Precursor Cells (MPC) for clinical application

F. Azzabi Zouraq, S. Salemi, R.A. Largo , K. Schallmoser, D. Strunk, T. Sulser, D. Eberli

Autologous cell therapies are envisioned as a promising therapy for many diseases including urinary incontinence, where sphincter muscle damage leads to urine leakage and significantly reduces the quality of life. Recent animal models demonstrated the validity of the method showing regeneration of sphincter muscle tissue after injection of MPCs. Currently, these cells are expanded in xenogenic media containing fetal bovine serum (FBS). However, before MPCs can be applied clinically it is mandatory to reduce the potential immunogenic reaction and infection risk by removing any xenogenic contaminants.

In this research human MPCs were expanded in xeno-free medium using pooled human platelet lysates (phPL) or pooled human Serum (HS). We assessed the expansion potential, the differentiation by FACS and the fibre formation *in vitro*. Further, we assessed the *in vivo* muscle tissue formation after injection and contractility by organ bath. Cells grown in standard FBS medium served as controls. Our results clearly demonstrate that HS is no substitute for FBS with the MPC showing signs of senescence and decreasing in growth. Using phPL we were able to expand the MPCs while maintaining the myo-phenotype as demonstrated by FACS and IHC for MyoD, desmin and MHC. Expanded MPCs gave rise to contractile muscle tissue *in vivo*, comparable to tissues grown using cells expanded in FBS.

In conclusion, our results show that hPL is a suitable substitute for FBS and may be used for clinical application.

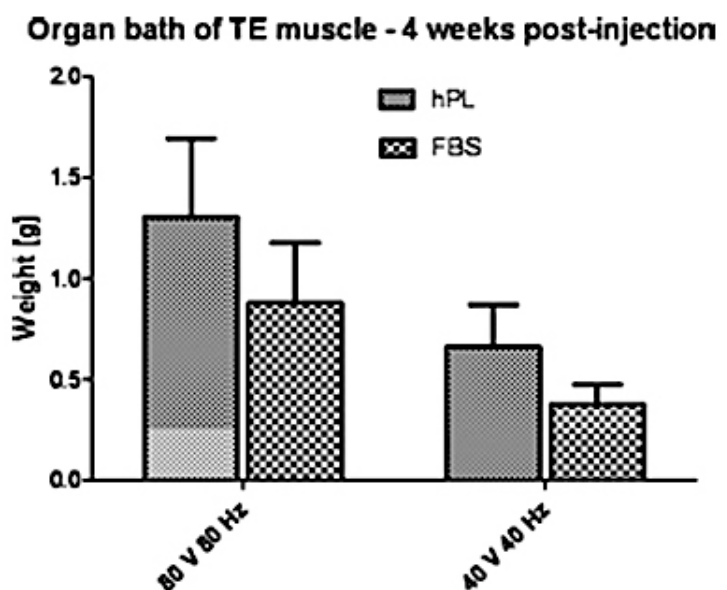


Figure.1: Organ bath of formed tissue engineered muscle. Injected MPCs grown in different mediums based either on FBS or pooled human platelet lysate were injected subcutaneously in nude mice. Four weeks post-injection, the tissue engineered muscle were harvested and tested for their contraction with organ bath techniques. The tissue engineered muscles rising from cells grown in xeno-free mediums were also capable in giving functional muscles.

Induction of Mature Vascular Networks *in vivo* by Longterm Cell-demanded Release of TG-VEGF121

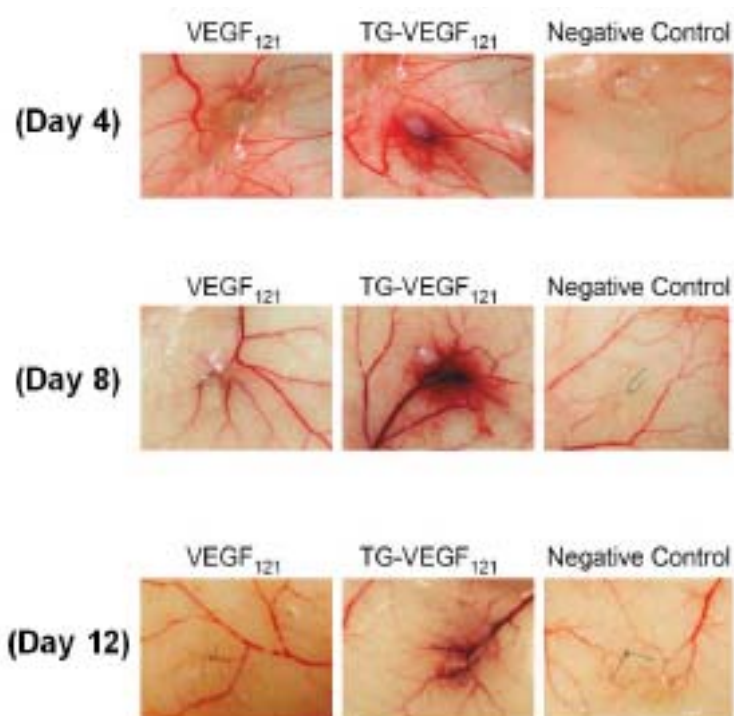
R.A. Largo, J. Marschall, V.M. Ramakrishnan, A. Ziogas, J. Plock, T. Sulser, J. Hubbell, K. Lorentz, D. Eberli, M. Ehrbar

The establishment of mature vascularisation in ischemic and engineered tissues by biomaterial engineering and growth factor delivery remains a major challenge. Recently, a fibrin engineering platform that allows for the covalent immobilization of peptides and proteins has been described. This scheme has been employed to deliver engineered angiogenic growth factors such as angiopoietin-1 (TG-Ang-1), Ephrin B2 (TG-EphrinB2), and vascular endothelial growth factor (TG-VEGF). However, control over growth factor delivery from such fibrin gels has been hampered by their *in vivo* ephemerality. To modulate the proteolytic stability of fibrin gels and consequently the release profile of the VEGF we have simultaneously incorporated TG-VEGF and protease inhibitor Aprotinin (TG-Aprotinin). Fibrin gels that were formed in presence or absence of TG-VEGF and contained different concentrations of TG-Aprotinin were subcutaneously implanted in the back of immunocompromized mice. The covalent immobilization of variable amounts of TG-Aprotinin resulted in a series of fibrin gels whose lifespan in murine subcutaneous pockets could be tuned from 2 to more than 4 weeks. Our gross morphological, histological, and histomorphometrical evaluations indicate that vascular leakiness and angiogenic response (vessel number and maturity) is greatly dependant on the fibrin gel stability. As the magnitude of angiogenesis was only due to materials properties and not to growth factor dosing, these findings indicate that the growth factor efficacy and bioactivity can be largely influenced by its mode of delivery. Furthermore, by varying the materials composition the release profile of growth factors can be tailored towards site and treatment specific requirements. Thus, this translational work not only represents a significant step forward towards developing mature vascular networks for engineered tissues but might also find use in other tissue engineering and drug delivery applications.

Improving Urinary Sphincter Engineering by Pre-Establishment of a Vascular Network

R.A. Largo, V.M. Ramakrishnan, J. Marschall, A. Ziogas, J. Plock, T. Sulser, M. Ehrbar, D. Eberli

The use of autologous cells could be ideal in reversing sphincter muscle damage. Until now, the construction of large volumes of functional muscle tissue with muscle precursor cells (MPC) is limited by insufficient angiogenic induction. Certain strategies, like transient expression of VEGF₁₆₅-transplanted MPCs, were not sufficient in supporting sustained muscle growth. Therefore, we engineered a fibrin gel which allows cell-demanded release of covalently bound TG-VEGF₁₂₁ (TGV). Our *in vitro* data demonstrated the stability (confirmed by ELISA) and maintenance of biological activity of TGV over 3 weeks, which was confirmed by HUVEC proliferation assay and Western blot of proteins involved in downstream signalling pathways (pVEGF-R, ERK1/2). Fibrin gels with covalently bound TGV implanted into the subcutaneous space of nude mice revealed robust induction of new vessels by fibrin-bound TGV over a period of 12 days. Non-bound VEGF₁₂₁ failed to support vessel formation (histology/IHC/vessel density). Further, we demonstrated that remaining TGV liberated from explanted fibrin gels (day 12) retained its biological activity. Taken together, these data demonstrate that fibrin constructs containing covalently-bound TGV can form a robust neo-vascular network. Within a translational context, this slow release material can be injected directly into a damaged sphincter before cell therapy. Well-vascularized tissue could support functional muscle tissue development after cell injection. This method could impact many organ systems and help to overcome current limits in organ engineering.



Use of Adipose Derived Stem Cells for Bladder Engineering

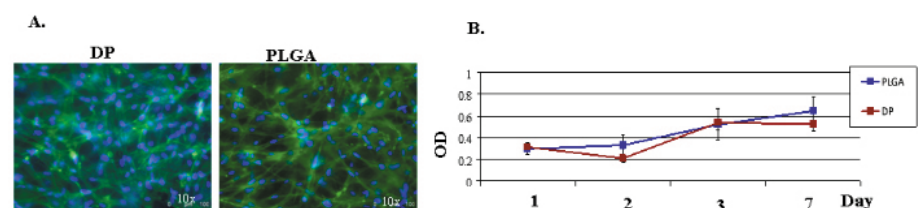
S. Salemi, M. Tremp, R. Gobet, T. Sulser, D. Eberli

Adipose derived stem cells (ADSCs) can be differentiated to smooth muscle cells (SMCs) and might offer a cell source for hollow organ engineering. However, differentiation is a complex process and has a dramatic effect on cell size, shape, membrane potential, metabolic activity and responsiveness to external signals. The optimal level of differentiation of ADSCs to SMCs for use in tissue engineering is not defined. Therefore, we have investigated the cellular alterations during differentiation of ADSCs into SMCs and evaluated the effects on cell behavior in two 3D scaffold systems.

Primary rat ADSCs were characterized by morphological analysis, immunofluorescent (IF) and FACS. ADSCs were differentiated towards SMCs and changes were investigated by FACS, Real time PCR and Western blot (WB). To evaluate whether all differentiated ADSCs or SMCs are able to grow and further differentiate in a 3D environment we seeded the cells on two different bioabsorbable materials (poly (lactic-co-glycolic) acid (PLGA), polyesterurethane polymers (DegraPol[®], DP). The cells viability and proliferation were evaluated by MTT assay, morphology and attachment were observed by microscopy. The cell ingrowth and 3D structure of both the materials were compared by confocal microscopy.

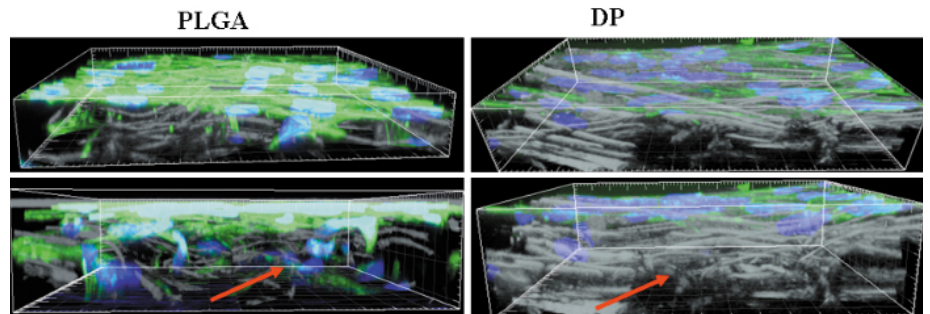
At passage 3 ADSCs showed positive expression of lineage specific markers beta-1 integrin (CD29; $45.5\% \pm 13.6$), hyaluronate receptor (CD44; 48.2 ± 10.7), stro-1 (35.5 ± 3.4) and hematopoietic marker (CD34; 4.5 ± 2.7). Real-time PCR demonstrated gradual fold increase in mRNA expression of caldesmon, myosin heavy chain 11 (MHC), and smoothelin during 1 to 4 weeks of differentiation to SMCs compared to undifferentiated ADSCs. Furthermore WB analysis revealed increased levels of smoothelin and calponin protein expression during differentiation process.

Seeded ADSCs on PLGA and DP adhered very well on the scaffolds and an increased proliferation was observed. Using confocal microscopy we could see good cells ingrowths in both the scaffolds. However more ingrowths were observed in PLGA seeded cells than DP.



Immunostaining of ADSCs

ADSCs were cultured on DP and PLGA for 72h. Green colour indicates cell growth and proliferation of ADSCs within the scaffold. Green; Phalloidin staining for cytoplasm. Blue: DAPI nucleus staining. **B:** MTT assay demonstrating cell survival and proliferation of ADSCs on DP and PLGA.



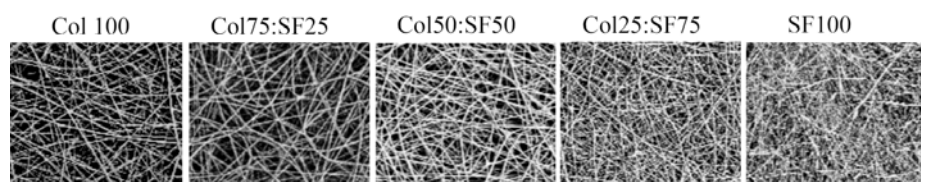
Confocal microscopy.

3D images of FDSCs growth on PLGA and DP demonstrating a superior cell growth and penetration on PLGA.

Hybrid composite scaffold delivering guidance structures and multiple neurotrophic factors for hollow organ innervation

S. Madduri, D. Eberli

Autonomic axonal innervation of tissue engineered hollow organs is critical. We have developed a composite scaffold for delivering 3D guidance structures and multiple neurotrophic factors (nerve growth factor (NGF) and glial derived neurotrophic factor (GDNF)), to promote sympathetic axonal regeneration. 5 different composite biomaterials consisting of a polymeric membrane and electrospun nanofibrous scaffold incorporated with single factor NGF or GDNF alone or both NGF + GDNF were fabricated from collagen (Col 100), silk fibroin (SF 100), Col75: SF25, Col50: SF50 and Col75:SF25, in order to tailor the growth factors release kinetics. All delivery systems showed sustained, but significantly different release kinetics of biologically active NGF and GDNF. Pure collagen based delivery system showed a high burst release of NTFs over first 4 days. Where as, hybrids of Col and SF showed significantly decreased initial burst release, but more sustained NTFs release with increase in SF content. Bioactivity of NTFs release over 30 days was confirmed by PC12 and N2A cells. Further, significant differences in the growth response of chicken embryonic sympathetic ganglionic explants cultured on 5 different scaffolds were observed showing the importance of release kinetics. Engineered polymeric composite scaffold with controlled release of multiple NTFs supports axonal regeneration and holds great promise for functional innervation of tissue engineered hollow organs.



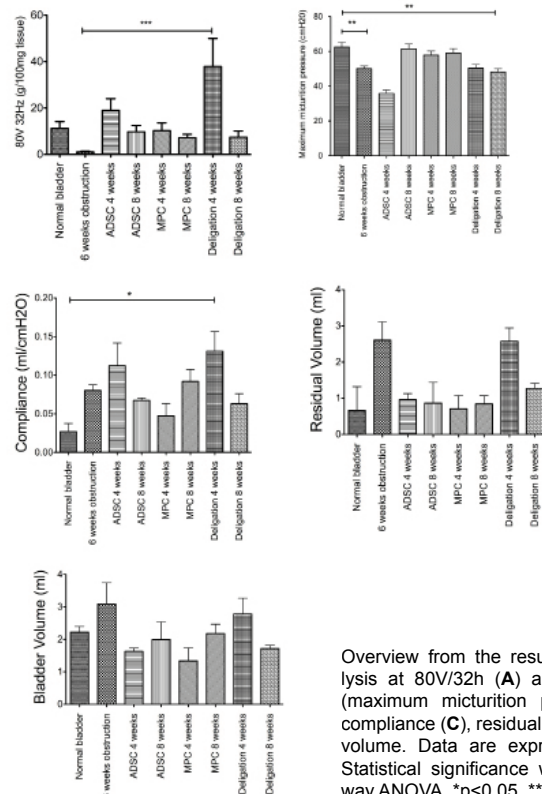
Scanning electron microscopic images of electrospun nanofibrous hybrid scaffold incorporated with neurotrophic factors

Adipose-derived Stem Cells (ADSCs) and Muscle Precursor Cells (MPCs) for the Treatment of Bladder Voiding Dysfunction

M. Tremp, S. Salemi, R. Largo, T. Aboushwareb, T. Sulser, D. Eberli

Bladder outflow obstruction is common in the elderly and can result in bladder voiding dysfunction (BVD). The goal of this research was to evaluate the use of adult stem cells for the treatment of BVD in a rat model.

Adipose-derived stem cells (ADSCs) from the inguinal region and Muscle Precursor Cells (MPCs) from the soleus muscle of adult male Lewis rats were harvested, expanded in culture and characterized. Bladder outflow obstruction was induced by tying a suture around the urethra in male Lewis rats (6-8 weeks old). After 6 weeks the development of a hypocontractile bladder was confirmed by urodynamic studies, organ bath and molecular expression. Injection of ADSCs or MPCs into the bladder wall and synchronous deligation was performed six weeks after the obstruction. 4 and 8 weeks after cell injection, morphological and functional changes were assessed. Obstructed rats had a significant larger bladder weight, lower maximum bladder pressure and lower contractility than age-matched rats. Labelled ADSCs and MPCs were detected after 4 weeks in the bladder wall expressing smooth muscle-specific markers. Organ bath analysis and urodynamic studies showed an improved contraction and higher maximal bladder pressure 4 and 8 weeks after cell injection. The same trend was seen on RT-PCR and Western-Blotting where gene expression and protein translation of important contractile proteins after stem cell therapy were upregulated.



The effect of porosity on tissue ingrowth and vascularization in electrospun hybrid scaffolds for bladder regeneration

M. Horst, V. Milleret, S. Noetzli, R. Gobet, T. Sulser, D. Eberli

Scaffold porosity governs cellular infiltration, tissue ingrowth and early revascularization which promotes oxygenation of the graft. We investigated the role of porosity of hybrid scaffolds consisting of bladder acellular matrix (BAM) and electrospun poly (lactide-co-glycolide) (PLGA) mimicking morphological characteristics of the bladder wall. Scaffolds with different porosity seeded with smooth muscle cells (SMCs) were evaluated in a cystoplasty model. Single-spun scaffolds (SSS) were compared with a scaffold with increased porosity (CSS) obtained by co-spinning of PLGA and Polyethylene glycol. Scaffolds were characterized by scanning electron-microscopy. *Ex vivo* proliferation assays and histological examinations were performed. 16 rats received partial cystectomy followed by augmentation cystoplasty with seeded SSS or CSS. Morphological and histological studies were performed after 2 and 4 weeks.

The porosity of the micro-fiber scaffold ($4.4 \pm 0.7 \mu\text{m}$) was $75.8 \pm 1.2 \%$ (SSS) and $80.7 \pm 1.8 \%$ (CSS). *Ex vivo* evaluation showed an increased cell proliferation on CSS. *In vivo* histology revealed a bladder wall-like structure with urothelial lining, and SMC infiltration. The micro vessel density was significantly increased in CSS after 2 and 4 weeks ($p=0.04$, $p<0.001$ respectively).

Conclusion: We were able to demonstrate that increased scaffold porosity significantly enhances cell infiltration and revascularization in bladder TE.

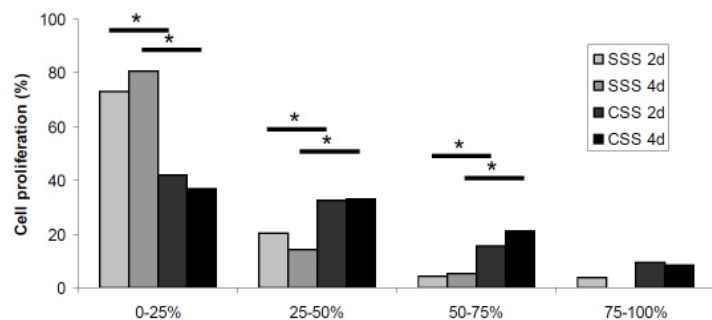


Figure 1: *In vitro* seeding: Infiltration depth of SMCs into SSS and CSS showing a deeper infiltration in the more porous scaffolds after 2 and 4 days

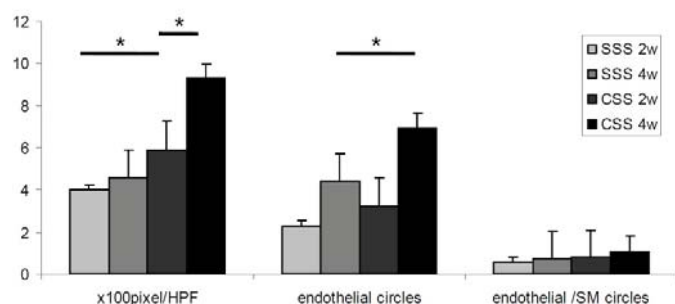


Figure 2: Histological evaluation: Micro vascular density showing significantly increased vascularization of CSS after 2 and 4 weeks.

Injected Muscle Precursor Cells (MPC) recover muscle function and inhibit tumor growth

M. Stölting, S. Ferrari, A. Becskei, Ch. Handschin, T. Sulser, D. Eberli

MPCs are capable of regenerating muscle fibers and are therefore investigated for the treatment of several muscular diseases.

Yet, safety and potential interactions of transplanted MPCs with cancers have not yet been investigated. In this study, we have evaluated the interactions of transplanted MPCs on the growth and malignant potential of neighboring prostate carcinomas and sarcoma *in vitro* and *in vivo*.

Primary human MPC and cancer cell lines (DU145, PC3, LnCAP, SK-LMS1) in co-culture and cell co-injection *in vivo* were used to assess the influence on cell growth rate, tumor size, apoptosis, cell cycle arrest and changes in protein expression. Further, cancer growth and metastasis formation was assessed *in vivo*.

MPC differentiated into normal and functional muscle in the proximity of tumor. Their presence reduced tumor growth ($p < 0.001$) and induced cancer apoptosis and cell cycle arrest by $TNF\alpha$. The effect was blocked in large part by $TNF\alpha$ inhibition. Histological studies and PET scan (F-choline) demonstrated lymph node and bone metastasis on control animals but not in animals with co-injected cancer and MPCs.

These results indicate that MPCs, while differentiating into functional muscle fibers, do secrete TNF alpha and thereby inhibit tumor growth, inducing apoptosis and tumor cell death. These results underline the safety of MPCs for cellular therapy even in proximity of a tumor.

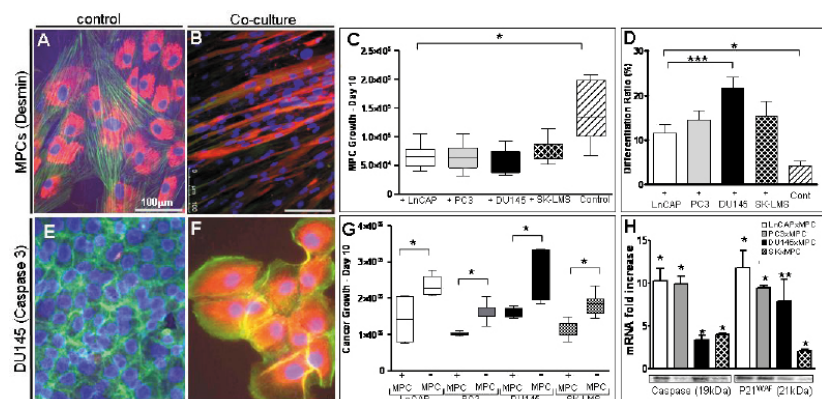
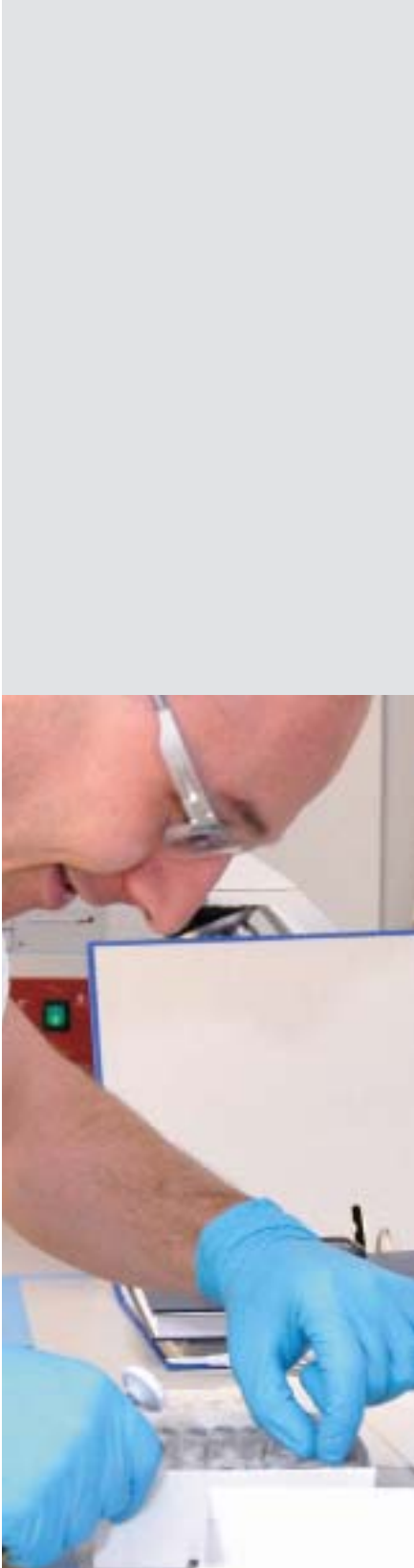


Figure 1: Co-culture effects on myoblasts and Cancer cells. Cell growth rate, differentiation ratio, morphology and gene expression were influenced by co-culture. Myoblasts differentiated rapidly in the presence of tumor, significantly increasing differentiation ratio (D) and, consequently, decreasing cell growth (C). In contrast, prostate carcinoma and sarcoma cells significantly decreased in growth (G) and underwent apoptosis and/or cell cycle arrest (E,F,H). Desmin staining in co-culture (A) and control (B), Caspase 3 staining of DU145 cells in co-culture with myoblasts (F) and control (E), cytoskeleton labelled in green (Phalloidin 488) and secondary antibody in red (Cy3). Caspase 3 and p21 mRNA fold increase and protein expression (H) significantly increased when compared to control. Samples in co-culture with myoblast were represented as (+ Mb) and control without myoblasts as (- Mb). mRNA fold increase was normalized with 18S house keeping gene and calculated as previously described (* $p < 0.001$, ** $p = 0.005$, *** $p = 0.011$)



Age and gender limitation for the bioengineering of contractile muscle tissue for human Muscle Precursor Cells (MPC)

M. Stölting, L.J. Hefermehl, M. Tremp, F. Azzabi Zouraq, R. Largo, T. Sulser, D. Eberli

MPCs are quiescent muscle cells capable of muscle fiber reconstruction. Therefore, autologous MPC transplantation is envisioned for the treatment of muscle diseases, many occurring in the aged population. However, density of MPCs and proliferation potential gradually decline with age.

The goal of this research was to assess the limitations of age and gender on the ability to bioengineer contractile muscle with human MPCs.

Human MPCs were harvested from the *rectus abdominalis* of 30 patients [15M, 15F] undergoing abdominal surgery [23-82y]. Growth curves, muscle phenotype and function were analyzed by FACS and cytological assays. *In vivo* muscle formation and contractility was assessed by histology, WB and organ bath.

We were able to confirm the myogenic phenotype, a great expansion potential and fiber formation for all ages and both gender. Male cultured cells had an increase differentiation ratio *in vitro* ($p=0.03$). Female cells were more stable *in vitro*, grew faster ($p=0.016$) and contracted better upon electrical stimulation ($p<0.001$). To gain sufficient cells the biopsy size needed to be bigger in male and older patients ($p<0.001$). MPCs of all ages were able to form muscle *in vivo*, but an age-dependent decline in contractile response could be detected. Our results suggest that human MPCs for cellular therapies can be successfully isolated and grown from patients of all ages and gender.

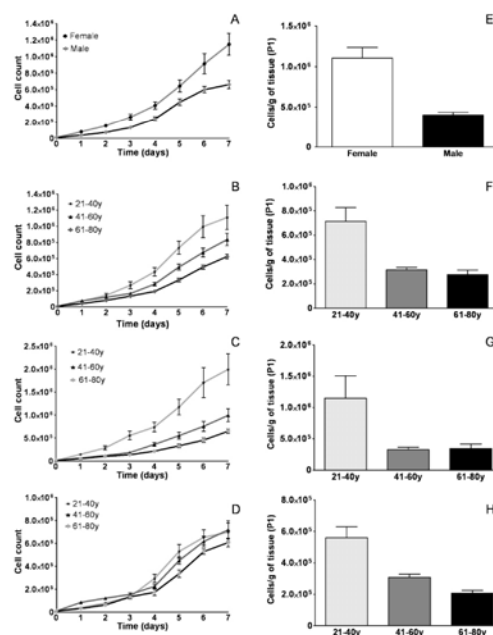


Figure 1: Age and gender impact on MPC growth and cell recover. MPC growth is a function of gender (A) and age (B). Cells isolated from females grow faster (A) and are strongly influenced by the age of the donor, a critical difference could be observed in the group of young female cells, which displayed an outstanding boosted growth in comparison to the other two age groups of the same gender (C). Aging is also important for male patients but in a later stage, only after 40 years of age (D). The same relations could be found regarding the cell recover per gram of muscle. Biopsies of younger and female provenience displayed a higher number of cells per gram of tissue in all groups analysed (E, F, G, H).

Muscle Precursor Cells for the Treatment of Fecal Incontinence

L. Brügger, R. Inglin, D. Candinas, D. Eberli

The surgical repair of external anal sphincter is still limited today.

We hypothesize that autologous Muscle Precursor Cells (MPC) injected into the damaged anal external sphincter muscle are able to form new functional muscle tissue.

In this research rodent MPCs were harvested and characterized by FACS, immunostaining and fiber formation assays. We established a fecal insufficiency model, which induces a constant sphincter damage and allows for detailed functional assessment of the external and internal anal sphincter. Morphological and functional outcome after MPC injection was compared up to 6 weeks. Collagen-only injections served as controls.

We demonstrated that rodent MPCs were reproducibly harvested, cultured and expanded *in vitro*. MPC-injection for anal sphincter reconstruction resulted in improved sphincter contraction in response to electrical stimulation ($p=0.016$, **Figure 1**). Significant improvement of sphincter contraction at 4 weeks (18.3 vs 8.7 cmH₂O; $p=0.003$) and at 6 weeks after MPC injection (27.6 vs 11.1 cmH₂O; $p<0.001$) was demonstrated. No difference between the groups was found for the resting pressures. Formation of new tissue with myofibers was demonstrated by immunostaining (**Figure 2**).

We conclude that cell therapy using cultured MPCs might be a promising option for the treatment of anal sphincter insufficiency in near future.

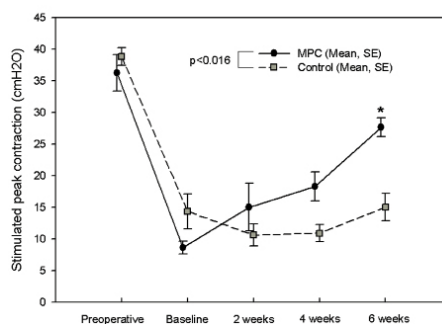


Figure 1: Asterisk indicates significant difference from baseline

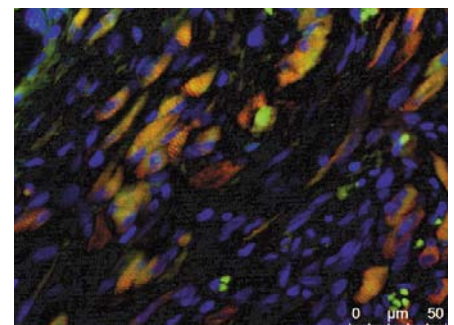


Figure 2: Newly formed tissue with myofibers demonstrated by immunostaining with anti- α -actinin (red) and tracing of injected MPCs with PKH-67 (green). Nuclear counterstaining with DAPI (blue).

Multi-layered hybrid biomaterial for the engineering of colon tissue

R. Inglin, L. Brügger, S. Nötzli, D. Candinas, D. Eberli

Surgical augmentation or patching of colon tissue still represents a major medical problem. We have developed a novel biomaterial designed for the bioengineering of large intestine, and evaluated its biocompatibility, tissue formation and integration in a mouse model.

Hybrid biomaterials consisting of a decellularized basal membrane (BAM) and a wet-bond layer of PLGA fibers directly electrospun onto the abluminal side of the BAM were produced. Elliptical patches were populated *in vitro* with primary smooth muscle cells (SMC) on the PLGA side and/or oral mucosal cells (OMC) on the BAM side. We then implanted these constructs into the native colon of normally colonized black six mice. Unseeded biomaterials served as control. The grafts were retrieved at postoperative day 14 or 28, and tissue formation, integration and biocompatibility were assessed.

Primary SMC survived and proliferated well on the hybrid biomaterial *in vitro*. Surgical implantation of the biomaterial was successful and served as barrier for colon bacteria. No animal died due to infection. The hybrid biomaterial, whether previously seeded with cells or not, gave support to the regeneration of new colon wall *in vivo*. Cell seeding of the biomaterial prior to implantation resulted in a reduction of graft shrinkage of 20% (SMC) and 25% (SMC and OMC), respectively, compared to controls.

This novel hybrid scaffold might be useful for colon engineering in the near future.

***In vivo* evaluation of O₂ releasing suture material for improved wound healing in hypoxic environments**

R. Inglin, B. Harrison, L. Brügger, T. Sulser, D. Candinas, D. Eberli

O₂ plays a pivotal role in wound healing. We therefore have developed an O₂-releasing suture material and evaluated its influence on healing of hypoxic colon tissue.

A PGA suture material was coated with PLGA containing oxygen-producing calcium peroxide (CPO) nanoparticles. To evaluate the limitations of our approach Lewis rats underwent an ischemia induction of a bowel segment that consequently was transected and reunified using O₂-producing (group A), untreated (B) or PLGA-coated (C) sutures. Mechanical, physiological and histomorphological measurements were performed, at postoperative day (pod) 1, 3, or 7, respectively.

Perianastomotic *in vivo* tissue oxygen saturation was maintained above baseline level in group A at all assessed pod's, and was significantly higher ($p=0.020$) compared to B at pod 3 (**Figure 1**). Thickness of colonic mucosa, a surrogate parameter for healing, demonstrated to be significantly more pronounced using O_2 -producing sutures compared to untreated or PLGA-sutures (**Figure 2**). Mechanical stability of the anastomosis was also improved in group A compared to B and C at pod 7. Oxygen-producing sutures promote anastomotic healing even in challenging environments, and may be clinically used under critical wound conditions in near future.

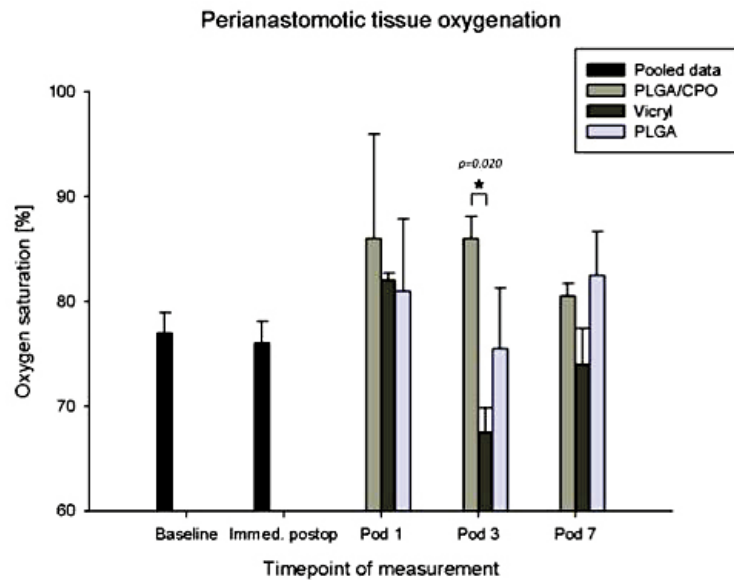


Figure 1: Significantly higher perianastomotic tissue oxygenation in anastomoses performed with O_2 -producing sutures (PLGA/CPO) compared to untreated Vicryl at postoperative day 3 ($p=0.020$). Baseline = measurement performed at the presumed site of the anastomosis, before induction of the ischemia. Immed. postop. = measurement performed immediately after confection of the anastomosis in a colon segment with previously induced ischemia as described before.

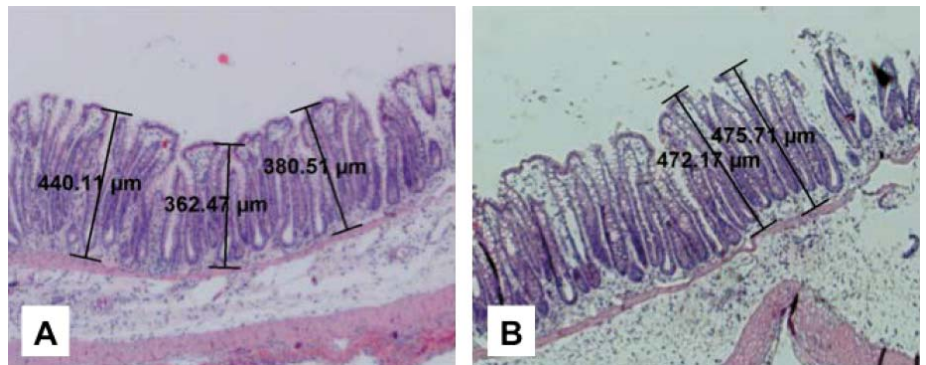


Figure 2: Significantly thicker mucosa and, hence, better wound healing in anastomoses sutured with O_2 -producing (**B**) compared to untreated Vicryl suture (**A**).

Collaborations:

- Prof. Anthony Atala, Wake Forest University School of Medicine, Medical Center Boulevard, Winston-Salem
- Prof. James Yoo, Wake Forest University School of Medicine, Medical Center Boulevard, Winston-Salem
- Dr. Benjamin Harrison, PhD, Wake Forest University School of Medicine, Winston-Salem
- Prof. Rita Gobet, Division of Pediatric Urology, University Children's Hospital Zurich
- PD Dr. Heike Hall-Bozic, Department of Materials, Federal Institute of Technology, Zurich, Switzerland
- Prof. Grégoire Courtine, Experimental Neurorehabilitation Laboratory, Department of Neurology, University Hospital Zurich
- Prof. Attila Becskei, Institute of Molecular Biology, University of Zurich
- Prof. Christoph Handschin, Biozentrum, Focal Area Growth and Development, University of Basel
- Dr. Stefano Ferrari, PhD, Institute of Molecular Cancer Research, University of Zurich
- Prof. Simon Ametamey, Federal Institute of Technology, Zurich, Switzerland
- Prof. Markus Rudin, Inst. f. Biomedizinische Technik, Universität und ETH Zürich, Schweiz
- Prof. Janos Vörös, Institut f. Biomedizinische Technik, Federal Institute of Technology, Zurich, Switzerland
- PD Dr. med. Caroline Maake, Institute of Anatomy, University of Zurich, Switzerland

2.8 Cranio-Maxillofacial Surgery Research



Prof. Dr. Dr.
Franz E. Weber,
PhD



Prof. Dr. Dr.
Klaus W. Grätz,
MD

Cranio-Maxillofacial Surgery Research

Oral Biotechnology and Bioengineering

Oral Oncology

Orofacial Deformities

Computer-assisted surgery and imaging

2.8.1 Oral Biotechnology and Bioengineering

Bone, cartilage and tooth regeneration

F. Weber, C. Ghayor, R. Correro, N. Rounsawasdi, P. Hänseler, A. Tchouboukov, Y. Bloemhard

Growth factor mediated bone regeneration and their enhancers

The regeneration of hard tissue is central for the patients care in Cranio-Maxillofacial and Oral Surgery, orthopaedics, and dentistry. For bone regeneration the outstanding growth factors utilized for this purpose are the BMPs. Since 2002 BMP-2 is clinically used mainly for spinal fusion. The drawback of this treatment is that the BMP dosage needed for effect in humans exceeds the natural BMP concentration by the factor of 1000. To reduce this high amount of BMP we evaluate the use of improved BMP carriers as bone substitute material and the use of BMP enhancers. Both concepts could help to reduce the dosage of BMP and with it the safety but at the same time also the very high price of this treatment option. In the last years we have identified the small chemical N-methyl pyrrolidone (NMP) to enhance bone regeneration by its enhancing effect on the kinase activity of the BMP/BMP receptor complex for key signalling molecules for bone formation. In 2011 we have discovered that the same small chemical reduces osteoclast maturation and osteoclast activity and therefore bone degradation. In essence we have now a small chemical in our hands that enhances bone regeneration via BMP pathways and reduces bone degradation via osteoclastogenesis related pathways and could prove useful for the prevention and treatment of osteoporosis or to reduce the development of metastasis in bone.

Synthetic hydrogels

Cellular components of bone tissue are osteoclasts, osteoblasts, and osteocytes. To study the interaction between different cell types in bone we have developed a synthetic backbone matrix, where we can incorporate cues in a spatial defined way. Last year we generated a bone-like construct composed of osteoblasts, osteocytes and endothelial cells and studied the effect of osteoclasts and osteoblasts on the tube formation of the endothelial cells.



Prof. Dr. Dr.
Franz E. Weber,
PhD



Dr.
Chafik Ghayor,
PhD



Dr.
Lindsay Sulzer,
PhD



Rita Correro
M.Sc.



Nisarath
Rounsawasdi
DDS



Patrick Hänseler
M.Sc.



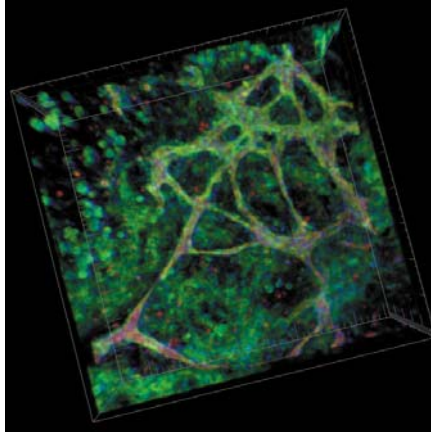
Alexander
Tchouboukov



Yvonne
Bloemhard



The results showed that tube length was 4 times increased when osteoblasts and osteocytes were present compared to constructs with only osteoblasts or osteocytes. This proof of concept study paved now the way for future work on the communication between different cell types in tissues.



Tube formation by endothelial cells in synthetic hydrogel

Bone substitute materials

Bone substitute materials are developed to substitute for the use of autologous grafts, which are associated with a second site of surgery, morbidity, pain and additional discomfort for the patient. Since bone is mainly composed of hydroxyapatite the majority of synthetic bone substitute materials contain 60-80% hydroxyapatite. In our group we characterize and develop novel bone substitute materials based on

- 1) Synthetic hydroxyapatite/tricalciumphosphates (HA/TCP).
The goal of this subproject is the characterization and development of synthetic HA/TCP based materials with emphasis on the attachment and release of growth factors.
- 2) Synthetic and natural hydrogels.
Hydrogels are ideal ingrowth matrices for regeneration purposes but their mechanical properties are insufficient for bone regeneration purposes. Therefore we want to combine hydrogels with mechanically more stable materials like hydroxyapatite to form novel bone substitute composites.
- 3) *In situ* forming implants for the double delivery of NMP and BMP.
Since NMP is a small, water- and organo-miscible molecule, many traditional drug delivery strategies are not adapted to the sustained release of this molecule. In the present work, we have employed polyesters as in situ-forming implants (ISFI) for prolonged NMP delivery and combine them with BMP to generate a double delivery system.
- 4) Titanium reinforced 3D scaffolds produced by rapid prototyping for the treatment of large bone defects in the mandible. Large bone defects can result from trauma or might even be generated during the resection of tumours. To subsequently restore aesthetics and function such defects have to be filled with bone tissue able to withstand the high mechanical forces generated during mastication right after surgery. The aim of this project is to generate titanium reinforced 3D scaffolds for bone ingrowth and placement of dental implants.

Biomimetic nano-fiber-based nucleus pulposus regeneration for the treatment of degenerative disc disease

Confucius said, “Do not use a cannon to kill a mosquito.” In spine, the admonition could become, “Do not use fusion to treat an early stage degenerated disc.” In future, nucleus replacement may become an alternative to more invasive procedures in cases of early stage degenerative disc disease. These technologies may fill part of the gap in the continuum of spine care and also help abate the use of the controversial “cannon,” otherwise known as fusion.

The main objective of this EU-project is to develop a biomimetic nano-polymer based gel for minimally invasive disc regeneration treatment: Electro-spinning technology will be exploited to develop a nano-fiber based, biocompatible, biodegradable, synthetic scaffold mimicking the mechanical properties of the native Nucleus Pulposus for immediate and short term treatment.

Anti-inflammatory drugs will be carried by the biodegradable nano-fibers to be gradually released in situ for healing and preventing inflammation.

The synthetic scaffold will be integrated with a bioactive-nano-polymer highly potent in supporting Nucleus Pulposus cells (EPCs) for long-term cure. In addition growth factors will be integrated into the material in a way so that their release suits the needs of this avascular site. To that end several BMPs and their heterodimers are engineered to achieve appropriate binding and release characteristics.

Mechanobiology of cartilage and cartilage tissue engineering

Our objective is to gain knowledge of the mechanobiology of temporomandibular joint (TMJ) cartilage, by designing functional tests of TMJ disc tissue and cartilage tissue in general. The long-term objective of this research is to understand the pathomechanics of TMJ degeneration and OA. This interdisciplinary research can be extended to other joints, such as e.g. the knee, also yielding functional tests for synthetic or tissue engineered replacement materials. The functional tests will be performed by means of a self-developed cartilage explant mechanical testing system that will reproduce physiological and pathological conditions on live tissue. **Aim I:** Analysis of wear and biological effects of rolling/sliding/plowing on pristine cartilage. The cartilage explant mechanical testing system will be used on pristine cartilage explants under different conditions, such as e.g. the type of stress and friction (rolling, sliding or plowing), the stress magnitudes, the geometry of the artificial condyles, the thickness and the fibre orientation of the tissue specimens. The range of loading conditions will be varied to simulate the physiological environment and will be extended to overloading. We will then investigate the thresholds for the testing conditions with regard to tissue wear and biological response, in particular cell viability, collagen integrity, proteoglycan biosynthesis and matrix metalloproteinase content/synthesis. The results will be compared among the different types of loading, i.e. rolling, sliding or plowing. Finally, we will mimic the stress-field translation in the TMJ through cartilage samples with *in vivo* acquired structural and kinematic information.

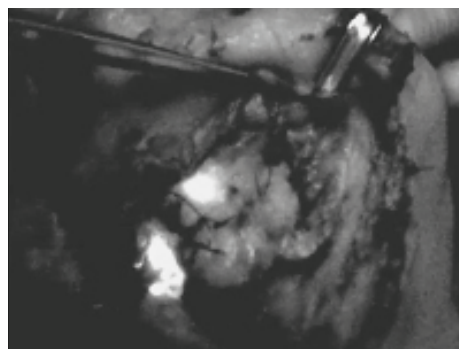
Aim II: Analysis of wear and biological effects of rolling/sliding/plowing on cartilage after mechanical damage and/or cartilage surface degradation. Cartilage samples will be artificially damaged either mechanically (i.e. by impact loading, perforation or tearing) or biochemically (e.g. by means of chondrolytic agents such as collagenase, aggrecanase, IL-1, cathepsin D, elastase etc.). Subsequently, experiments like those in Aim I will be performed. The loads will be at first at physiological level and then increased to overloading. The wear and biological parameters at the different loading regimes will be compared to the corresponding data obtained for pristine cartilage and among the different types of loading.

2.8.2 Oral Oncology

The estimated number of newly diagnosed cancers of the oral cavity and pharynx is 97,800 patients per year in Europe; the estimated number of deaths due to these carcinomas is 40,100 per year. The 5-year disease specific survival rate for patients with primary oral cancer ranges from 53% to 74%. This 5-year survival rate seems to be unchanged, despite improved diagnostic tools, chemo- and radiotherapy, and improved surgical techniques. In a first step during the last two years, we evaluated our clinical tumor patient's data base concerning clinical prognostic markers. Preoperative factors were C-reactive protein, leukocytes, haemoglobin, the value of CT and PET-CT scans for preoperative staging. Concerning intraoperative factors we studied the role of the submandibular gland in neck dissections, the value of frozen sections, lymph node metastases in maxillary carcinomas, reconstruction possibilities for soft tissue defects. Furthermore we studied the role of CT routine in follow-up control, head and neck cancer in elderly and non-smoking and non-drinking patients as well as mucosal malignant melanomas and minor salivary gland tumours.

At present we are planning to study metabolites in tumor tissue and saliva in order to evaluate possible tumor markers in regard to prognosis/lymph node metastases and to compare these data with our clinical parameters that we gathered during the last two years.

After our proof of concept studies we plan to determine the role of Indocyanin Green in the identification of sentinel lymph nodes as well as its role in ensuring complete removal of lymph draining tissue.



Lymphatic drainage pattern seen after injection of Indocyanin Green



Dr. Dr. dent.
Marius Bredell,
MD



PD Dr. Dr. dent.
Astrid Kruse,
MD

2.8.3 Orofacial Deformities



Prof. Dr. Dr. dent.
Joachim Obwegeser,
MD



Dr. Dr. dent.
Christine Jacobsen,
MD

Until today, several standardized therapy methods for the surgical correction of craniofacial deformities were developed. In some severe cases, surgical distraction of syndromic craniofacial deformities is the method of choice to achieve the best possible functional and aesthetic result.

During the last decade different devices for surgical distraction in the facial area were developed, but for all of them it remains difficult to determine the correct vectors. Additionally some devices show early loosening and un-aesthetic scarring, especially in small children. For this a new external distraction device for distraction in Le Fort III level was developed in collaboration with KLS Martin Group. This device was successfully applied in a child with syndromic craniosynostosis.

2.8.4 Computer-assisted surgery and imaging



PD Dr. Dr. dent.
Heinz-Theo Lübbers,
MD

Three-dimensional imaging of the facial surface: In cranio-maxillofacial and plastic surgery, but also in orthodontics and prosthetic dentistry, anthropometry is especially challenging because of the complex structure of faces, which do not allow an accurate assessment with simple measurements. For the underlying bony structures, the development of computer tomography solved the difficulties. An objective, accurate, and reliable system for quantifying the soft tissues of the face in dimension and color is still missing. Today, direct measurements and two-dimensional photography are state-of-the-art for craniofacial anthropometry, although the pitfalls are well known. However, interest in overcoming the limitations of these techniques has led to the development of numerous three-dimensional scanning devices that have an obvious appeal over the old-fashioned techniques.

Despite the huge amount of literature about the new three-dimensional systems, a clear and objective evaluation of accuracy and reliability under different circumstances is missing for many of them. Even more important: A clear strategy for evaluation and judgment of the captured 3D data is missing as well. The project is meant to evaluate the precision of 3D facial imaging under clinical circumstances, to integrate this technique into daily clinical routine and to develop evaluation strategies for the acquired data.

Three-dimensional radiographic imaging in dental medicine: The development of cone beam computed tomography brought three-dimensional imaging into the daily business of dental medicine. Only a few years after the introduction of this technique it is widely utilized not only in specialized centers but also in general dentistry. Most of the dentist appreciate the new insight into their patient's anatomy and strongly believe into the benefit of this technology. However, despite the broad application of this technology the evidence for most indications is quite unclear. Therefore we started this project to gain evidence for certain applications. In the initial phase of this project we will cover the surgical fields but in the long run we plan to cover all fields of dentistry.

Computer Assisted Surgery in Oral and Cranio-Maxillofacial Surgery: The complex three-dimensional geometry and the requirement for a precise facial symmetry are the main challenges in reconstructive maxillofacial surgery. Despite diligent planning e.g. with the help of patient specific models, the procedure remains subject to considerable imprecision due to the difficulty to assess the complex craniofacial anatomy during the operation. More recently, computer-based 3D pre-operation planning based on 3D imaging datasets opened the door to surgical navigation. Surgical navigation assists in transporting the pre-operative plan into the operation room and is an established method in today's cranio-maxillofacial surgery. Several key elements are relevant for favorable results: Correct indication, precise preoperative planning, and exact transformation of the plan into the surgical procedure and – of course – postoperative evaluation of the results in order to learn from the achieved. The project therefore focuses not only on the technical parts of Computer Assisted Surgery as e.g. preoperative planning techniques and precision in surgical navigation with its key element of patient registration, but also on clinical guidelines for specific indications and postoperative evaluation of the achieved results.

Collaborations:

- Department of Fixed and Removable Prothodontics and Dental Material Science, University of Zurich, Switzerland (Prof. Ch. Hämmerle, PD Dr. Ronald Jung, Dr. Daniel Thoma)
- Department of Masticatory Disorders, University of Zurich, Switzerland (Prof. Sandro Palla, Prof. Luigi Gallo)
- Division of Obstetrics (Prof. Roland Zimmermann, Dr. Martin Ehrbar)
- ETH Zurich, Laboratory of Biosensors and Bioelectronic (Prof. Janos Vörös)
- ETH Zurich, Department of Materials (Prof. Viola Vogel)
- ETH Zürich Institut f. Biomechanik (Prof. Ralph Müller)
- EPFL Institute of Bioengineering (Prof. Jeffrey Hubbell, Prof. Matthias Lütolf)
- ETH Zurich, Department of Chemistry and Applied Biosciences (Prof. Wendelin Stark)
- University of Belgrade (Serbia-Montenegro), (Dr. Vladimir Kokovic, Prof. Aleksa Markovic und Prof. Milan Jurisic)
- University of Hongkong, (Prof. Roger Zwahlen)
- Kuros Biosurgery (Zurich, Switzerland)
- Straumann AG (Waldenburg, Switzerland)
- Geistlich AG (Wohlen, Switzerland)
- Degradable solution (Zurich, Switzerland)

2.9. Surgical Intensive Care Medicine



Prof. Dr.
John F. Stover,
MD



Jutta Sommerfeld



Mario Fasshauer



Angela Fendel
Lab. Technician

Patients suffering from severe traumatic brain injury are prone to additional lesion-aggravating injuries. To improve neurological recovery and to prevent potentially deleterious effects during intensive care treatment the following investigations were successfully published showing that

- 1) jugular venous glutamate is inferior to $SjvO_2$ in unmasking metabolic impact of increased ICP
- 2) amino acid composition of routine enteral nutrition influences brain metabolism and ICP

1. Influence of sedation on arterio- jugular venous glutamate difference and $SjvO_2$

R. Vuille-Dit-Bille, R. Ha-Huy, M. Tanner, J.F. Stover

Cerebral metabolic impairment is feared to induce secondary brain damage following traumatic brain injury (TBI). The present study was designed to assess the temporal profile of calculated arterio- jugular venous differences in glutamate (AJVDglu) and $SjvO_2$ in patients subjected to continuous pharmacologic coma. Metabolic impairment was assumed to be reflected by increased jugular venous glutamate levels and decreased $SjvO_2$.

Arterial and jugular venous blood was drawn once daily for up to 14 days from 14 patients to assess the temporal profile. Plasma glutamate was measured by high performance liquid chromatography. $SjvO_2$, lactate and $paCO_2$ were determined in routine blood gas analysis. Calculated AJVD indirectly reflects cerebral uptake (positive values) or cerebral release (negative values).

During pharmacologic coma an increase in ICP approaching 20 mmHg was associated with significantly reduced $paCO_2$ (4.7 ± 0.5 kPa; mean \pm standard deviation), markedly decreased $SjvO_2$ ($66.0 \pm 4.2\%$) without reaching ischemic values, and a trend to more negative AJVDglu values (-6.0 ± 14.3 $\mu\text{mol/L}$), suggesting cerebral glutamate release. Arterio- jugular venous lactate difference (AJVDlac) remained unchanged.

During pharmacologic coma increased ICP was associated with significantly decreased $SjvO_2$ which coincided only with a trend to increased cerebral glutamate release. Calculated AJVDglu appears to be inferior in unmasking altered brain metabolism compared to $SjvO_2$ whenever ICP is increased.

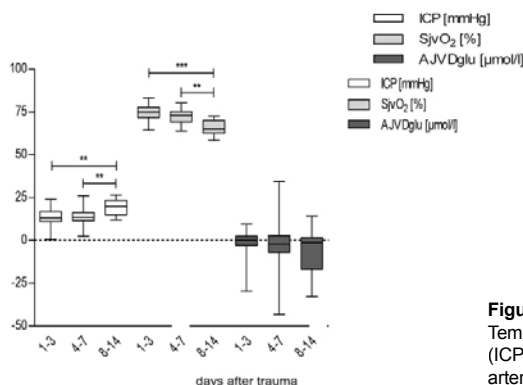
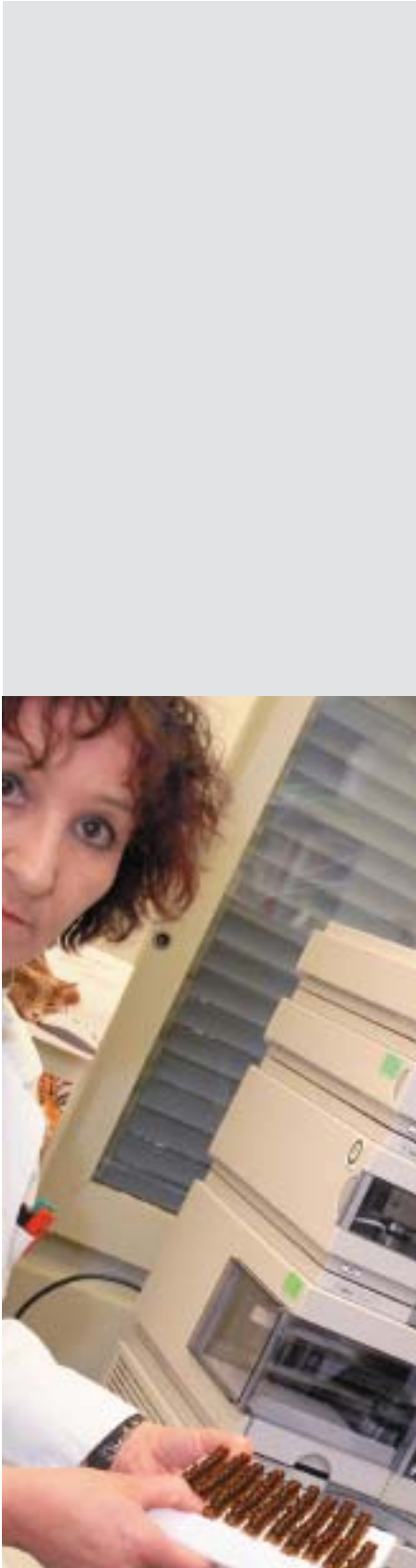


Figure 1

Temporal profile of changes in intracranial pressure (ICP), jugular venous oxygen saturation ($SjvO_2$) and arterio- jugular venous glutamate difference (AJVDglu)



2. Influence of enteral nutrition on brain metabolism

R. Vuille-Dit-Bille, R. Ha-Huy, J.F. Stover.

Brain metabolism is influenced by systemic changes. In this context, amino acids exert specific functions: while aromatic amino acids (AAA) are precursors of excitatory transmitters (noradrenaline, adrenaline, dopamine) and serotonin, branched chain amino acids (BCAA) are used for detoxification of ammonium. We assumed that changes in plasma AAA and BCAA could influence intracranial pressure (ICP) and cerebral oxygen consumption ($SjvO_2$)

Arterial and jugular venous blood was drawn once daily for up to 14 days from 19 patients to assess the temporal profile. Plasma amino acids were measured by high performance liquid chromatography. $SjvO_2$, lactate and $paCO_2$ were determined in routine blood gas analysis. Calculated AJVD indirectly reflects cerebral uptake (positive values) or cerebral release (negative values).

Compared to 44 healthy volunteers, jugular venous plasma BCAA were significantly decreased by 35% ($p < 0.001$) while AAA were markedly increased in TBI patients by 19% ($p < 0.001$). The BCAA to AAA ratio was significantly decreased by 55% ($p < 0.001$) which persisted during the entire study period. Elevated plasma phenylalanine was associated with decreased ICP and increased $SjvO_2$, while higher plasma isoleucine and leucine levels were associated with increased ICP and higher plasma leucine and valine were linked to decreased $SjvO_2$. The amount of enterally administered amino acids was associated with significantly increased plasma levels with the exception of phenylalanine.

Contrary to the initial assumption that elevated AAA and decreased BCAA levels are detrimental, increased plasma phenylalanine levels were associated with beneficial signs in terms of decreased ICP and reduced cerebral oxygen consumption reflected by increased $SjvO_2$; concomitantly, elevated plasma isoleucine and leucine levels were associated with increased ICP while leucine and valine were associated with decreased $SjvO_2$ following severe TBI, respectively. The impact of enteral nutrition on this observed pattern must be examined prospectively to determine if higher amounts of phenylalanine should be administered to promote beneficial effects on brain metabolism and if normalization of plasma BCAA levels is without cerebral side effects.

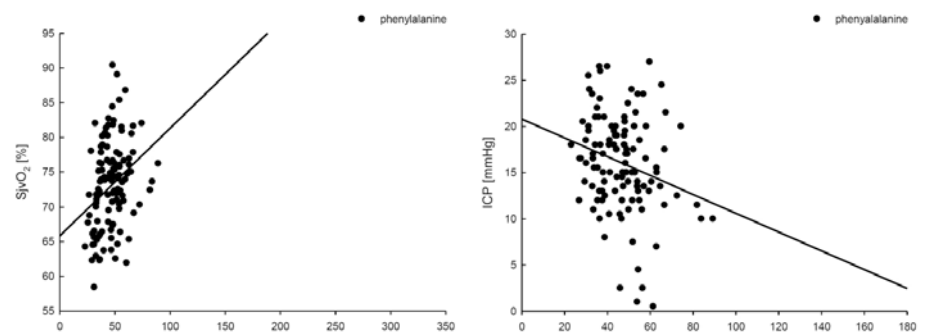


Figure 2
Influence of arterial phenylalanine on intracranial pressure (ICP) and cerebral oxygen consumption ($SjvO_2$)



Dr.
Markus Béchir,
MD



Dr.
Renato Lenherr,
MD



Dr.
Urs Wenger,
MD



Dr.
Christian
Oberkofler, MD

Intensive care medicine/Transplantation

Ongoing Research

New ICU Prediction score

To date there are different prognostic scores to predict outcome in critical care medicine, e.g. SAPS II or APACHE score. ICG liver test (LIMON®) can predict outcome in critically ill patients. Therefore, the aim of this study was to evaluate the prognostic value of the combination of ICG test and SAPS II score together as a new - easy to assess - score for outcome prediction in intensive care medicine.

We included 144 consecutive critically ill patients in to this study. At admission the ICG liver test was performed and after 24 hours SAPS II score was calculated. By means of multivariate Cox analysis and Kaplan-Meier survival curve, we tested the ability of SAPS II and ICG as an outcome prediction score. The score consists of 3 possible conditions: Zero (both negative), 1 (one positive and one negative) or 2 (both positive). Cut off for positivity - derived by ROC analysis - was a SAPS II score > 40 and an ICG measurement $< 12.6\%$. The cumulative 1 year survival of the 3 groups (score 0, 1 or 2) were 92.5%, 78.0% and 29.4%, respectively ($p=0.03$, log rank test). In Conclusion the combination of SAPS II and ICG Test – as an easy to perform test - seems to be accurate in outcome prediction of critically ill patients.

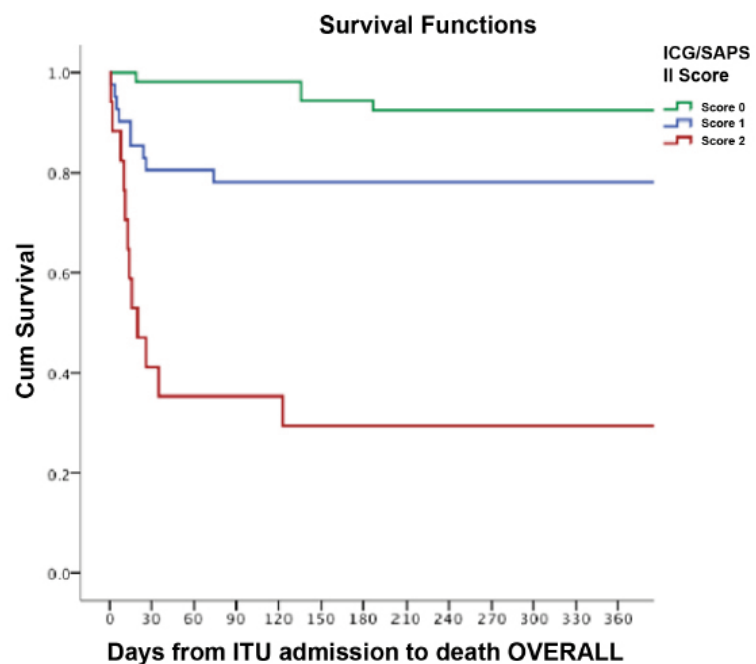


Figure1 Survival according to the new score in ICU patients

Combination of MELD score and ICG-liver testing predicts outcome in liver transplant recipients.

Prediction of outcome after liver transplantation with an easy assessment would be useful for ICU management of such patients. Therefore, we tested the ICG –liver test (LiMON[®]) in comparison with other known outcome predictors. We included 50 liver transplant recipients in to this study. We analysed length of stay in the ICU, hospital stay and mortality in respect of MELD score, liver function test (LiMON[®]), factor V after 24 hours postoperative, praeoperative creatinine serum level and postoperative bilirubin peak level. Therefore, we performed ROC curves determining accuracy of those parameters and a Kaplan-Meier survival analysis. ICG liver testing (LiMON[®]) and MELD score predicted LOS in the ICU with an accuracy of 67% and 81%, hospital stay with 77% and 66%, mortality with 79% and 85%, respectively.

The best prognostic tool is the combination of MELD score (cut off > 25) and ICG (cut off < 20) together. When combined they predict twice as long ICU stay and hospital stay and when negative, mortality is 0%, while when positive, mortality is 40%. To conclude the combination of MELD score and ICG liver monitoring allows a good prediction of length of stay in the ICU, length of hospital stay and mortality.

Combined MELD>25 & ICG<20			
Outcomes	Negative	Positive	P value
ICU stay, median (IQR)	4 (3-6)	9 (5-43)	0.004
ICU stay, mean (SEM)	5 (0)	28 (9)	-
Hospital stay, median (IQR)	22 (15-28)	42 (21-74)	<0.001
Hospital stay, mean (SEM)	24 (2)	55 (11)	-
Mortality, number (%)	0/36 (0%)	4/10 (40%)	0.003

Table 1. Combined MELD & ICG and outcomes

Pretransplant dyslipidaemia determines outcome in lung transplant recipients

Dyslipidemia is associated with an increased risk of cardiovascular events and as such with an increased mortality. In patients undergoing lung transplantation the effects of serum lipids on mortality is not clear – considering the side effects of calcineurin inhibitors one would expect a pronounced effect of dyslipidemia. We have conducted a retrospective analysis of our lung transplantation program. From January 2000 to December 2008 the charts of 172 consecutive lung transplantation recipients were analysed. At baseline and after one year laboratory values of renal function (creatinin) and serum lipid profile (total cholesterol, triglycerides, high-density lipoprotein and cholesterol/HDL ratio) were collected. During the follow-up major cardiovascular events (MCE; beginning of dialysis, cerebro-vascular insult or myocardial infarction) were recorded. The follow-up period ended December 2010. Because of incomplete baseline data 28 patients were excluded, so in the end 144 patients were analysed. Total cholesterol (4.3 ± 1.6 vs. 5.4 ± 1.3 mmol/l, $p < 0.0001$), triglycerides (1.2 ± 0.7 vs. 2.4 ± 1.3 mmol/l, $p < 0.0001$), HDL-cholesterol (1.5 ± 0.6 vs. 1.7 ± 0.6 mmol/l, $p = 0.003$) and cholesterol/HDL ratio (3.0 ± 1.0 vs. 3.6 ± 1.2 , $p = 0.002$) increased significantly after 1 year.

Until the end of the observational period 10 patients (6.9%) suffered from a MCE. In a univariate analysis these were associated with baseline total cholesterol. In the event-group baseline cholesterol was 10% higher than in the event free group (odds ratio for MCE 2.5 (CI: 1.1-2.6, $p = 0.012$)). In a multivariate model the odds ratio per increased 1.0 mmol/l total cholesterol was 2.5 (1.2-6.1, $p = 0.013$).

During the observational period 36 patients died (25%). The univariate analysis showed that mortality was associated with increased cholesterol/HDL ratio. The nonsurvivors had a 23% higher baseline cholesterol/HDL ratio with a hazard ratio of 2.7 (CI: 1.2-3.3, $p = 0.007$). In a multivariate model the hazard ratio was 1.5 (1.2-1.9, $p = 0.001$) per increase of 0.4 Cholesterol/HDL ratio. In conclusion this retrospective study has shown that the total cholesterol before transplantation is associated with the incidence of MCE and the cholesterol/HDL ratio with mortality. Suggesting that it is worthwhile correcting the lipid profile in advance of lung transplantation. In the mirror of the side effects of the commonly used statins the potential beneficial effect of a better lipid profile has to be proven.

Collaborations:

- Prof. Dr. Ph. Dutkowski, Visceral- and Transplantation, UniversityHospital Zurich
- Prof. Dr. G. Noll, Cardiology, UniversityHospital Zurich
- PD Dr. Th. Neff, Kantonsspital Münsterlingen



PD Dr.
Reto Schüpbach,
MD, M.Sc



Dr.
Miriam Ender,
PhD



Dr.
Jerzy Madon,
MD



Dr.
Stephanie Klinzing,
MD

Coagulation and Inflammation

Ongoing Research

The clotting protease activated protein C (aPC) has powerful protective effects in systemic inflammation and was approved to treat patients with severe sepsis. However, efficiency is controversially discussed and the recently completed PROWESS-SHOCK trial failed to show a survival benefit, resulting in withdrawal of the drug from the market. No other specific treatment options for sepsis are available and therefore a thorough understanding on how aPC mediates protective effects on the molecular basis is necessary and may help to design novel treatment options for patients with sepsis.

Our group focuses on understanding **i)** how aPC mediates protective effects on a molecular basis, **ii)** what potential non desired side effects of aPC are and **iii)** how cell protective effects of aPC could be enhanced.

Cleavage by and activation of the protease activated receptor by aPC is recognized to mediate cytoprotective effects in *in vitro* as well as in mouse injury models. It however remained elusive how aPC can mediate cytoprotective effects through PAR1 while thrombin mediates opposite effects through the very same PAR1. In a project sponsored by the University of Zurich we could show that protease specific cleavage sites on PAR1 exist (**Figure 1A-B**) and translate into agonist specific cellular responses (**Figure 1C-E**). These observations implicate that for PAR1, similarly to other G-coupled protein receptors, several agonist specific active conformations exist. Our novel model for the first time allows to explain agonist specific G-protein coupling and divergent signaling patterns in PAR1. Our findings carry the potential for future therapeutic use of specific PAR1 (ant-)agonists in the setting of inflammatory disorders in the future (manuscript submitted for publication).

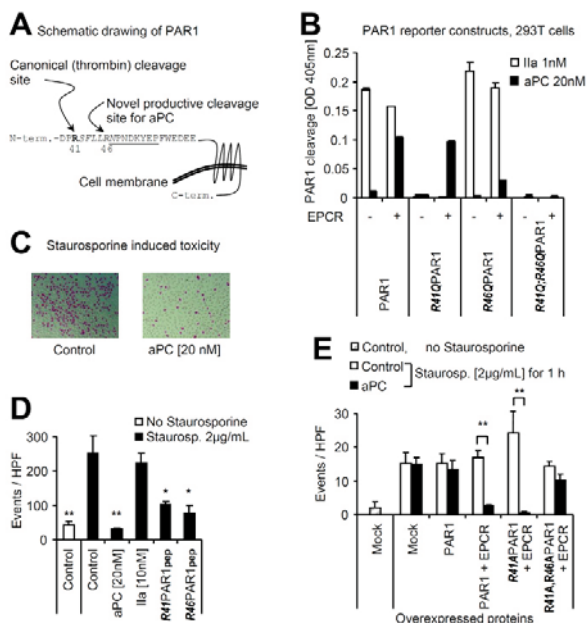


Figure 1: Non canonical R46 cleaved PAR1 mediates cytoprotective effects.

(A) Schematic drawing of PAR1 with cleavage sites (bold) and cytoprotective R-46 cleaved N-terminus (under-scored).

(B) Cleavage of PAR1 cleavage reporter construct by aPC and thrombin. Substitutes in PAR1 variants are indicated (italics).

(C) Visualisation and quantification (D) of staurosporine induced cytotoxicity. Agonists are given, R41PAR1pep and R46PAR1pep are soluble octapeptides corresponding to the R41 and R46 cleaved N-terminus of PAR1.

(E) Over-expressing system testing for requirement of EPCR and R46 cleavable PAR1 to allow aPC mediating anti-toxic effects.

Activated protein C inhibits the procoagulant tenase and prothrombinase complexes through cleavage of activated clotting factors Va and VIIIa. We wondered whether aPC has similar anticoagulant effects on the key initiation complex. Surprisingly, we found aPC to exert procoagulant effects on the initiation complex (**Figure 2A**) through degrading its natural inhibitor (**Figure 2B**), the tissue factor pathway inhibitor (TFPI). On a molecular basis aPC's procoagulant effects were found to be explained by a newly discovered cleavage event between TFPI's Kunitz I and II domains at Lys86 (**Figure 2B**). Our findings demonstrate a novel unexpected procoagulant role of the protein C pathway that may have important implications for the regulation of TF- and TFPI-dependent biologic responses and for fine tuning of the hemostatic balance in the vascular system (*published Blood. 2011 Jun 9;117(23):6338-46*). To eventually bring our findings back to clinics we have proposed to dissect the procoagulatory effects of aPC's from its cytoprotective properties. We hypothesized that a variant of aPC with enhanced cytoprotective but no coagulant function could be obtained by altering aPC's Gla-domain. The Gla-domain allows aPC to bind onto the endothelial protein C receptor which favourably positions aPC for activation of PAR1. APC-PAR1 then mediates the desired protective effects.

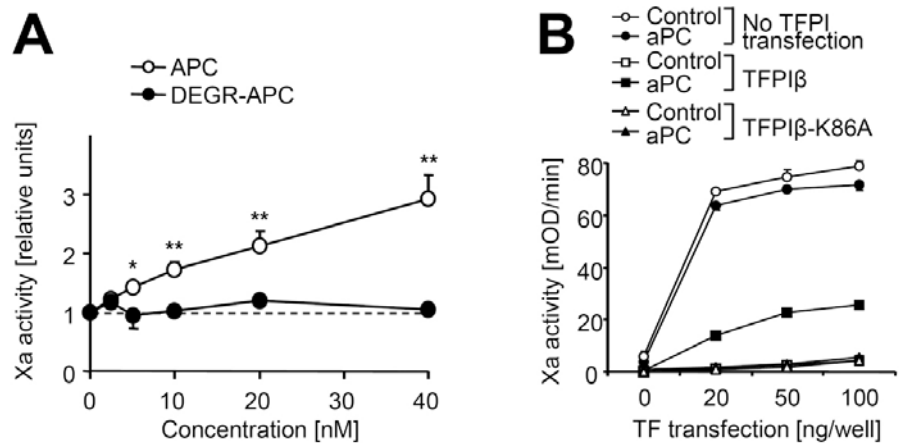
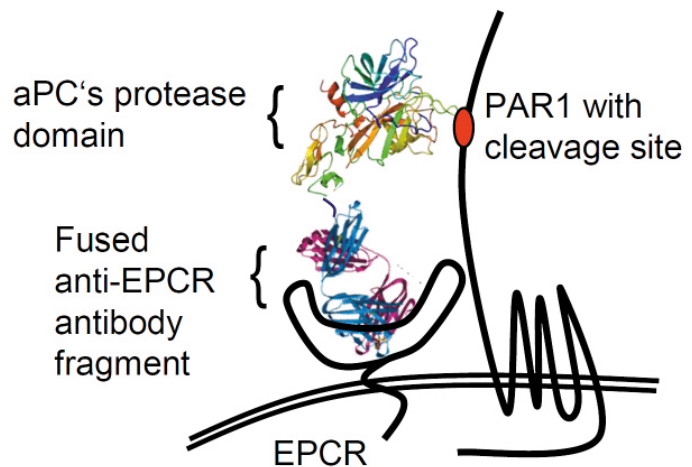


Figure 2: Procoagulant degradation of tissue factor pathway inhibitor by APC. (A) EAhy926 cells were TNF α induced and treated with agonists for 3h. Washed cells were incubated with factors VIIa (20nM) and X (100nM) followed by colorimetric quantification of Xa activity. (B) HEK293t cells overexpressing TF, EPCR, and wildtype TFPI β or TFPI β K86A were aPC treated (3h, 60nM) followed by quantification of Xa generation.

The Gla-domain however also binds to negatively charged cell membrane domains resulting in the non desired degradation of clotting factors. To target aPC only to PAR1 we have replaced the Gla-domain by an EPCR-specific antibody fragment (**Scheme 1**) and now plan to test if this variant of aPC indeed efficiently mediates cytoprotective effects. (This work is funded by the SNF grant# PZ00P3_136639).

The overall goal of our research is to better understand on a molecular basis how the clotting system influences pro- and anti-inflammatory pathways. We hope that this knowledge can be translated into novel therapeutic possibilities for inflammatory driven diseases in the future.



Scheme 1: Endothelial protein C receptor (EPCR) recruits aPC towards PAR1 to enhance cleavage efficiency. To enhance aPC recruitment we proposed to replace aPC's natural but inefficient EPCR-binding Gla-domain by an high affinity anti-EPCR antibody fragment.

Collaborations:

- PD Dr. A. Zinkernagel PhD, Klinik für Infektionskrankheiten und Spitalhygiene, UniversitätsSpital Zürich, Schweiz
- Prof. Dr. Ch. Renner, Klinik für Onkologie, UniversitätsSpital Zürich, Schweiz
- Prof. M. Riewald MD, Department of Immunology and Microbial Science, The Scripps Research Institute, La Jolla, CA 92037, USA

2.10. New and Improved Anaesthesia Methods for Use in Laboratory Mice



PD Dr. vet.
Margarete Arras,
MD



Dr. vet.
Nikola Cesarovic,
MD



Flora Nicholls
Dipl. nat.



Andreas Rettich
Dipl. nat.



Prof. Dr. vet.
Jörg Haberstroh,
MD



Paulin Jirkof
Dipl. nat.



Thea
Fleischmann,
Dipl. nat.

The utilization of laboratory mice in surgical research has been continuously increasing over the years, in particular due to the availability of a magnitude of genetically modified mouse lines. The optimization of data output from existing models and the creation of new surgical models in this species requires development of safe, hours-long anaesthesia as well as effective pain relief. Owing to their small size, high metabolic rate, lack of easily accessible arteries and veins and several other species-specific and/or genetically induced properties, mice represent an anaesthetic challenge. Thus, the goal of our research in this field is to develop reliable anaesthetic protocols for the use in laboratory mice.

In summary, targeted in-depth research in the field of laboratory animal anaesthesia and the alleviation of pain undoubtedly contributes to the improvement of techniques in surgical research and enhances our ethical responsibility towards animals used in science.

Combining Sevoflurane Anaesthesia with Fentanyl–Midazolam or S-Ketamine in Laboratory Mice

N. Cesarovic, P. Jirkof, A. Rettich, F. Nicholls, M. Arras

Laboratory mice typically are anaesthetized by either inhalation of volatile anaesthetics or injection of drugs. Here we compared the acute and postanaesthetic effects of combining both methods with standard inhalant monoanaesthesia using sevoflurane in mice. After injection of fentanyl–midazolam or S-ketamine as premedication, a standard 50-min anaesthesia was conducted by using sevoflurane. Addition of fentanyl–midazolam (0.04 mg/kg–4 mg/kg) induced sedation, attenuation of aversive behaviors at induction, shortening of the induction phase, and reduced the sevoflurane concentration required by one third (3.3% compared with 5%), compared with S-ketamine (30 mg/kg) premedication or sevoflurane alone. During anaesthesia, heart rate and core body temperature were depressed significantly by both premedications but in general remained within normal ranges. In contrast, with or without premedication, substantial respiratory depression was evident, with a marked decline in respiratory rate accompanied by hypoxia, hypercapnia, and acidosis. Arrhythmia, apnea, and occasionally death occurred under S-ketamine–sevoflurane. Postanaesthetic telemetric measurements showed unchanged locomotor activity but elevated heart rate and core body temperature at 12 h; these changes were most prominent during sevoflurane monoanaesthesia and least pronounced or absent during fentanyl–midazolam–sevoflurane. In conclusion, combining injectable and inhalant anaesthetics in mice can be advantageous compared with inhalation monoanaesthesia at induction and postanaesthetically. However, adverse physiologic side effects during anaesthesia can be exacerbated by premedications, requiring careful selection of drugs and dosages.

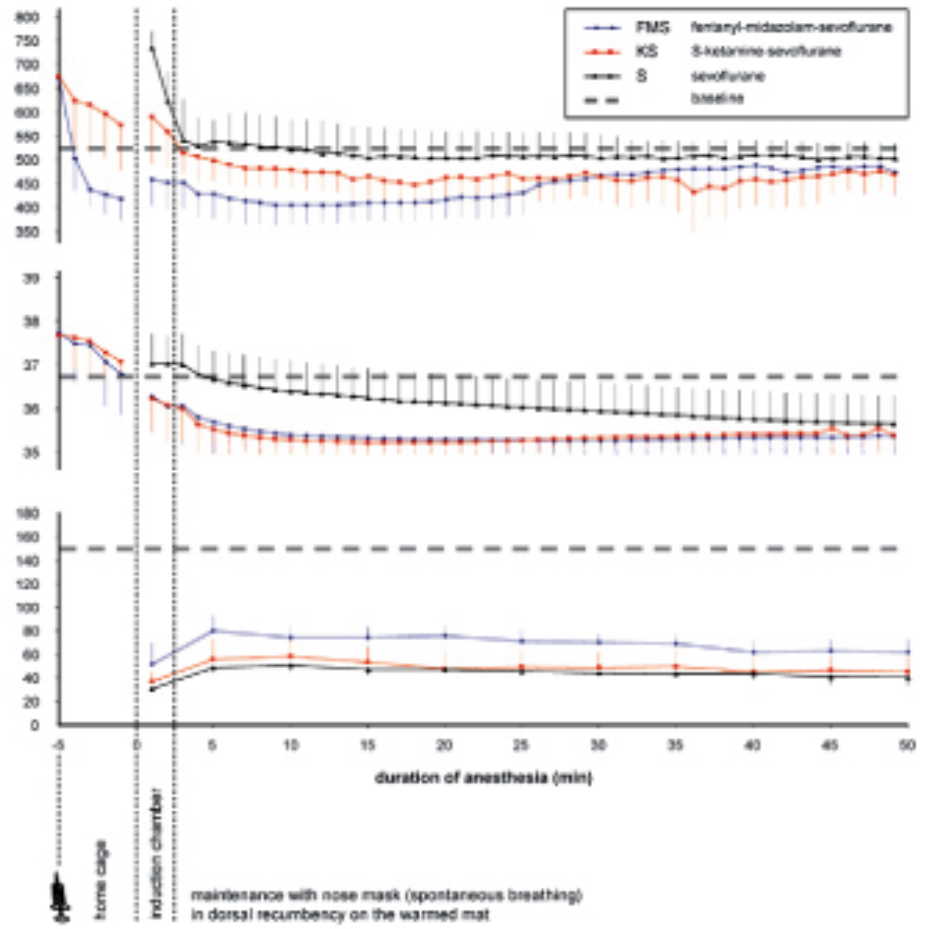
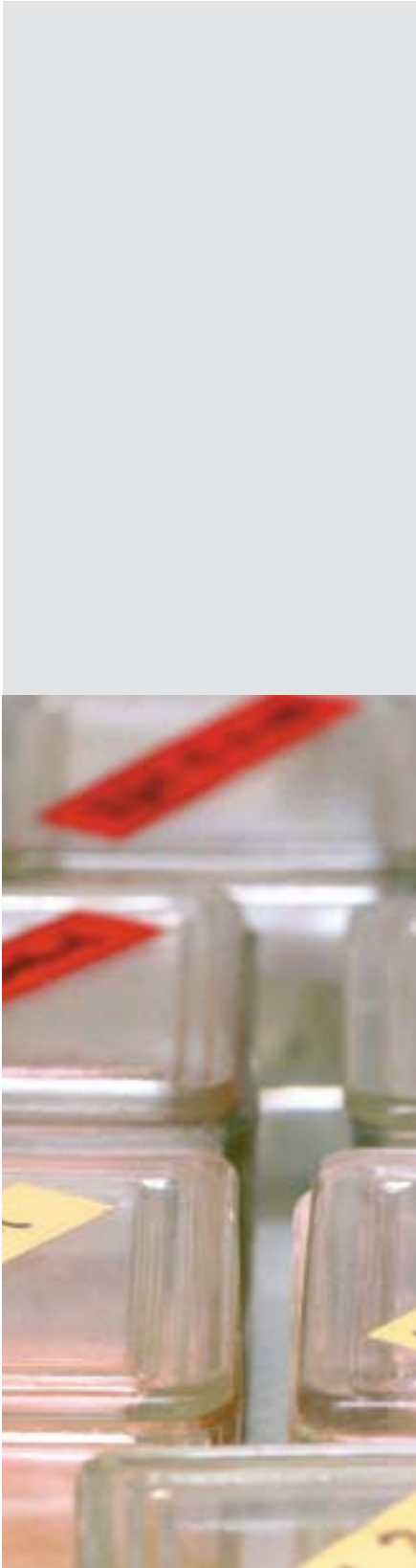


Figure 1. Mean ($n = 8$ mice; bar, 1 SD) heart rate, core body temperature, and respiratory rate after pre-medication in the home cage, in the induction chamber, and during 50-min sevoflurane anaesthesia while mice breathed spontaneously and lay in dorsal recumbency on the warming mat. Dashed lines indicate mean baseline values (measured before anaesthesia) at the same time of day in conscious mice. The baseline respiratory rate was established by counting the movement of the thorax wall in resting mice before anaesthesia.

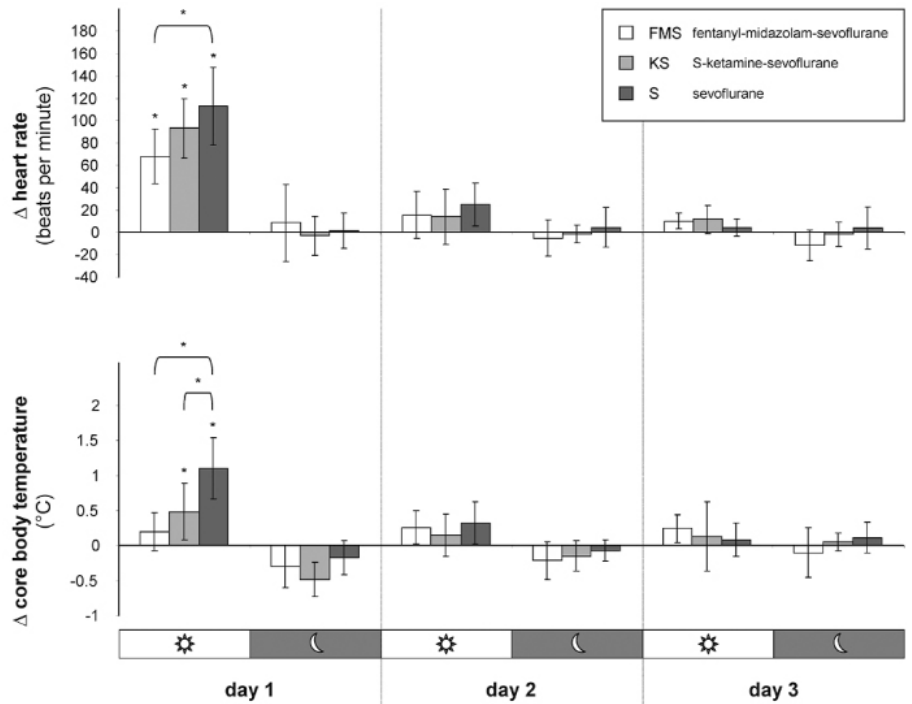
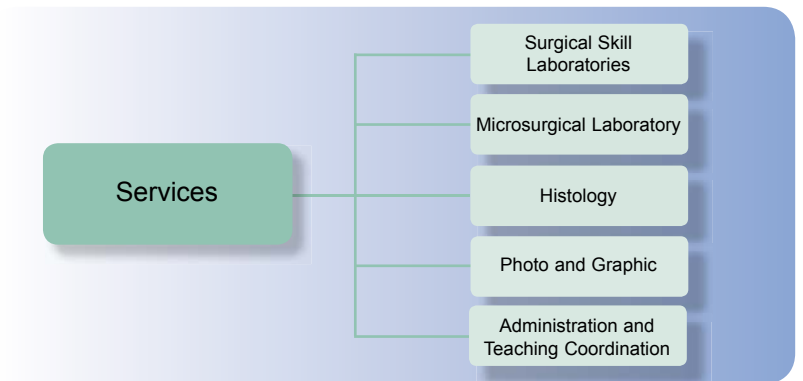


Figure 2. Mean ($n = 8$ mice; bar, 1 SD) postanaesthetic measurements of the effects of 3 anaesthesia protocols on heart rate and core body temperature. Delta (Δ) values represent deviations from baseline values (established prior to anaesthesia) during the corresponding 12-h day and night periods. *, $P \leq 0.05$ compared with baseline values and between protocols.

Collaborations:

- Department of Cardio-Vascular Surgery, UniversityHospital Zurich, Dr. M. Emmert, Dr. M. Gessat, Dr. S. Sündermann
- Institute of Laboratory Animal Sciences, University of Zurich, A. Rettich, Dr. G. Fischer, Prof. K. Bürki
- Experimentelle Chirurgie, BioMed Zentrum, Universitätsklinikum Freiburg, Deutschland, Prof. Dr. Jörg Haberstroh
- Department of Pediatrics, Endocrinology, University Children`s Hospital Zurich, Dr. S. Wüest, PD Dr. D. Konrad
- Institute of Veterinary Physiology, University of Zurich, Prof. Dr. J. Vogel
- Department of Gastroenterology and Hepatology, University Hospital Zurich, K. Leucht, PD Dr. M. Hausmann
- Institute of Neuropathology, UniversityHospital Zurich, P. Dametto, T. Läufer, PD Dr. M. Neumann, Prof. Dr. A. Aguzzi

3. Services



PD Dr. vet.
Margarete Arras,
MD



Dr. vet.
Nikola Cesarovic,
MD



Boris Leskosek
(retired 7/31/11)



Alush Avdyli
(retired 4/30/11)



Pia Fuchs

3.1 Surgical Skill Laboratories

Surgery requires a number of practical and manual skills that can be trained in skill laboratories. In our facilities which are open to all members of the department we provide a number of tools and machines in a surgical environment. To perform operations under conditions similar to the clinical situation, technical help is provided by our staff which is also responsible for the maintenance of our facilities.

3.2 Microsurgical Laboratory

The microsurgery laboratory is a separate section in which several operating-microscopes are available to all members of the department requiring special equipment. Maintenance of this laboratory includes all aspects of preparation of surgical instruments, sterilization and handling of waste materials. In addition, an intravital microscope including video equipment is available. This facility also provides for histological work-up.

3.3 Histology

The laboratory for Histology provides a histological work-up from preserved specimen to sectioning and staining. The laboratory contains an embedding machine, several microtomes and staining devices. Several techniques including paraffin embedded, frozen and plastic embedded tissue can be processed.

3.4 Photo and Graphic Services

A quick, flexible, versatile and professional service.

We offer

- photographic documentation of patients and events
- technical photography, on location or in our well equipped studio
- graphic and design of illustrations for papers and books
- reproductions from any original
- layout of printing matters
- preparation of files for external printing
- print service
- cutting and converting of movie-files for presentation
- construction and maintainance of websites
- maintainance of the digital image archives



Nico Wick
Photographer



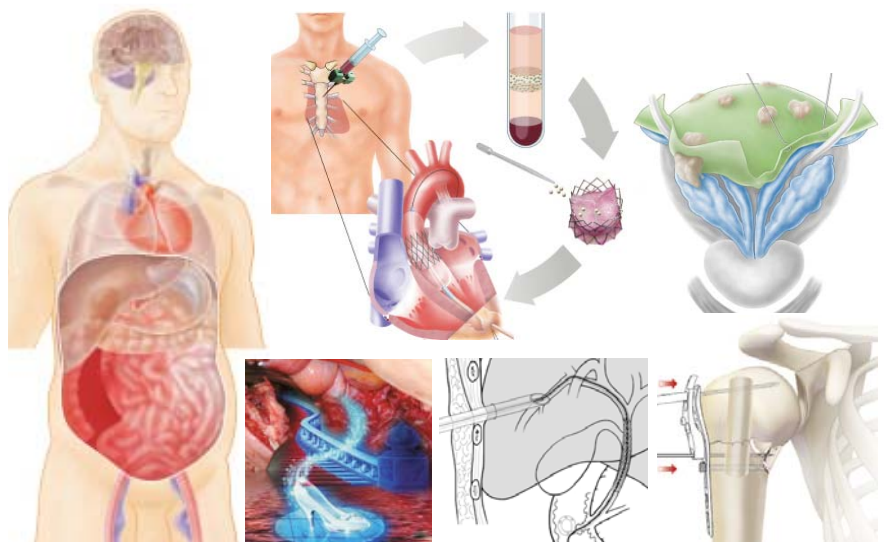
Lea Schütz-Cohen
Photographer



Stefan Schwyter
Scientific
Illustrator



Carol De Simio
Scientific
Illustrator



3. 5 Administration



Susanne Frehner
Administration
Division of Surgical
Research

- Administrative office management
- Financial accounting of the Research Division
- Organisation, planning and coordination of workshops and vocational training
- Workshop, tutorials and seminars
- Quarterly reports
- Meeting organisation and coordination
- Personnel administration

3. 6 Teaching Coordination



Corinne Renold
Teaching Coordination
Division of Surgical
Research



Donata Gröflin
Teaching Coordinator
Division of Surgical
Research

- Coordination and organization of the learning and teaching units in the Department of Surgery from 1st to 6th years of study including lectures and clinical courses in the compulsory part of the curriculum as well as in the electives.
- Coordination and organization of the clinical rotations during the 5th year of study.

The work is done in cooperation with the University of Zurich and the UniversityHospital Zurich for the Department of Surgery.

4. Events and Workshops at the Division of Surgical Research in 2011

120



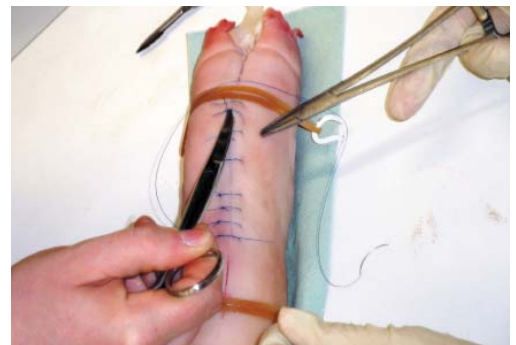
10th Day of Clinical Research



Sewing class



Sewing course



Inauguration "Zentrum für Regenerative Medizin" (ZRM)



Goodbye Alush Avdyli



Aesculap sewing course for medical students



Symposium on Pharmaceutical Medicine



Goodbye Boris Leskosek



Christmas party



5. Publications 2011

Cardiovascular Surgery

- Chu, M W A; Falk, V; Mohr, F W; Walther, T (2011). Percutaneous endoscopic transapical aortic valve implantation: three experimental transcatheter models.
In: *Interactive Cardiovascular and Thoracic Surgery* 13(3), 251-256
- Emmert, M Y; Weber, B; Behr, L; Frauenfelder, T; Brokopp, C E; Grünenfelder, J; Falk, V; Hoerstrup, S P (2011) Transapical aortic implantation of autologous marrow stromal cell-based tissue-engineered heart valves: first experiences in the systemic circulation.
In: *JACC: Cardiovascular Interventions* 4(7), 822-823
- Ender, J; Eibel, S; Mukherjee, C; Mathioudakis, D; Borger, M A; Jacobs, S ; Mohr, F W; Falk, V (2011). Prediction of the annuloplasty ring size in patients undergoing mitral valve repair using real-time three dimensional transoesophageal echocardiography.
In: *European Journal of Echocardiography* 12(6), 445-453
- Feuchtnner, G M; Spoeck, A; Lessick, J; Dichtl, W; Plass, A; Leschka, S; Mueller, S; Klausner, A; Scheffel, H; Wolf, F; Jaschke, W; Alkadhi, H (2011). Quantification of aortic regurgitant fraction and volume with multi-detector computed tomography comparison with echocardiography.
In: *Academic Radiology* 18(3), 334-42
- Gessat, M; Altwegg, L; Frauenfelder, T; Plass, A; Falk, V (2011). Cubic hermite bezier spline based reconstruction of implanted aortic valve stents from CT images.
In: *IEEE Engineering in Medicine and Biology Society. Conference Proceedings 2011*, 2667-2670
- Karar, M E; John, M; Holzhey, D; Falk, V; Mohr, F W; Burgert, O (2011). Model-updated image-guided minimally invasive off-pump transcatheter aortic valve implantation.
In: *Medical Image Computing and Computer-Assisted Intervention - MICCAI 2009* , 275-282
- Karar, M E; Merk, D R; Chalopin, C; Walther, T; Falk, V; Burgert, O (2011). Aortic valve prosthesis tracking for transapical aortic valve implantation.
In: *International Journal of Computer Assisted Radiology and Surgery* 6(5), 583-590
- Maisano, F; Cioni, M; Seeburger, J; Falk, V; Mohr, F W; Mack, M J; Alfieri, O; Vanermen, H (2011). Beating-heart implantation of adjustable length mitral valve chordae: acute and chronic experience in an animal model.
In: *European Journal of Cardio-Thoracic Surgery* 40(4), 840-847
- Martinez, E C; Kofidis, T (2011). Adult stem cells for cardiac tissue engineering.
In: *Journal of Molecular and Cellular Cardiology* 50(2), 312-319
- Merk, D R; Karar, M E; Chalopin, C; Holzhey, D; Falk, V; Mohr, F W; Burgert, O (2011). Image-guided transapical aortic valve implantation: sensorless tracking of stenotic valve landmarks in live fluoroscopic images.
In: *Innovations* 6(4), 231-236
- Schoenauer, R; Emmert, M Y; Felley, A; Ehler, E; Brokopp, C E; Weber, B; Nemir, M; Faggian, G G; Pedrazzini, T; Falk, V; Hoerstrup, S P; Agarkova, I (2011). EH-myomesin splice isoform is a novel marker for dilated cardiomyopathy.
In: *Basic Research in Cardiology* 106(2), 233-247
- Theusinger, O M; Baulig, W; Seifert, B; Emmert, M Y; Spahn, D R; Asmis, L M (2011). Relative concentrations of haemostatic factors and cytokines in solvent/detergent-treated and fresh-frozen plasma.
In: *British Journal of Anaesthesia* 106(4), 505-511
- Weber, B; Emmert, M Y; Behr, L; Brokopp, C E; Frauenfelder, T; Kretschmar, O; Falk, V; Hoerstrup, SP (2011). Fetal trans-apical stent delivery into the pulmonary artery: prospects for prenatal heart-valve implantation.
In: *European Journal of Cardio-Thoracic Surgery* 41(2), 398-403
- Weber, B; Scherman, J; Emmert, M Y; Grünenfelder, J; Verbeek, R; Bracher, M; Black, M; Kortsmitt, J; Franz, T; Schoenauer, R; Baumgartner, L; Brokopp, C E; Agarkova, I; Wolint, P; Zund, G; Falk, V; Zilla, P; Hoerstrup, S P (2011). Injectable living marrow stromal cell-based autologous tissue engineered heart valves: first experiences with a one-step intervention in primates.
In: *European Heart Journal* 32(22), 2830-2840

Visceral and Transplant Surgery

- Ashrafian, H; Athanasiou, T; Li, J V; Bueter, M; Ahmed, K; Nagpal, K; Holmes, E; Darzi, A; Bloom, S R (2011). Diabetes resolution and hyperinsulinaemia after metabolic Roux-en-Y gastric bypass. In: *Obesity Reviews* 12(5), e257-e272
- Boeck, L; Graf, R; Eggimann, P; Pargger, H; Raptis, D A; Smyrniotis, N; Thakkar, N; Siegemund, M; Rakic, J; Tamm, M; Stolz, D (2011). Pancreatic stone protein: a marker of organ failure and outcome in ventilator-associated pneumonia. In: *Chest* 140(4), 925-932
- Bueter, M; Ashrafian, H; Frankel, A H; Tam, FWK; Unwin, R J; le Roux, CW(2011). Sodium and water handling after gastric bypass surgery in a rat model. In: *Surgery for Obesity and Related Diseases* 7(1),68-73
- Bueter, M; Miras, A D; Chichger, H; Fenske, W; Ghatei, M A; Bloom, S R; Unwin, R J; Lutz, T A; Spector, A C; le Roux, C W (2011). Alterations of sucrose preference after Roux-en-Y gastric bypass. In: *Physiology & Behavior* 104(5), 709-721
- Drebber, U; Madeja, M; Odenthal, M; Wedemeyer, I; Mönig, S P; Brabender, J; Bollschweiler, E; Hölscher, A H; Schneider, P M; Dienes, H P; Vallböhmer, D (2011). beta-catenin and Her2/neu expression in rectal cancer: association with histomorphological response to neoadjuvant therapy and prognosis. In: *International Journal of Colorectal Disease* 26(9), 1127-1134
- Dutkowski, P; Oberkofler, C E; Slankamenac, K; Puhan, M A; Schadde, E; Müllhaupt, B; Geier, A; Clavien, P A (2011). Are there better guidelines for allocation in liver transplantation? A novel score targeting justice and utility in the model for end-stage liver disease era. In: *Annals of Surgery* 254(5), 745-753
- El-Badry, A M; Jang, J H; Elsherbiny, A; Contaldo, C; Tian, Y; Raptis, D A; Laczko, E; Moritz, W; Graf, R; Clavien, P A (2011). Chemical composition of hepatic lipids mediates reperfusion injury of the macrosteatotic mouse liver through thromboxane A(2). In: *Journal of Hepatology* 55(6), 1291-1299
- Fischer, M A; Gnannt, R; Raptis, D; Reiner, C S; Clavien, P A; Schmidt, B; Leschka, S; Alkadhi, H; Goetti, R (2011). Quantification of liver fat in the presence of iron and iodine: An ex-vivo dual-energy CT study. In: *Investigative Radiology* 46(6), 351-358
- Furrer, K; Rickenbacher, A; Tian, Y; Jochum, W; Bittermann, A G; Käch, A; Humar, B; Graf, R; Moritz, W; Clavien, P A (2011). Serotonin reverts age-related capillarization and failure of regeneration in the liver through a VEGF-dependent pathway. In: *Proceedings of the National Academy of Sciences of the USA* 108(7), 2945-2950
- Heinrich, S; Georgiev, P; Weber, A; Vergopoulos, A; Graf, R; Clavien, P A (2011). Partial bile duct ligation in mice: A novel model of acute cholestasis. In: *Surgery* 149(3), 445-451
- Le Roux, CW; Bueter, M; Theis, N; Werling, M; Ashrafian, H; Löwenstein, C; Athanasiou, T; Bloom, S R; Spector, A C; Olbers, T; Lutz, T A (2011). Gastric bypass reduces fat intake and preference. In: *American Journal of Physiology. Regulatory, Integrative and Comparative Physiology* 301(4), R1057-66
- Li, J V; Reshat, R; Wu, Q; Ashrafian, H; Bueter, M; le Roux, C W; Darzi, A; Athanasiou, T; Marchesi, J R; Nicholson, J K; Holmes, E; Gooderham, N J (2011). Experimental bariatric surgery in rats generates a cytotoxic chemical environment in the gut contents. In: *Frontiers in Microbiology* 2, 183
- Li, L; Bimmler, D; Graf, R; Zhou, S; Sun, Z; Chen, J; Siech, M; Bachem, M G (2011). PSP/reg inhibits cultured pancreatic stellate cell and regulates MMP/αTIMP ratio. In: *European Journal of Clinical Investigation* 41(2), 151-158
- März-Weiss, P; Kunz, D; Bimmler, D; Berkemeier, C; Özbek, S; Dimitriades-Schmutz, B; Haybaeck, J; Otten, U; Graf, R (2011). Expression of pancreatitis-associated protein after traumatic brain injury: a mechanism potentially contributing to neuroprotection in human brain. In: *Cellular and Molecular Neurobiology* 31(8), 1141-1149
- Raptis, D A; Graf, R; Peck, J; Mouzaki, K; Patel, V; Skipworth, J; Oberkofler, C; Boulos, P B (2011). Development of an electronic web-based software for the management of colorectal cancer target referral patients. In: *Informatics for Health & Social Care* 36(3), 117-131

- Rickenbacher, A; DeOliveira, ML; Tian, Y; Jang, J H; Riener, MO; Graf, R; Moritz, W; Clavien, PA (2011). Arguments against toxic effects of chemotherapy on liver injury and regeneration in an experimental model of partial hepatectomy. In: *Liver International* 31(3), 313-321
- Silva, A; Weber, A; Bain, M; Reding, T; Heikenwalder, M; Sonda, S; Graf, R (2011). COX-2 is not required for the development of murine chronic pancreatitis. In: *American Journal of Physiology. Gastrointestinal and Liver Physiology* 300(6), G968-G975
- Tian, Y; Graf, R; El-Badry, A M; Lesurtel, M; Furrer, K; Moritz, W; Clavien, P A (2011). Activation of serotonin receptor-2B rescues small-for-size liver graft failure in mice. In: *Hepatology* 53(1), 253-62

Trauma Surgery

- Chan, E; Cadosch, D; Gautschi, O P; Sprengel, K; Filgueira, L (2011). Influence of metal ions on human lymphocytes and the generation of titanium-specific T-lymphocytes. In: *Journal of Applied Biomaterials & Biomechanics : JABB* 9(2), 137-143
- Favre, P; Kloen, P; Helfet, D L; Werner, C M L (2011). Superior versus anteroinferior plating of the clavicle: a finite element study. In: *Journal of Orthopaedic Trauma* 25(11), 661-665
- Osterhoff, G; Baumgartner, D; Favre, P; Wanner, G A; Gerber, H; Simmen, H P; Werner, C M L (2011). Medial support by fibula bone graft in angular stable plate fixation of proximal humeral fractures: an *in vitro* study with synthetic bone. In: *Journal of Shoulder and Elbow Surgery* 20(5), 740-746
- Osterhoff, G; Löffler, S; Steinke, H; Feja, C; Josten, C; Hepp, P (2011). Comparative anatomical measurements of osseous structures in the ovine and human knee. In: *The Knee* 18(2), 98-103
- Rüter, A; Werner, C M L; Trentz, O (2011). Ellenbogengelenk. In: Scharf, H P; Braun, M; et al. (ed.), *Orthopädie und Unfallchirurgie*. Urban&Fischer Verlag, Kapitel-26
- Sabile, A A; Arlt, M J; Muff, R; Bode, B; Langsam, B; Bertz, J; Jentsch, T; Puskas, G J; Born, W; Fuchs, B (2011). Cyr61 expression in Osteosarcoma indicates poor prognosis and promotes intratibial growth and lung metastasis in mice. In: *Journal of Bone and Mineral Research* 27(1), 58-67

Plastic, Hand and Reconstructive Surgery

- Altintas, A A; Guggenheim, M; Oezcelik, A; Gehl, B; Aust, M C; Altintas, M A (2011). Local burn versus local cold induced acute effects on *in vivo* microcirculation and histomorphology of the human skin. In: *Microscopy Research and Technique* 74(10), 963-969
- Buschmann, J; Müller, A; Feldman, K; Tervoort, T A; Fessel, G; Snedeker, J G; Giovanoli, P; Calcagni, M (2011). Small hook thread (Quill) and soft felt internal splint to increase the primary repair strength of lacerated rabbit Achilles tendons: biomechanical analysis and considerations for hand surgery. In: *Clinical Biomechanics* 26(6), 626-631
- Buschmann, J; Welti, M; Hemmi, S; Neuenschwander, P; Baltes, C; Giovanoli, P; Rudin, M; Calcagni, M (2011). 3D co-cultures of osteoblasts and endothelial cells in DegraPol foam: Histological and high field MRI analyses of pre-engineered capillary networks in bone grafts. In: *Tissue engineering. Part C* 17(3-4), 291-299
- Calcagni, M; Althaus, M K; Knapik, A D; Hegland, N; Contaldo, C; Giovanoli, P; Lindenblatt, N (2011). *In vivo* visualization of the origination of skin graft vasculature in a wild-type/GFP crossover model. In: *Microvascular Research* 82(3), 237-245
- Fakin, R; Hamacher, J; Gugger, M; Gazdhar, A; Moser, H; Schmid, R A (2011). Prolonged amelioration of acute lung allograft rejection by sequential overexpression of human interleukin-10 and hepatocyte growth factor in rats. In: *Experimental Lung Research* 37(9), 555-562

- Fessel, G; Frey, K; Schweizer, A; Calcagni, M; Ullrich, O; Snedeker, J G (2011). Suitability of Thiel embalmed tendons for biomechanical investigation.
In: *Annals of Anatomy = Anatomischer Anzeiger* 193(3), 237-241
- Forster, N A; Penington, A J; Hardikar, A A; Palmer, J A; Hussey, A; Tai, J; Morrison, W A; Feeney, S J (2011). A prevascularized tissue engineering chamber supports growth and function of islets and progenitor cells in diabetic mice.
In: *Islets* 3(5), 271-283
- Guggenheim, M; Thurnheer, T; Gmür, R; Giovanoli, P; Guggenheim, B (2011). Validation of the Zürich burn-biofilm model.
In: *Burns* 37(7), 1125-1133
- Meier, T O; Guggenheim, M; Vetter, S T; Husmann, M; Haile, S R; Amann-Vesti, B R (2011). Microvascular regeneration in meshed skin transplants after severe burns.
In: *Burns* 37(6), 1010-1014
- Radtke, C; Allmeling, C; Waldmann, K H; Reimers, K; Thies, K; Schenk, H C; Hillmer, A; Guggenheim, M; Brandes, G; Vogt, P M (2011). Spider silk constructs enhance axonal regeneration and remyelination in long nerve defects in sheep.
In: *PLoS ONE* 6(2), e16990
- Sarahrudi, K; Thomas, A; Heinz, T; Krumböck, A; Vécsei, V; Aharinejad, S (2011). Growth factor release in extra- and intramedullary osteosynthesis following tibial fracture.
In: *Injury* 42(8), 772-777
- Schweizer, R; Merz, K; Schlosser, S; Spanholtz, T; Contaldo, C; Stein, J V; Enzmann, V; Giovanoli, P; Erni, D; Plock, J A (2011). Morphology and hemodynamics during vascular regeneration in critically ischemic murine skin studied by intravital microscopy techniques.
In: *European Surgical Research* 47(4), 222-230

Thoracic Surgery

- Arbogast, S; Behnke, S; Opitz, I; Stahel, R A; Seifert, B; Weder, W; Moch, H; Soltermann, A (2011). Automated ERCC1 Immunohistochemistry in Non-small Cell Lung Cancer: Comparison of anti-ERCC1 Antibodies 8F1, D-10, and FL-297.
In: *Applied Immunohistochemistry & Molecular Morphology* 19(2), 99-105
- Dodd-o, J M; Lendermon, E A; Miller, H L; Zhong, Q; John, E R; Jungraithmayr, W M; D'Alessio, F R; McDyer, J F (2011). CD154 blockade abrogates allospecific responses and enhances CD4(+) regulatory T-cells in mouse orthotopic lung transplant.
In: *American Journal of Transplantation* 11(9), 1815-1824
- Draenert, A; Marquardt, K; Inci, I; Soltermann, A; Weder, W; Jungraithmayr, W (2011). Ischaemia-reperfusion injury in orthotopic mouse lung transplants - a scanning electron microscopy study.
In: *International Journal of Experimental Pathology* 92(1), 18-25
- Inci, I; Arni, S; Acevedo, C; Jungraithmayr, W; Inci, D; Vogt, P; Weder, W (2011). Surfactant alterations following donation after cardiac death donor lungs.
In: *Transplant International* 24(1), 78-84
- Meerwein, C; Korom, S; Arni, S; Inci, I; Weder, W; Jungraithmayr, W (2011). The effect of low-dose continuous erythropoietin receptor activator in an experimental model of acute Cyclosporine A induced renal injury.
In: *European Journal of Pharmacology* 671(1-3), 113-119
- Opitz, I; Erne, B V; Demirbas, S; Jetter, A; Seifert, B; Stahel, R; Weder, W (2011). Optimized intrapleural cisplatin chemotherapy with a fibrin carrier after extrapleural pneumonectomy: a preclinical study.
In: *Journal of Thoracic and Cardiovascular Surgery* 141(1), 65-71
- Tischler, V; Pfeifer, M; Hausladen, S; Schirmer, U; Bonde, A K; Kristiansen, G; Sos, M L; Weder, W; Moch, H; Altevogt, P; Soltermann, A (2011). L1CAM protein expression is associated with poor prognosis in non-small cell lung cancer.
In: *Molecular Cancer* 10, 127
- Wiedl, T; Arni, S; Roschitzki, B; Grossmann, J; Collaud, S; Soltermann, A; Hillinger, S; Aebersold, R; Weder, W (2011). Activity-based proteomics: identification of ABHD11 and ESD activities as potential biomarkers for human lung adenocarcinoma.
In: *Journal of Proteomics* 74(10), 1884-1894

Urology

- Beer, M; Montani, M; Gerhardt, J; Wild, P J; Hany, T F; Hermanns, T; Müntener, M; Kristiansen, G (2011). Profiling gastrin-releasing peptide receptor in prostate tissues: Clinical implications and molecular correlates.
In: *Prostate* 72(3), 318-325
- Beermann, A; Ghanjati, F; Hermanns, T; Poyet, C; Pereira, J; Fischer, J; Wernet, P; Santouridis, S (2011). Methods for separate isolation of cell-free DNA and cellular DNA from urine-application of methylation-specific PCR on both DNA fractions.
In: *The Open Biomarkers Journal* 4, 15-17
- Eberli, D; Atala, A; Yoo, J J (2011). One and four layer acellular bladder matrix for fascial tissue reconstruction.
In: *Journal of Materials Science: Materials in Medicine* 22(3), 741-751
- Eberli, D; Hefermehl, L J; Müller, A; Sulser, T; Knönagel, H (2011). Thermal spread of vessel-sealing devices evaluated in a clinically relevant *in vitro* model.
In: *Urologia Internationalis* 86(4), 476-482
- Fritzsche, F R; Hasler, A; Bode, P K; Adams, H; Seifert, H H; Sulser, T; Moch, H; Barghorn, A; Kristiansen, G (2011). Expression of histone deacetylases 1, 2 and 3 in histological subtypes of testicular germ cell tumours.
In: *Histology and Histopathology* 26(12), 1555-1561
- Gabi, M; Hefermehl, L; Lukic, D; Zahn, R; Vörös, J; Eberli, D (2011). Electrical microcurrent to prevent conditioning film and bacterial adhesion to urological stents.
In: *Urological Research* 39(2), 81-88
- Gerhardt, J; Montani, M; Wild, P J; Beer, M; Huber, F; Hermanns, T; Müntener, M; Kristiansen, G (2011). FOXA1 promotes tumor progression in prostate cancer and represents a novel hallmark of castration-resistant prostate cancer.
In: *American Journal of Pathology* 180(2), 848-861
- Gerhardt, J; Steinbrech, C; Büchi, O; Behnke, S; Bohnert, A; Fritzsche, F; Liewen, H; Stenner, F; Wild, P; Hermanns, T; Müntener, M; Dietel, M; Jung, K; Stephan, C; Kristiansen, G (2011). The androgen-regulated Calcium-Activated Nucleotidase 1 (CANT1) is commonly overexpressed in prostate cancer and is tumor-biologically relevant *in vitro*.
In: *American Journal of Pathology* 178(4), 1847-1860
- Morra, L; Rechsteiner, M; Casagrande, S; Duc Luu, V; Santimaria, R; Diener, P A; Sulser, T; Kristiansen, G; Schraml, P; Moch, H; Soltermann, A (2011). Relevance of periostin splice variants in renal cell carcinoma.
In: *American Journal of Pathology* 179(3), 1513-1521
- Rechsteiner, M P; von Teichman, A; Nowicka, A; Sulser, T; Schraml, P; Moch, H (2011). VHL gene mutations and their effects on hypoxia-inducible factor HIF{alpha}: Identification of potential driver and passenger mutations.
In: *Cancer Research* 71(16), 5500-5511
- von Boehmer, L; Keller, L; Mortezaei, A; Provenzano, M; Sais, G; Hermanns, T; Sulser, T; Jungbluth, A A; Old, L J; Kristiansen, G; van den Broek, M; Moch, H; Knuth, A; Wild, P J (2011). MAGE-C2/CT10 protein expression is an independent predictor of recurrence in prostate cancer.
In: *PLoS ONE* 6(7), e21366

Cranio-maxillofacial Surgery

- Besic Gyenge, E; Darphin, X; Walt, H; Maake, C (2011). Uptake and distribution of silica-shell nano particles in head-and-neck cancer cell lines.
In: *Journal of Nanobiotechnology* 9(1), 32-45
- Besic Gyenge, E; Hiestand, S; Graefe, S; Walt, H; Maake, C (2011). Cellular and molecular effects of the liposomal mTHPC derivative Foslipos in prostate carcinoma cells *in-vitro*.
In: *Photodiagnosis and Photodynamic Therapy* 8(2), 86-96
- Colombo, V; Corroero, M R; Riener, R; Weber, F E; Gallo, L M (2011). Design, construction and validation of a computer controlled system for functional loading of soft tissue.
In: *Medical Engineering & Physics* 33(6), 377-683

- Correro-Shahgaldian, M R; Colombo, V; Spencer, N D; Weber, F E; Imfeld, T; Gallo, L M (2011). Coupling plowing of cartilage explants with gene expression in models for synovial joints. In: *Journal of Biomechanics* 44(13), 2472-2476
- Ehrbar, M; Sala, A; Lienemann, P; Ranga, A; Mosiewicz, K; Bittermann, A; Rizzi, S C; Weber, F E; Lutolf, M P (2011). Elucidating the role of matrix stiffness in 3D cell migration and remodeling. In: *Biophysical Journal* 100(2), 284-293
- Ghayor, C; Correro, R M; Lange, K; Karfeld-Sulzer, L S; Grätz, K W; Weber, F E (2011). Inhibition of osteoclast differentiation and bone resorption by N-methylpyrrolidone. In: *Journal of Biological Chemistry* 286(27), 24458-24466
- Jung, R E; Kokovic, V; Jurisic, M; Yaman, D; Subramani, K; Weber, F E (2011). Guided bone regeneration with a synthetic biodegradable membrane: a comparative study in dogs. In: *Clinical Oral Implants Research* 22(8), 802-807
- Kruse, A; Jung, R E; Nicholls, F; Zwahlen, R A; Hämmerle, C H F; Weber, F E (2011). Bone regeneration in the presence of a synthetic hydroxyapatite/silica oxide-based and a xeno-genic hydroxyapatite-based bone substitute material. In: *Clinical Oral Implants Research* 22(5), 506-511
- Lübbers, H T; Kruse, A; Messmer, P; Grätz, K W; Obwegeser, J A; Matthews, F (2011). Precise screw positioning at the mandibular angle: computer assisted versus template coded. In: *Journal of Craniofacial Surgery* 22(2), 620-624
- Sala, A; Hänseler, P; Ranga, A; Lutolf, M P; Vörös, J; Ehrbar, M; Weber, F E (2011). Engineering 3D cell instructive microenvironments by rational assembly of artificial extracellular matrices and cell patterning. In: *Integrative Biology* 3(11), 1102-1111
- Schneider, D; Weber, F E; Hämmerle, C H F; Feloutzis, A; Jung, R E (2011). Bone regeneration using a synthetic matrix containing enamel matrix derivate. In: *Clinical Oral Implants Research* 22(2), 214-222
- Thoma, D S; Subramani, K; Weber, F E; Luder, H U; Hämmerle, C H F; Jung, R E (2011). Biodegradation, soft and hard tissue integration of various polyethylene glycol hydrogels: a histomorphometric study in rabbits. In: *Clinical Oral Implants Research* 22(11), 1247-1254

Intensive Care Unit

- Oberkofler CE, Stocker R, Raptis DA, Stover, J. F., Schuepbach, R. A. Mullhaupt, B. Dutkowsky, P. Clavien, P. A. Bechir, M. (2011). Same quality - higher price? The paradox of allocation: the first national single center analysis after the implementation of the new Swiss transplantation law: the ICU view. In: *Clin Transplant* 25:921-928
- Quiblier C, Zinkernagel AS, Schuepbach RA, Berger-Bachi B, Senn MM. (2011) Contribution of SecDF to Staphylococcus aureus resistance and expression of virulence factors. In: *BMC Microbiol* 11:72
- Vuille-Dit-Bille RN, Ha-Huy R, Stover JF. (2011) Changes in plasma phenylalanine, isoleucine, leucine, and valine are associated with significant changes in intracranial pressure and jugular venous oxygen saturation in patients with severe traumatic brain injury. In: *Amino Acids* 2011
- Vuille-Dit-Bille RN, Ha-Huy R, Tanner M, Stover JF. (2011) Changes in calculated arterio-jugular venous glutamate difference and SjvO₂ in patients with severe traumatic brain injury. In: *Minerva Anestesiol* 77:870-876

6. Grants 2011

Cardiac Surgery

Grants	Title of Project	Project Leader
Swiss National Science Foundation	Advanced Cell Therapies for Cardiac Repair-SPUM	S.P. Hoerstrup
Swiss National Science Foundation	Characterization / evaluation & cell fate <i>in vivo</i> analysis of fetal stem cells used for CV TE applications	S.P. Hoerstrup
Commission of the European Communities	Living autologous heart valves for MIV implantable procedures	S.P. Hoerstrup
Novartis Stiftung für Biologisch-Medizinische Forschung	miRNA manipulations to improve the regenerative potential of bone-marrow derived MSCs	S.P. Hoerstrup
SCIEX-NMSch Fellowship	SCIEX Fellowship Jaro Slamecka	S.P. Hoerstrup
Fakultät der Universität Zürich	Sarcomeric M-band as a novel marker for the remodelling process in cardiomyopathy	R. Schönauer
Swiss National Science Foundation	Biomechanische Simulation der katheterbasierten Aortenklappenimplantation.	M. Gessat
Deutsche Forschungsgemeinschaft (DFG)	Deutsche Forschungsgemeinschaft	V. Falk
Medtronic Ventor Technologies NL-Maastricht	Medtronic Engager Feasibility and Pivotal Trial	V. Falk
Valtech Cardio LTD, ISRAEL	"Valtech Cardinal adjustable Semi-Rigid annuloplasty Ring System for Treatment of Mitral Valve Regurgitation in Open Surgical Repair" and "Valtech V-Chordal adjustable System for chordal repair in Mitral Valve Insufficiency due to leaflet prolaps"	V. Falk
Edwards Lifesciences LLC, Irvine, CA, USA (Zahlung evtl. via Edwards Lifesciences, Nyon)	Carpentier-Edwards / Perimount Magna / Mitra Pericardial Bioprotheses	V. Falk
Schweizerische Herzstiftung Bern	The clinical value of 3D template based planning for percutaneous aortic valve implantation	M. Gessat
Schweizerische Herzstiftung Bern	Patient specific annuloplasty rings for mitral valve repair - an initial surgical tria.	S. Jacobs

Visceral & Transplant Surgery

Grants	Title of Project	Project Leader
Hepatobiliary laboratory		
Olga Mayenfisch Stiftung	Versagen der Leberregeneration nach ausgedehnter Leberresektion als Ursache des "Small-for-Size Syndroms"	K. Lehmann P.A. Clavien
Swiss National Science Foundation	Hypothermic oxygenated perfusion (HOPE) of non-heart beating donor livers prior to transplantation	P. Dutkowski
Swiss National Science Foundation	Multicellular tumor spheroids derived from esophageal cancer cell lines as a model system to characterize chemo- and radiation sensitivity and resistance	P. Schneider
Swiss National Science Foundation	Reversible portal vein embolization for safer liver surgery and transplantation	M. Lesurtel
Swiss National Science Foundation	Serotonin and regeneration in the normal, old and diseased liver	P.A. Clavien
Sassella-Stiftung	Adjuvant gemcitabine versus neoadjuvant gemcitabine / oxaliplatin and adjuvant chemotherapy with gemcitabine in patients with resectable pancreatic cancer	P.A. Clavien
Swiss National Science Foundation	Konditionierung mit volatilen Anästhetika in der Lebertransplantation	S. Breitenstein
Kurt und Senta Herrmann Stiftung, Vaduz, FL	Targeting Reactive Oxygen Levels	K. Lehmann P.A. Clavien
Hartmann Müller Stiftung	Serotonin in der Magensäuresekretion	A. Nocito P.A. Clavien
ETH Zurich as the Swiss leading house for the SSSTC	Sino-Swiss Science and Technology Cooperation	P.A. Clavien
Swiss National Science Foundation	Adjuvant gemcitabine versus NEOadjuvant gemcitabine / oxaliplatin plus adjuvant gemcitabine in resectable Pancreatic Cancer: a randomized multicenter phase III study (NEOPAC study).	P.A. Clavien
Swiss National Science Foundation	Switzerland - Uzbekistan International Cooperation: Transition to Modern Hepato-Pancreato-Biliary Surgery.	M.Lesurtel P.A. Clavien
Swiss National Science Foundation	Establishment of a Morbidity Index to Assess Surgery	Dr. K. Slankamenac
Pancreatitis Laboratory		
Swiss National Science Foundation	Role of serotonin in inflammation, repair and regeneration of the pancreas	R. Graf
Gottfried und Julia Bangerter Rhyner-Stiftung	Serotonin in pancreas	R. Graf
Amélie Waring Stiftung	Pankreatitis	P.A. Clavien
Velux Stiftung	The role of macrophages in chronic pancreatic inflammation	R. Graf

Plastic Hand & Reconstructive Surgery

Grants	Title of Project	Project Leader
Swiss National Science Foundation	Characterization of the vascularization of skin grafts, skin substitutes and biomaterials <i>in vivo</i> and identification of the vascular mechanisms	N. Lindenblatt
Fonds für Medizinische Forschung - Universität Zürich	Molekulare Charakterisierung der Revaskularisierung von Hauttransplantaten	N. Lindenblatt
Hartmann Müller-Stiftung	Tendon repair in hand surgery	J. Buschmann
Wolferrmann-Nägeli-Stiftung	Tendon repair in hand surgery	J. Buschmann
Fonds für Medizinische Forschung - Universität Zürich	Tendon repair in hand surgery	J. Buschmann
Helmut Horten Stiftung	„Role of exogenously administered recombinant erythropoietin in plastic surgery“	C. Contaldo
Elite-med Stiftung Zürich	Microcirculation study	C. Contaldo
Swiss National Science Foundation	Breast tissue reconstruction: Potential and therapeutic implications of mesenchymal stem cells	Dr. Jan Plock

Trauma Surgery

Grants	Title of Project	Project Leader
AO Research Fund	Assessment of soft-tissue and periosteal microcirculation in severely open fractures using orthogonal polarization spectral imaging	G. Wanner

Thoracic Surgery

Grants	Title of Project	Project Leader
Swiss National Science Foundation	Immune targeted therapy for lung cancer	S. Hillinger
Swiss National Science Foundation	NF In-Vivo Bioreactor for the reepithelialization of tissue engineered trachea	W. Weder
Swiss National Science Foundation	The role of CD26/DPP IV and SDF-1 in pulmonary ischemic injury in a mouse lung transplantation model	W. Jungraithmayr
Swiss National Science Foundation	Föderungsprofessur Isabelle Schmitt-Opitz	I. Schmitt-Opitz
Covidien Inc	Covidien LUN-06-002	W. Weder
Krebsliga Zürich	Adjuvante intrapleurale Spüllösung nach Pleuropneumonektomie beim malignen Pleuramesotheliom	I. Schmitt-Opitz
F. Hoffmann-La Roche Ltd., Bern (Zahlung evtl. durch ETOP, Bern)	ETOP Lungscape Database collaboration between ETOP and Chinese investigators	W. Weder
Lungen Liga	Lungenliga Ex vivo evaluation and resuscitation of human donor lungs rejected for transplantation	W. Weder
ETOP European Thoracic Oncology Platform	ETOP Lungscape	W. Weder
Krebsliga Zürich	Activity based protein profiling in human lung cancer biopsies	W. Weder

Urological Research

Grants	Title of Project	Project Leader
SNF Projektförderung	„Generation of a Recombinant Vaccinia Virus encoding immunogenic BKV Large T antigen epitopes	M. Provenzano
SNF SCORE Förderung	Muscle Precursor Cells for the treatment of Urinary Incontinence	D. Eberli
Swiss National Science Foundation	Improving human muscle engineering by PGC-lalpha expression and molecular imaging using pet.	D. Eberli
AstraZeneca, SE-151 85 Södertälje	Eine randomisierte, Placebo-kontrollierte, doppel-blinde Phase-III-Studie zur Beurteilung der Wirksamkeit und Sicherheit von 10 mg ZD4054, einmal täglich oral verabreicht, bei Patienten mit nicht metastasierendem hormonresistentem Prostatakrebs.	T. Sulser
Forschungskredit UZH	Adult Muscle Progenitor Cells for Clinical Applications: Function, Safety and Interactions	M. Stölting T. Sulser
Eli Lilly (Suisse) S.A., Vernier (Zahlungen kommen evtl. durch ICON Clinical Research Ltd., Dublin	Evaluating the Effect on erectile function of Tadalafil in a randomised, double-blind, placebo-controlled study in subjects undergoing bilateral nerve-sparing radical prostatectomy	M. Müller T. Sulser

Cranio-Maxillofacial Surgery Research

Grants	Title of Project	Project Leader
Commission of the European Communities	Biomimetic nano-fiber-based nucleus pulposus regeneration for the treatment of degenerative disc disease	F. E. Weber
International Bone Research Association	Frontbloc Distraction-Evaluation and clinical assessment	Anas Al-jadaa K. W. Grätz
Novartis	Neue Forschungsergebnisse in der Oralen Onkologie	K. W. Grätz
Emina Besic Gyenge	Photodynamic Therapy for the Treatment of Oral Pathogens	E. Besic Gyenge K. W. Grätz

Surgical Intensive Care Medicine

Grants	Title of Project	Project Leader
Forschungs- und Nachwuchsförderung der Universität Zürich	Role of PAR1 in vascular barrier regulation	R. Schüpbach
Hartmann Müller-Stiftung für medizinische Forschung Hartmann Müller Stiftung	Role of PAR1 in Vascular Barrier Regulation	R. Schüpbach
UBS Wealth Management	Einfluss von Noradrenalin auf die Funktion isolierter arterieller und jugularvenöser Thrombo bei intensivpflichtigen Patienten mit schwerem SHT Pathophysiologische Relevanz aktivierter Thrombozyten und Einfluss von Noradrenalin auf die Funktion isolierter Thrombozyten nach schwerem Schädel Hirn Trauma	J. Stover
Fresenius Kabi (Schweiz) AG	Early fluid resuscitation with balanced HES 130/0.4 [6\%] in severe burn injury	M. Béchir
Schweizerischer Nationalfonds	Cytoprotection through non Anticoagulant Engineered Chimeric Activated Protein C	R. Schüpbach

7. Awards 2011

- Dr. med. Benedikt Weber
Young Investigator Finalist Selection
American College of Cardiology (ACC), April 11, 2011
- Dr. med. Thomas Hermanns:
Best poster of session BPH, Interventional Therapy and PVP, 26th Annual Congress of the European Association of Urology (EAU), Vienna, A, 2011
- Dr. med. Thomas Hermanns:
Best poster of session BPH, 63st Congress of the German Society of Urology, Hamburg, D, 2011
- C. Frei, I. Opitz, A. Soltermann, B. Fischer, U. Moura, H. Rehrauer, W. Weder, R. Stahel, E. Felley-Bosco
10th Day of Clinical Research, 9th June, 2011 – **Poster Prize**
- Dr. Ing. Michael Gessat:
Best Paper Award – Jahrestreffen der CURAC (Deutsche Gesellschaft für Computer- und roboterassistierte Chirurgie e.V.), vom 15.-16. Sept. 2011 in Magdeburg
- Paulin Jirkof, Nikola Cesarovic, Andreas Rettich, Flora Nicholls, Burkhardt Seifert, Margarete Arras
Poster Award – 8th World Congress on Alternatives and Animal Use in the Life Sciences, Montreal – 25.08.2011
- Dr. Christian Oberkofler
Best oral presentation ARS (Association for Research in Surgery) - 98. Jahreskongress der SGC, Genf, 25.-27. Mai 2011
- D. Rittirsch, V. Schoenborn, K. Sprengel, L. Härter, S. Albers, C.M. Werner, H.-P. Simmen, G. A. Wanner
Best oral presentation ARS (Association for Research in Surgery) - 98. Jahreskongress der SGC, Genf, 25.-27. Mai 2011
- K. Lehmann, A. Rickenbacher, J.-H. Jang, C.E. Oberkofler, O. Tschopp, S. Schultze, A. Weber, R. Graf, B. Humar, P.-A. Clavien (Zürich)
Best oral presentation ARS (Association for Research in Surgery) - 98. Jahreskongress der SGC, Genf, 25.-27. Mai 2011
- K. Lehmann, A. Rickenbacher, J.-H. Jang, C. E. Oberkofler, R. Vonlanthen, B. Humar, P. Gertsch, P.-A. Clavien (Zürich)
Best poster presentation ARS (Association for Research in Surgery) – 98. Jahreskongress der SGC, Genf, 25.-27. Mai 2011
- Stölting M.N.L, Kramer S, Ametamey S, Ferrari S, Becskei A, Sulser T, Eberli D. **Research prize: Best Poster of Session**
Annual Meeting of the European Association of Urology, Vienna 2011.
- Horst M , Madduri S, Hall H, Milleret V, Gobet R , Sulser T , Eberli D
2nd Research Prize
22nd Annual Meeting of the European Society for Pediatric Urology, Copenhagen, 2011
- Tremp T, Salemi S, Largo R, Aboushwareb T, Sulser T, Eberli D
Research Poster Prize of the Swiss Urological Association
Annual Meeting of the Swiss Urological Association, Basel 2011
- Dr. med. Maximilian Emmert
Bridge to Academic Career Grant 2010 ARS/SGC (CHF 15'000) – Awarded in 2011

- Dr. med. Marco Bueter, PhD
World Congress of the International Federation for the Surgery of Obesity and metabolic disorders (IFSO) in Hamburg, 30.08.-03.09.2011
Awarded on 02.09.2011
IFSO Scholarship 2011 (2.500,00 USD)
- PD Dr. Wolfgang Jungraithmayr
European Society of Thoracic Surgeons. 19th European Conference in General Thoracic Surgery, Marseille, France, 5-8 June, 2011
ESTS-GRILLO AWARD – 8th June, 2011
- PD Dr. Wolfgang Jungraithmayr
Schweizerische Gesellschaft für Thoraxchirurgie - 2011
Best Publication in Thoracic Surgery in the year 2011
- W. Jungraithmayr, I. De Meester, L. Baerts, L. Härter, V. Matheussen, S. Arn, S. Korom, W. Weder (Zürich, Antwerpen)
Best poster presentation ARS (Association for Research in Surgery) - 98. Jahreskongress der SGC, Genf, 25.-27. Mai 2011
- Dr. Sabrina Sonda
Best poster presentation at the 43rd Annual European Pancreatic Club meeting in Magdeburg, Germany. June 22-25, 2011.
- Prof. PA Clavien
Research Prize of the United European Gastroenterology Federation, Stockholm, October 24, 2011

Photo & Graphic, Division of Surgical Research
Nico Wick, Carol De Simio

Sponsors:

